Earth-Science Reviews 143 (2015) 62–97

Contents lists available at ScienceDirect

Earth-Science Reviews

journal homepage: www.elsevier.com/locate/earscirev

Mediterranean climate and oceanography, and the periodic development of anoxic events (sapropels)

E.J. Rohling [a,b,*], G. Marino [a], K.M. Grant [a]

[a] Research School of Earth Sciences, The Australian National University, Canberra, ACT 2601, Australia
[b] Ocean and Earth Science, University of Southampton, National Oceanography Centre, Southampton, Hampshire SO14 3ZH, United Kingdom

ARTICLE INFO

Article history:
Received 17 June 2014
Accepted 23 January 2015
Available online 7 February 2015

Keywords:
Mediterranean
Sapropel
Organic carbon
Anoxic event
Monsoon
Deep-water renewal

ABSTRACT

Mediterranean sapropels are layers with elevated organic carbon concentrations that contrast with surrounding sediments, which are organic poor. Sapropels occur (quasi-) periodically in sedimentary sequences of the last 13.5 million years, and exist both in the eastern and western Mediterranean sub-basins. They have been the subject of extensive study, based on records from both short (conventional) and long (Ocean Drilling Program) sediment cores, and from a wide variety of uplifted marine sediment sequences on the basin margins and islands. Previous syntheses in the 1990s and 2000s have discussed how the formation of sapropels is commonly ascribed to deep-sea anoxia, enhanced export productivity, or a combination of these effects. However, a wealth of new evidence and insights has emerged during the past 1–2 decades, based on traditional and novel proxy data as well as modelling, which has revealed intriguing new aspects and nuances to the reconstructed conditions. Hence, it is timely to present a new synthesis of current understanding of the processes behind the formation of sapropels, which have over the past decade also become a matter of commercial interest in sub-salt hydrocarbon exploration. In this review, we present a context of modern Mediterranean climate and oceanography, followed by an integrated assessment of the growing understanding of climatological and ocean circulation changes that were associated with sapropel deposition. We find that sapropels predominantly formed during (astronomically timed) episodes when climatic and oceanographic conditions and ecological responses broadly preconditioned the basin for sapropel deposition. There is strong correspondence with times of monsoon intensification, fuelling runoff from North Africa into the Mediterranean Sea, while preconditioning due to sea-level rise, and regional precipitation and runoff may have contributed as well. Within these broad episodes of surface buoyancy gain and resultant decline in deep-water ventilation, specific deposition under dysoxic, anoxic, or even euxinic conditions occurred within a clearly dynamic system that was characterised by complex spatial and depth-dependent patterns/gradients, with distinct temporal variability on (at least) decadal to centennial–millennial timescales. In the final section, we evaluate the implications of different modes of deep-water removal from silled basins, to investigate why sapropels are more frequently and often more intensely developed in the eastern Mediterranean than in the western Mediterranean.

Contents

---

* Corresponding author.
E-mail address: eelco.rohling@anu.edu.au (E.J. Rohling).

http://dx.doi.org/10.1016/j.earscirev.2015.01.008

1. Introduction

The Mediterranean Sea is a land-locked, semi-enclosed marginal sea of the Atlantic Ocean (Fig. 1) with a vigorous thermohaline circulation. This thermohaline circulation transforms relatively warm and fresh Atlantic surface waters that enter the basin through the Strait of Gibraltar into cooler and saltier waters that return to the North Atlantic at depth through the strait, and also maintains well-oxygenated conditions in the Mediterranean deep sea (e.g., Wüst, 1960; McGill, 1961; Wüst, 1961; Miller et al., 1970; Bryden and Stommel, 1984; Béthoux, 1989; Schlitzer et al., 1991; Zavatarelli and Mellor, 1995; Klein et al., 1999; Pinardi and Masetti, 2000; Roether and Well, 2001; Béranger et al., 2005, 2010; Rogerson et al., 2012a; Pinardi et al., in press; and references therein). Meridionally, the basin spans a maximum of ~3860 km, and zonally it spans a maximum of ~1600 km; its surface area is ~2,500,000 km^2 (Fig. 1). Despite this limited size, the Mediterranean represents an exceptionally complex marine environment, and this combination has stimulated intensive research of a wide variety of modern physical and biogeochemical processes, and their interactions (among many others: Wüst, 1961; MEDOC group, 1970; Miller et al., 1970; Roether et al., 1983; Malanotte-Rizzoli and Hecht, 1988; POEM group, 1992; Samuel et al., 1999; Send et al., 1999; Pinardi and

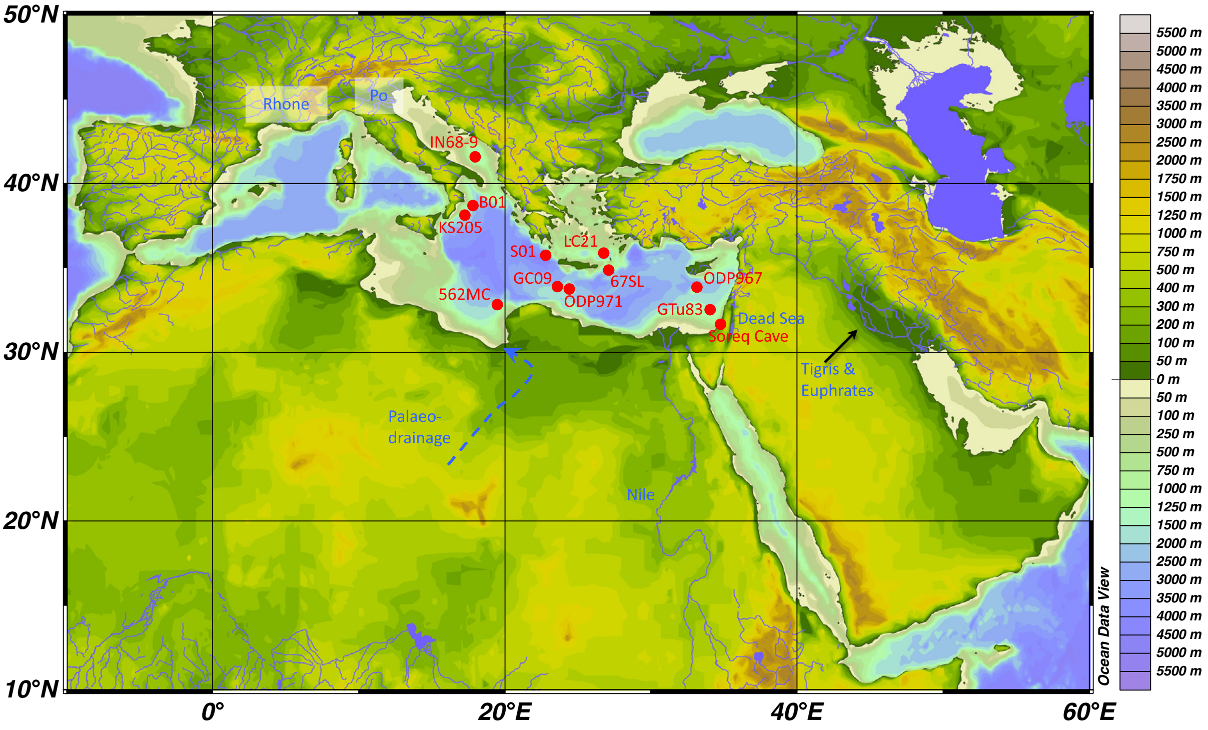

Fig. 1. Topographic map of the wider Mediterranean region (generated with Ocean Data View; Schlitzer, 2014). Blue names indicate main rivers and (palaeo-)drainage systems. Red dots indicate main study sites mentioned in this review: IN68-9 (Rohling et al., 1997); B01 (short for BD02-GC01; Morigi, 2009); KS205 (Rohling et al., 2002b, 2004); 562MC (Casford et al., 2003); S01 (short for SIN97-GC01; Capotondi et al., 2006; Morigi, 2009); GC09 (short for BAN89-GC09; Morigi, 2009); ODP971 (A and C; Kemp et al., 1999; Rohling et al., 2002b, 2004, 2006; Marino et al., 2007); LC21 (Casford et al., 2002; Rohling et al., 2002a; Casford et al., 2003; Rohling et al., 2004; Casford et al., 2007; Marino et al., 2007; Abu-Zied et al., 2008; Osborne et al., 2010; Grant et al., 2012); 67SL (short for M40-4/67SL; Schmiedl et al., 2003); ODP967 (Emeis et al., 1998; Rohling et al., 2002b, 2004); GTu83 (short for GeoTüKL83 (Schmiedl et al., 2003); Soreq Cave (Bar-Matthews et al., 1999, 2000, 2003; Grant et al., 2012). To avoid clutter, major basins are named in Fig. 3.

Masetti, 2000; Hecht and Gertman, 2001; Roether and Well, 2001; MEDAR group, 2002; Theocharis et al., 2002; Ribera d'Alcalà et al., 2003; Béthoux et al., 2005; Millot and Taupier-Letage, 2005; MerMex Group, 2011; Pinardi et al., in press). In addition, these attributes have allowed intensive research into the nature and development of past episodes of deep-sea oxygen starvation and attendant organic carbon accumulation in sediments, both in the eastern and (less frequently) in the western Mediterranean basins, which are divided by the Strait of Sicily (Olausson, 1961; Cita and Grignani, 1982; Rossignol-Strick, 1985; Mangini and Schlosser, 1986; Emeis et al., 1991; Rohling, 1994; Cramp and O'Sullivan, 1999; Rohling and Thunell, 1999; Emeis et al., 2003; Meyers, 2006; De Lange et al., 2008; Emeis and Weissert, 2009; Rohling et al., 2009). These episodes resulted in the formation of so-called 'sapropels', which occurred (quasi-) periodically throughout (at least) the last 13.5 million years (Krijgsman et al., 1995; Lourens et al., 1996; Schenau et al., 1999; Sierro et al., 1999; Krijgsman et al., 2001; Hilgen et al., 2003).

Apart from forming a perfect mini-ocean laboratory for 'blue-skies' scientific process studies, there is a growing 'applied' interest in the Mediterranean as well, namely for sub-salt exploration by the petroleum industry (e.g., Farmer et al., 1996). Because of its accessibility, the Mediterranean geological history has been uniquely well researched (e.g., Krijgsman, 2002 and references therein), and delivers a detailed understanding of the processes behind organic-rich sediment accumulation in an evaporative marginal basin. This, in turn, can help advance understanding of the nature of subsalt resources in other regions, which are less accessible for mainstream research; e.g., the South Atlantic (with important subsalt plays offshore Brazil), the Red Sea, and the Gulf of Mexico.

Here we review the current state of knowledge about the development of sapropels in the Mediterranean Sea, beginning (Section 2) with a summary and update of a previous review of modern Mediterranean climate (Rohling et al., 2009). Starting from the same review, Section 3 greatly extends the discussion of subsurface circulation. There is particular emphasis on the nature of well-monitored deep-water circulation changes of the past three decades, because these provide important new information for use in palaeoreconstructions. Section 4 presents key characteristics of sapropels and their palaeoclimatological and palaeoceanographic relevance. This section assesses, updates, and extends arguments that were started in earlier reviews (Rohling and Hilgen, 1991; Rohling, 1994; Cramp and O'Sullivan, 1999; Rohling and Thunell, 1999; Emeis et al., 2000a; Meyers, 2006; Emeis and Weissert, 2009), and adds several critical new aspects. Finally, we account for an increasing focus on changes through time in the processes behind water-column stratification and deep-water removal from below sill depth in the western and eastern Mediterranean sub-basins (e.g., Stommel et al., 1973; Rohling, 1994; Béthoux and Pierre, 1999; Rogerson et al., 2008, 2012a; Grimm et al., submitted for publication). Different processes dominate in each sub-basin, due to differences in their water-column characteristics and in the exchange transports through the straits of Gibraltar and Sicily. Section 5 builds on recent work that explores some key implications of these concepts for palaeo-reconstructions.

2. Modern climate

2.1. Direct climatic influences

The typical present-day Mediterranean climate is characterised by warm and dry summers, and mild and wet winters. It results from the basin's location on the transition between the subtropical high-pressure belt over North Africa and the temperate westerlies over central and northern Europe (Boucher, 1975; Lolis et al., 2002) (Fig. 2). In summer, northward displacement of this transition causes drought over most of the Mediterranean, and especially in the south-eastern sector. The influences of Atlantic depressions may still reach the western Mediterranean, but only exceptionally penetrate the eastern Mediterranean (Rohling and Hilgen, 1991). In winter, southward displacement of the transition brings (especially the northern sector of) the Mediterranean under the influence of the temperate westerlies, with associated Atlantic depressions that track eastward over Europe.

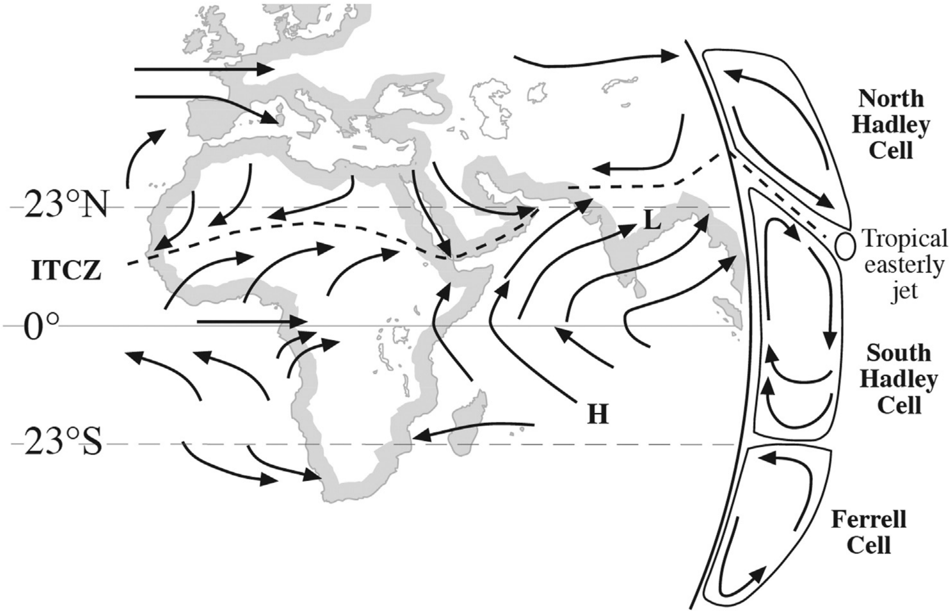

Fig. 2. Atmospheric circulation pattern during Northern Hemisphere summer. The main winds are indicated as arrows. ITCZ = Inter-Tropical Convergence Zone; H = areas of high sea-level pressure; L = areas of low sea-level pressure.
After Rohling et al. (2009).

Polar/continental air masses over Europe are channelled towards the Mediterranean through valleys that cross the mountain ranges of the northern Mediterranean margin. During winter and spring, intense cold and dry air flows thus affect the Gulf of Lions ('Mistral'), the Adriatic ('Bora'), and the Aegean Sea ('Vardar'), where they induce strong evaporation and cooling of the sea surface (e.g., Berenger, 1955; Leaman and Schott, 1991; Saaroni et al., 1996; Poulos et al., 1997; Maheras et al., 1999; Casford et al., 2003; and references therein). Winter-time northerly air flow into the western and eastern Mediterranean is governed by interaction between an intense Low over the warm central and eastern Mediterranean surface waters, and northeastward extension of the Azores High (over Iberia, France, and southern Britain) or westward ridging of the Siberian High towards northwestern Europe and southern Scandinavia (Maheras et al., 1999; Lolis et al., 2002). The most pronounced basin-wide cold winter events complement widespread cold conditions over Europe, associated with positive sea-level pressure anomalies to the west or northwest of the British Isles and particularly low pressure over the Mediterranean, a configuration that is suggested to reflect an extreme phase of the North Atlantic Oscillation (NAO) (Moses et al., 1987; Maheras et al., 1999). However, detailed climate reanalysis has identified the so-called "East Atlantic" and "East Atlantic/West Russian" modes as the main drivers for extensive heat loss from the (northern) Mediterranean Sea, with little direct impact from the NAO, especially in the east (Josey et al., 2011).

The main mode of climate variability in the Mediterranean is the so-called Mediterranean Oscillation (MO), a west–east pressure seesaw that is apparent both at the surface and at 500 hPa, especially in winter and spring (Maheras et al., 1999; Lolis et al., 2002). A statistical correlation has been inferred between the MO and the NAO, where the low NAO index phase is associated with wet conditions in the western Mediterranean (Maheras et al., 1999; Lolis et al., 2002; Dünkeloh and Jacobeit, 2003; and references therein). In the eastern basin, however, the relationship between local conditions and the NAO remains weakly established, except via dependence of the MO on the NAO (Dünkeloh and Jacobeit, 2003).

The second main mode of winter variability is the Mediterranean Meridional Circulation (MMC), with important influences on cyclogenesis (formation of new depressions) within the basin and consequent precipitation in the northeastern and south-central sectors (Dünkeloh and Jacobeit, 2003). Intense cyclogenesis in the northern sectors of the Mediterranean is driven by the invasion of cold and relatively dry northerly (meridional) air masses over warm sea surfaces. Most cyclones observed in the Mediterranean are thus formed over the basin itself, although some Atlantic depressions may enter the western basin (Rumney, 1968; Trigo et al, 1999).

After the Gulf of Genoa and Ligurian Sea in the western Mediterranean, the Aegean Sea, extending to the Cyprus area, forms another region of important winter cyclogenesis (Trewartha, 1966; Rumney, 1968; Boucher, 1975; Cantu, 1977; Trigo et al., 1999). Most Genoan depressions track southeastward down the coast of Italy and then eastward or northeastward across the Aegean Sea or northern Levantine Sea (Trewartha, 1966; Rumney, 1968; Trigo et al., 1999; Lolis et al., 2002). Along the way, both these depressions and those developing over other centres of cyclogenesis cause the modern Mediterranean's characteristic winter precipitation. The dominant contribution to this precipitation of moisture evaporated from the Mediterranean Sea itself is reflected by the precipitation's stable hydrogen and oxygen isotope composition, which follows a Mediterranean-specific mixing line (the Mediterranean Meteoric Water Line, MMWL), due to evaporation into low-humidity air masses (Gat and Carmi, 1970; Matthews et al., 2000; McGarry et al., 2004; Piccini et al., 2008; and references therein). Geological archives indicate that Mediterranean depressions have controlled Mediterranean climate in the Levant as an enduring feature over glacial–interglacial timescales (Goodfriend, 1991; Matthews et al., 2000; Bar-Matthews et al., 2003; McGarry et al., 2004; Rohling, 2013; and references therein).

Today, summer rainfall is low, especially in the eastern basin. Steady, dry, northwesterly winds (the 'Etesians'; Mariolopoulos, 1961; Furlan, 1977) develop over southeastern Europe down to the Levantine area, due to development of a thermal low-pressure extension of the Asiatic monsoon low over the Iranian Plateau (Goldsmith and Sofer, 1983). Some cyclogenesis occurs around Cyprus and the Middle East in summer, but dry summer conditions are maintained by adiabatic descent in the upper troposphere associated with the Asian summer monsoon (Rodwell and Hoskins, 1996; Trigo et al., 1999; Raicich et al., 2003; Ziv et al., 2004).

Mean annual precipitation over the Mediterranean ranges from less than 12.5 cm in North Africa, to over 200 cm in portions of southwest Turkey and in the eastern Adriatic Sea along the slopes of the Dinaric Alps (Naval Oceanography Command, 1987). Total evaporation increases towards the east over the basin, with estimated averages of 1.45 m y^{-1} (Malanotte-Rizzoli and Bergamasco, 1991) and 1.36–1.57 m y^{-1} (Béthoux et al., 1990; Béthoux and Gentili, 1994). Recent compilations report ranges for evaporation and precipitation of 0.92–1.57 m y^{-1}, and 0.26–0.70 m y^{-1}, respectively (Adloff et al., 2011; Criado-Aldeanueva et al., 2012). Enhanced rates of evaporation occur in areas subjected to strong winds, such as the Gulf of Lions and Ligurian Sea, the Aegean and Cretan Seas, and the southern part of the Turkish coast (MEDOC Group, 1970; Miller, 1974; Pinardi and Masetti, 2000; Josey et al., 2011; Pinardi et al., in press). Prevalence of relatively humid Atlantic air masses causes relatively weak evaporation along the Moroccan and Algerian coasts (the Alboran Sea), which is reflected in regionally low latent heat loss (Criado-Aldeanueva et al., 2012).

The overall Mediterranean excess of evaporation over freshwater input [$X = E$ (evaporation) $- P$ (precipitation) $- R$ (runoff)] has been estimated at ~1.0 m y^{-1} (Béthoux et al., 1999), 0.75 m y^{-1} (Gilman and Garrett, 1994), or 0.56–0.66 m y^{-1} (Bryden and Kinder, 1991), or between 0.42 and 1.23 m y^{-1} (Criado-Aldeanueva et al., 2012). Northern areas such as the Gulf of Lions, Adriatic and Aegean Seas show relatively low X values due to high freshwater inputs from the Rhone and Ebro rivers, the Po river, and the Black Sea, respectively. Southern regions show high X values, especially in the eastern Mediterranean (Béthoux and Gentili, 1994). Strong overall excess evaporation causes a pronounced west–east increase in surface water salinity (e.g., Wüst, 1960, 1961; MEDATLAS, 1997; MEDAR Group, 2002; Béranger et al., 2004; Adloff et al., 2011; Mikolajewicz, 2011).

The balance between solar irradiation during widespread subtropical high-pressure (clear) conditions in summer, and considerable (latent) heat loss during evaporation gives rise to an overall increase in Mediterranean sea surface temperature (SST) towards the east and south. In summer, SST ranges from ~21 °C in the northwest to ~26 °C in the southeast, and in winter SST ranges from ~10 °C in the northwest to 15–16 °C in the southeast (Naval Oceanography Command, 1987).

2.2. Indirect climatic influences: the African monsoon

The Mediterranean Sea is affected by the African monsoon, although this system does not itself penetrate into the basin. Prior to completion of the Aswan High Dam in 1964, the African monsoon caused extensive Nile River discharge into the Mediterranean. It averaged 8.4×10^{10} m^3 yr^{-1} (4.5×10^{10} m^3 yr^{-1} in low-flood years to 15.0×10^{10} m^3 yr^{-1} in high-flood years) and has dwindled to a negligible amount since the mid-1960s (Nof, 1979; Said, 1981; Wahby and Bishara, 1981; Béthoux, 1984; Rohling and Bryden, 1992).

Strong interannual variability between high and low discharge years in pre-1964 instrumental records resulted mainly from variations in the monsoon-fed contribution of the Blue Nile/Atbara rivers, which drain highly seasonal African monsoon precipitation from the Ethiopian highlands. Conversely, the White Nile drains the equatorial uplands of Uganda in a more regular and permanent manner. Based on a summary of Nile hydrology by Adamson et al. (1980) and Williams et al. (2000), at least 70% of the annual Nile discharge (prior to damming) originated from the Blue Nile/Atbara, and at most 30% from the White Nile. Historical discharge values (Hurst, 1944; Said, 1981) indicate that the White Nile contributed only 14% of the total annual discharge (see Table in Rohling et al., 2009). Seasonally, the monsoon-fed Blue Nile/Atbara provided 90% of the summer flow of the Nile (peak in August–October), while winter flow was dominated (83%) by the White Nile (little variation between peak and lowest monthly values, with a weak maximum between late September and January) (Adamson et al., 1980; Williams et al., 2000).

Before damming, the Nile plume used to be distinctly traceable with the prevailing surface circulation in the easternmost Mediterranean, causing a zone with notably reduced surface-water salinities and enhanced turbidity (suspended matter) from the Nile delta east- and northward along the eastern Levantine coast (Reiss et al., 1999; Hecht and Gertman, 2001). Anthropogenic control has severely reduced both Nile discharge and its associated sediment transport (cf., Sharaf El Din, 1977; UNDP/UNESCO, 1978; El Dardir, 1994; Stanley, 1996; Stanley et al., 1998). Damming of the Nile in combination with that of major rivers draining into the Aegean Sea via the Black Sea may have played an important role in the distinct increase of eastern Mediterranean salinities over the last 40–50 years, with associated impacts on the processes of deep-water formation (e.g., Rohling and Bryden, 1992; Boscolo and Bryden, 2001; Skliris and Lascaratos, 2004; Skliris et al., 2007).

3. Modern circulation in the Mediterranean Sea

3.1. Modern surface-water circulation

Circulation in the Mediterranean Sea results from wind stress and thermohaline forcing (POEM Group, 1992) (Fig. 3). Large net evaporative loss from the basin and subsurface saline outflow through the Strait of Gibraltar drive a compensatory surface inflow of Atlantic water (AW) through that strait. With 1 Sv being 1×10^6 m^3 s^{-1}, estimated inflows are 0.92 Sv (Bryden and Kinder, 1991), ~0.8 Sv (Béranger et al., 2005), or 0.82 ± 0.05 Sv (Criado-Aldeanueva et al., 2012). AW enters the Alboran Sea as a jet with velocities in excess of 1 m s^{-1} (Béranger et al., 2005). As AW enters through the Strait of Gibraltar with S = ~36 and T = ~16 °C (Stommel et al., 1973; Kinder and Parrilla, 1987; Bryden and Kinder, 1991; Béthoux and Gentili, 1994; Bryden et al., 1994; Béranger et al., 2005), it mixes with upwelled Mediterranean Intermediate Water (MIW), creating Modified Atlantic Water (MAW) with higher salinities (36.5‰) (La Violette, 1986; Tintoré et al., 1988; Arnone et al., 1990; Heburn and La Violette, 1990).

Within the Alboran Sea, MAW hugs the Spanish coast in a 20 km wide and 150 m deep jet (Pistek et al., 1985) that initiates two fluctuating anticyclonic gyres (Heburn and La Violette, 1990). Near Almeria (Spain, eastern Alboran Sea), MAW converges with resident Mediterranean waters and deflects towards Oran (Algeria), forming a distinct front (~35 km wide, 200 m deep; Cheney and Doblar, 1982), whose position and intensity depend on the degree of development of the Eastern Alboran Gyre (Tintoré et al., 1988).

Upon exit from the Alboran Sea, MAW splits into a northward flow towards Ibiza, and an eastward flow along the African coast (Pinardi et al., in press). Northward flows through the Tyrrhenian Sea join northern cyclonic gyres in the Gulf of Lions, where Mistral winds in winter initiate the formation of Western Mediterranean Deep Water (WMDW) (e.g., MEDOC group, 1970; Gascard, 1978; Leaman and Schott, 1991; Robinson and Golnaraghi, 1994; Rohling et al., 1998; Send et al., 1999; Pinardi and Masetti, 2000; Smith et al., 2008; Pinardi et al., in press). Eastward flowing MAW passes through the Strait of Sicily into the eastern Mediterranean (e.g., Wüst, 1960; POEM group, 1992; Pinardi and Masetti, 2000; Hecht and Gertman, 2001; Stansfield et al., 2003; Pinardi et al., in press).

In the Strait of Sicily, MAW salinity ranges between 37.0 and 38.2, with a core salinity of 37.5 (Stansfield et al., 2003) (Figs. 3, 4). The level of observed zero cross-transect velocity has a mean salinity of 38.2 (Stansfield et al., 2003), slightly lower than earlier estimates of 38.5 for the flow reversal boundary (Garzoli and Maillard, 1979). Béranger et al. (2005) infer – from Herbaut et al. (1998) – that the major forcing of exchange through the Strait of Sicily is the transport of Atlantic Water from the Atlantic Ocean, rather than the density gradient between the western and eastern Mediterranean.

Once in the eastern Mediterranean, MAW feeds the Ionian Current and the 'Mid-Mediterranean Jet' (MMJ) through the Ionian Sea and Levantine Basin, respectively (POEM-group, 1992). One branch flows to Cyprus and then north- and westward to become the Asia Minor Current. Along its eastward path, MAW salinity increases steadily up to 39.0–39.6 (Wüst, 1961; Malanotte-Rizzoli and Hecht, 1988; Hecht and Gertman, 2001; Theocharis, 2009). Model results of Mikolajewicz (2011) capture the MMJ well, but Béranger et al. (2005) emphasise that high-resolution modelling (Alhammoud et al., 2005) and satellite data (Marullo et al., 1999; Hamad et al., 2005) question its existence as a discrete entity. Instead, they argue that it appears (statistically) as an expression of the northern limit of anticyclonic eddies/gyres associated with the southern coastal current (also Pinardi et al., in press).

3.2. Modern intermediate-water circulation

In winter, surface waters in the Levantine Basin experience enhanced mixing and evaporation due to strong winds associated with the flow of cold, dry air masses over the eastern Mediterranean (Ozsoy, 1981), especially in the Cyprus-Rhodes area. This leads to low surface-water temperatures (15–16 °C) and high salinities (39.0–39.2; Wüst, 1960; Malanotte-Rizzoli et al., 1999; Hecht and Gertman, 2001; Painter and Tsimplis, 2003; Béranger et al., 2010) (Fig. 3), which favour vertical convection and the consequent formation of Levantine Intermediate Water (LIW), and occasionally also of Levantine Deep Water (Theocharis, 2009; Pinardi et al., in press). The LIW salinity maximum can be traced – with modification due to mixing and entrainment of ambient waters – throughout the eastern and western Mediterranean basins, where it is sometimes referred to as Mediterranean Intermediate Water (MIW) (Fig. 4). There is no comparable major source region for intermediate water formation in the western Mediterranean basin, although some Winter Intermediate Water is formed due to moderate winter cooling of the surface layer within the western Mediterranean, which is insufficient to cause mixing with the high-salinity LIW (Send et al., 1999). In the open eastern Mediterranean, LIW resides between ~150 and ~600 m water depth, and is separated from overlying MAW by a distinct salinity gradient, or halocline (Fig. 4).

As LIW flows westward from its source area and approaches the Strait of Sicily, some is re-circulated back into the eastern basin (where it helps to precondition Eastern Mediterranean Deep Water formation; Wu and Haines, 1996), while the rest continues to enter the Western Mediterranean basin. The ratio of re-circulation to efflux remains to be established (POEM-group, 1992). At the Strait of Sicily, LIW temperature (14.0–14.3 °C) and salinity (38.73–38.78) are reduced relative to values in the LIW source area, due to admixtures along its path (e.g., Garzoli and Maillard, 1979; Malanotte-Rizzoli et al., 1997; Stansfield et al., 2003).

About 1 Sv of LIW exits from the Strait of Sicily at a mean velocity of ~0.2 m s^{-1} (Stansfield et al., 2003; Béranger et al., 2004, 2005). Notably since the late 1980s to early 1990s change in eastern Mediterranean deep-water ventilation, known as the Eastern Mediterranean Transient (EMT; see Section 3.3.1), this outflow has contained components of Eastern Mediterranean Deep Water (EMDW, see Section 3.3.1) that originate from depths of ~800 m in the eastern Mediterranean. Upon entry into the western Mediterranean, these deep-water components cascade to depths as great as ~2000 m in the Tyrrhenian Sea, while mixing with ambient Western Mediterranean Deep Water (WMDW, see Section 3.3.2) to produce Tyrrhenian Deep Water, or TDW (e.g., Astraldi et al., 1999; Millot, 1999; Astraldi et al., 2001; Béranger et al., 2005; Gasparini et al., 2005; Millot et al., 2006; García Lafuente

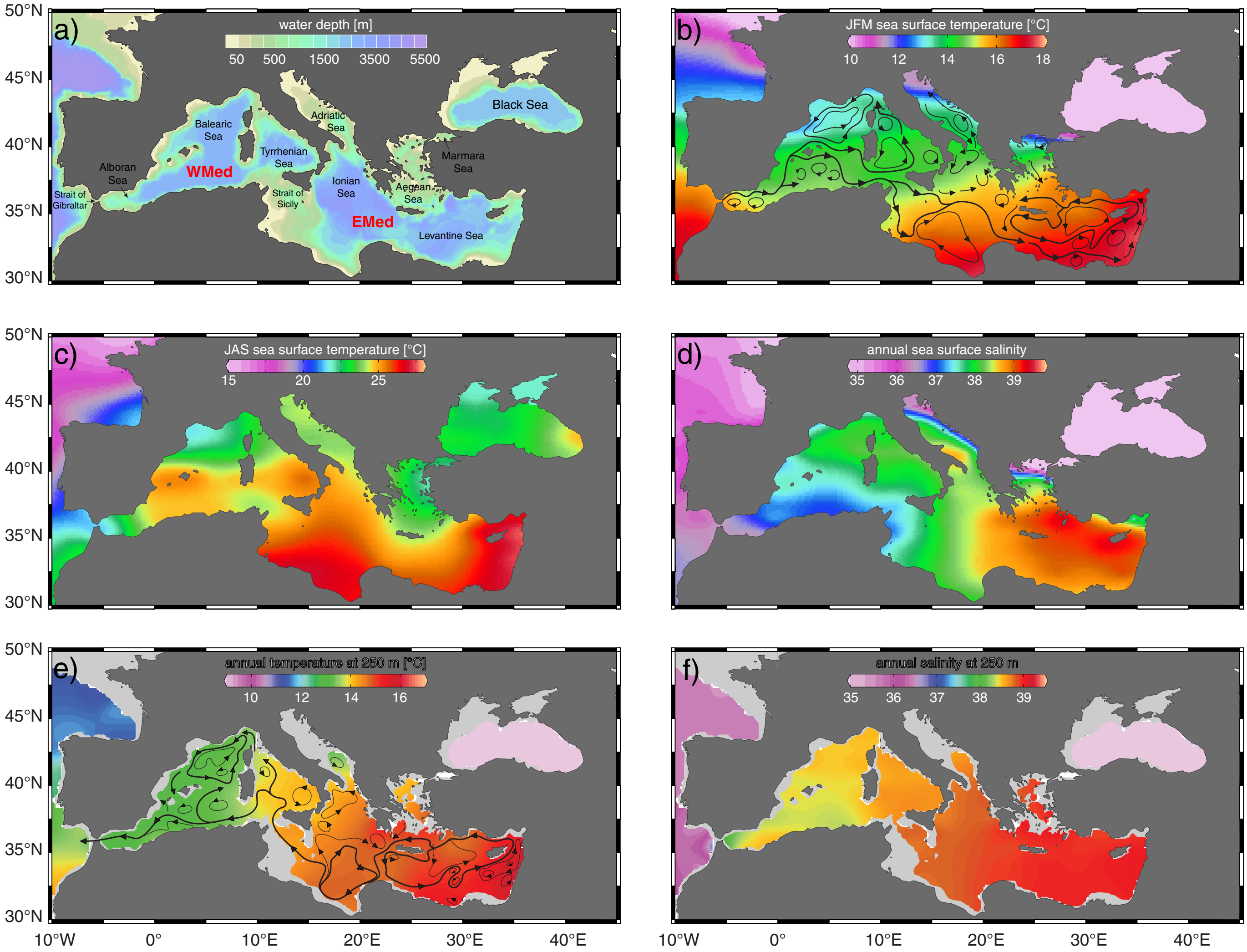

Fig. 3. Key features of the Mediterranean. a. Bathymetric map with most important geographic names. b. Winter sea surface temperature distribution (Locarnini et al., 2010) and schematic surface circulation pattern (arrows, Pinardi et al., in press). c. Summer sea surface temperature distribution (Locarnini et al., 2010). d. Annual sea surface salinity distribution (Antonov et al., 2010). e. Annual temperature distribution at 250 m and schematic circulation pattern of LIW (arrows, Pinardi et al., in press). f. Annual salinity distribution at 250 m (Antonov et al., 2010). Plots were generated with Ocean Data View (Schlitzer, 2014).

et al., 2007; Millot, 2009). TDW was found in the western Mediterranean below LIW, down to ~1800 to ~2000 m, overlying 'proper' WMDW (Send et al., 1999; Millot et al., 2006). Meanwhile, LIW itself settles to depths between ~200 and ~700 m, and is distributed throughout the western Mediterranean, until its exit through the Strait of Gibraltar into the North Atlantic (e.g., Wüst, 1960; Send et al., 1999; Pinardi and Masetti, 2000; Pinardi et al., in press). LIW occupies the Alboran Sea between ~200 and ~600 m depth, with a temperature of 13.1–13.2 °C and salinity of ~38.5 (Fig. 4), flowing westward towards the Strait of Gibraltar at velocities of 1–2 cm s^{-1} (e.g., Parrilla et al., 1986; Richez and Gascard, 1986; Kinder and Parrilla, 1987).

The subsurface Mediterranean Outflow through the Strait of Gibraltar has a temperature of ~13 °C and salinity of ~38.5, while the surface (AW) inflow is characterised by values of ~15–16 °C and 36.1–36.2 (e.g., Wüst, 1960, 1961; Gascard and Richez, 1985; Kinder and Parrilla, 1987; Bryden et al., 1994; García Lafuente et al., 2007; Rogerson et al., 2012a). This highlights that the Mediterranean experiences both net evaporation and net cooling (Garrett, 1994), and the resulting density difference between the Mediterranean and the Atlantic Ocean forces the Mediterranean Outflow (Bryden and Stommel, 1984; Bryden and Kinder, 1991; Garrett, 1996; Béranger et al., 2005), with a flux of 0.7–1.0 Sv (e.g., Bryden and Kinder, 1991; Send et al., 1999; Béranger et al., 2005) at mean velocities of ~1 m s^{-1} (e.g., Stommel et al., 1973; Tsimplis and Bryden, 2000; Béranger et al., 2005; García Lafuente et al., 2007). In detail, 4 or 5 recognisable water-masses may contribute to the total exchange through the Strait of Gibraltar (including TDW) (Millot, 2009, 2014). Today, the core of Mediterranean Outflow reaches ~800 m depth in the North Atlantic Ocean, and its deepest influences reach ~1700 m (e.g., Wüst, 1960; Stommel et al., 1973; Reid, 1979; Price et al., 1993; O'Neill-Baringer and Price, 1999; Rogerson et al., 2012a,b).

3.3. Modern deep-water circulation

The western and eastern Mediterranean basins each have their own source of deep water, which settles below LIW. Eastern Mediterranean Deep Water (EMDW) is formed in the Adriatic and Aegean Seas, and Western Mediterranean Deep Water (WMDW) in the northern sector of that basin, notably the Gulf of Lions. All processes of deep-water formation to some extent involve LIW. As a result, all Mediterranean water masses are closely related, so that significant modification to one will also affect the others. The freshwater flux through the Mediterranean Sea surface thus is a key control on the exchange between the Atlantic and the Mediterranean (Béranger et al., 2005).

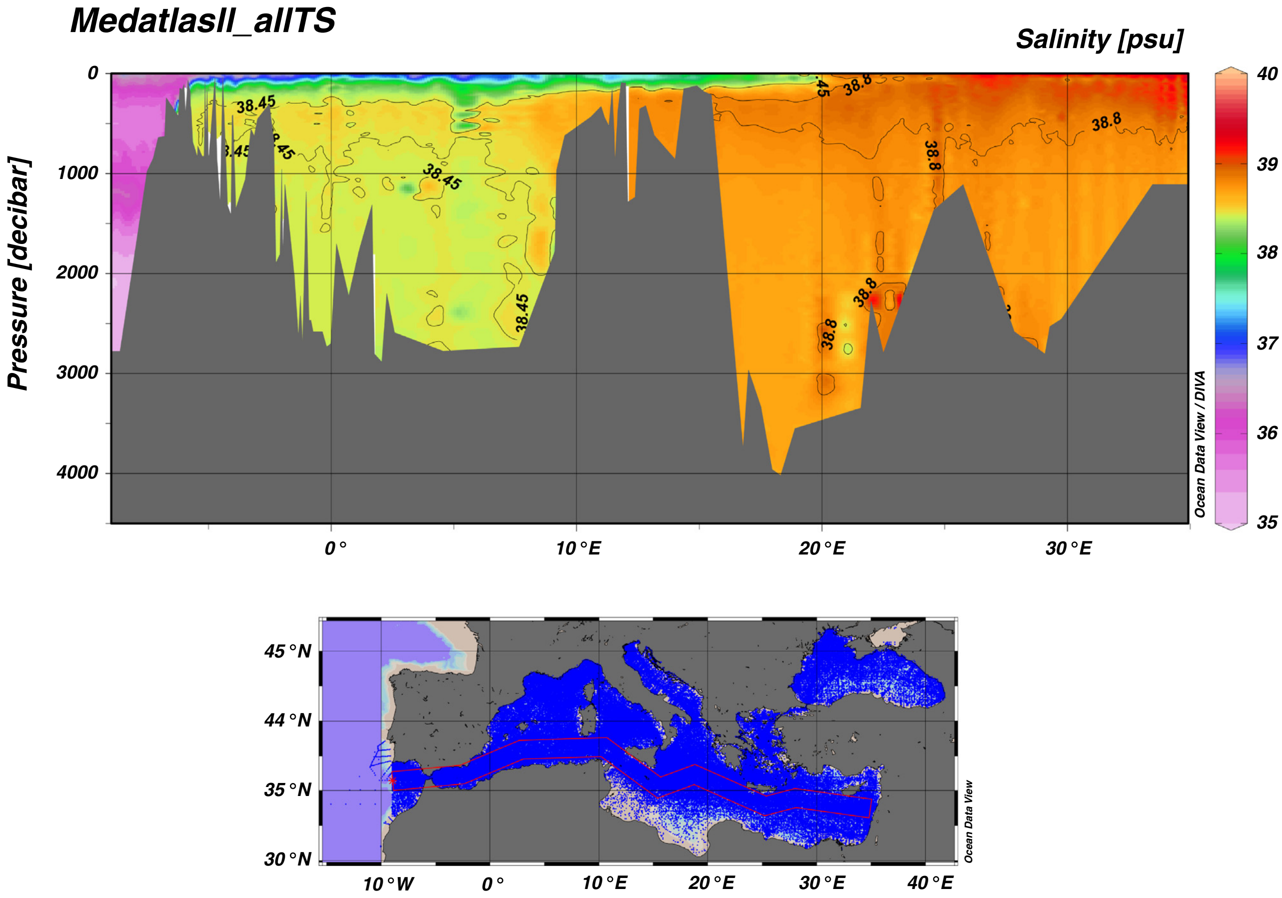

Fig. 4. Salinity profile from West to East through the Mediterranean Sea. Apart from the colour coding, two isohalines (38.45 and 38.80) have been contoured to best illustrate patterns of change. The inset map shows hydrographic stations in the basin (blue, after MEDAR group, 2002) and the 150 km wide transect for which data is assimilated into the profile (red). Plotted with Ocean Data View (Schlitzer, 2014).

Consistent deep-water ventilation from the aforementioned regions ensures that both the eastern and western Mediterranean are filled with well-oxygenated deep and bottom waters, with oxygen concentrations in the range 4.0–4.7 ml l^{-1} or 180–210 μmol kg^{-1} (Wüst, 1960; McGill, 1961; Miller et al., 1970; Béthoux, 1989; Schlitzer et al., 1991; Klein et al., 1999; Roether and Well, 2001). Mean rates of EMDW and WMDW formation used to be similar, at ~0.3 Sv each, compared with LIW formation at ~1–1.5 Sv (Lascaratos, 1993; Theocharis, 2009), yielding deep-water renewal times of 100 ± 20 years (Theocharis, 2009). CFC and oxygen-based estimates suggest 84 years (Schlitzer et al., 1991) and 150 years (±30%) (Roether and Well, 2001) for the eastern Mediterranean. Although higher than earlier deep-water residence-time estimates of ~20 years and ~50 years for the western and eastern Mediterranean, respectively (Béthoux et al., 1990), these numbers still imply highly efficient deep-water ventilation in both basins. Below, EMDW formation and WMDW formation are discussed in more detail.

3.3.1. Eastern Mediterranean Deep Water (EMDW)

Until 1987, the Adriatic Sea was the dominant source area of EMDW formation (Pollak, 1951; Wüst, 1961; Malanotte-Rizzoli and Hecht, 1988; POEM-group, 1992; Theocharis, 2009). Winter-time cold and dry north-easterly winds (Bora) cause intense cooling of the North Adriatic shelf waters, which have relatively low salinities due to dilution with Po river discharge (Ozsoy, 1981). These cold waters flow towards the deep South Adriatic Basin, where they mix with warmer but more saline LIW that penetrates the South Adriatic across the Otranto Sill. The mixing of cold and relatively low-salinity shelf waters with warm and highly saline LIW results in the formation of Adriatic Deep Water (ADW). Although ADW has a lower salinity ($S < 38.7$) than LIW, it is also cooler, between 13.0 and 13.6 °C. The resultant higher density of ADW allows it to settle below LIW, reaching (until the late 1980s–early 1990s) down to the greatest depths of the eastern Mediterranean basin and becoming a major component of EMDW. EMDW circulates in a deep western boundary current through the Ionian Sea before entering into the Levantine Basin (POEM-group, 1992). A 22-box model for the deep-water flow in the Ionian and Levantine basins by Roether and Schlitzer (1991) suggests that the eastern Mediterranean thermohaline circulation at that time consisted of a single vertical cell through both basins, driven by Adriatic deep-water formation. The inferred rate of deep-water supply from the Adriatic Sea into the eastern Mediterranean was 0.29 Sv and the turn-over time about 126 years (POEM-Group, 1992).

In contrast to the Adriatic, the importance of the Aegean Sea as a contributor to EMDW ventilation used to be strongly debated. Pollak (1951) argued that the Adriatic was the only significant source region. Wüst (1961) found the Aegean role to be minor but not negligible, and Miller (1963) observed that Aegean Deep Water (AeDW) formed sporadically in the Aegean Sea before flowing into the Levantine Basin via the Kasos and Karpathos Straits, contributing to EMDW. However, Roether et al. (1983) concluded from ^{3}H and ^{3}He data that eastern Mediterranean bottom waters were formed exclusively in the Adriatic. Then the debate changed completely, as observations from *RV Meteor* cruise M31-1 (January–February 1995) revealed that an influx of Aegean Sea water had replaced approximately 20% of the deep and bottom waters of the eastern Mediterranean, strongly enhancing deep/bottom-water salinities and displacing older waters upwards (Roether et al., 1996). Aegean Sea outflow contributed up to 65% of eastern Mediterranean deep and bottom water formation (Roether et al., 1996). This change has become known as the Eastern Mediterranean Transient (EMT), and is discussed in more detail at the end of this section.

As with ADW formation, the formation of Aegean Deep Water (AeDW) is again closely related to the influences of salty LIW. To understand this, some key features of the Aegean circulation must be considered. A generally cyclonic circulation prevails in the Aegean Sea, albeit fragmented by the complex topography. This circulation is mainly controlled by the regional climate, local riverine inputs that occur predominantly in winter, and the Black Sea surface-water outflow that increases in summer (Poulos et al., 1997). The relatively fresh Black Sea outflow plume from the Dardanelles flows westward and southward along the northern and western margins of the Aegean Sea, respectively. Salty northward flow from the Levantine basin is focussed along the eastern margin of the Aegean Sea. Aegean surface temperatures vary from less than 13 °C in winter to more than 24 °C in summer, and salinities from less than 31 to more than 39 (Poulos et al., 1997). Locally, salinity minima around 26 may be reached in summer, as a result of Black Sea outflow (Yüce, 1995). As the LIW-derived Aegean Intermediate Water (AeIW) travels northward along the Turkish coast, prevailing offshore winds cause upwelling to the surface (Lascaratos, 1989; Yüce, 1995). In shallow eastern shelf areas, AeIW consequently forms a single uniform water-mass from surface to sea floor. Exposed at the surface, upwelled AeIW is directly affected by the regional climate as it travels northward. During winter, it is (along with the entire Aegean Sea surface) exposed to cold and dry northerly outbreaks of polar/continental air masses, which cause strong surface buoyancy loss through cooling and evaporation (Theocharis and Georgopoulos, 1993). This drives formation of AeDW, mainly in the Cretan Sea (southern Aegean), which fills the Aegean Basin below 300 m (Bruce and Charnock, 1965; Burman and Oren, 1970; Miller et al., 1970; Miller, 1972; Theocharis, 1989; Yüce, 1995).

Starting at ~1990 and peaking in 1992–1994, the EMT was marked by formation of unusually dense, saline waters in the Aegean Sea (Roether et al., 1996; Klein et al., 1999; Lascaratos et al., 1999; Malanotte-Rizzoli et al., 1999; Samuel et al., 1999; Schröder et al., 2006; Font et al., 2009; Pinardi et al., in press). The existing, older, deep waters in the open eastern Mediterranean – which were of Adriatic origin – were uplifted by the higher-salinity AeDW influx (e.g., Schröder et al., 2006; Theocharis, 2009). At its peak, the AeDW formation rate reached about 1 Sv (Theocharis, 2009; Pinardi et al., in press). The EMT is thought to have decayed from 1995, with reduction of AeDW flux and penetration to no more than 1500–2000 m in the open eastern Mediterranean (Theocharis et al., 2002; Theocharis, 2009), until the outflow had ceased in 2002 (Theocharis, 2009). A recent re-analysis, however, suggests that the cessation was more abrupt after 1996 (Pinardi et al., in press), when the Adriatic resumed its role as main deep-water supplier to the eastern Mediterranean (Klein et al., 2000) with reinstatement of deep convection by 2002 (Roether et al., 2007) or even earlier in 1999–2000 (Manca et al., 2006).

The EMT was superimposed upon a longer-term trend of progressive salinification in the eastern Mediterranean, which has been (partly) ascribed to progressive damming of major river inputs into the basin (Rohling and Bryden, 1992; Boscolo and Bryden, 2001; Skliris and Lascaratos, 2004; Skliris et al., 2007). Boscolo and Bryden (2001) reason that this trend may have provided sufficient preconditioning for development of the EMT given one or two severe winters over the Aegean (see also Theocharis, 2009), while Skliris and Lascaratos (2004) and Skliris et al. (2007) propose that it also accounts for a large portion of the eventual salinity increase in WMDW (see below). Malanotte-Rizzoli et al. (1999) argue that development towards the EMT involved strong preconditioning of the Cretan/Aegean Sea through invasion of salty LIW from the northern Levantine Sea. The actual trigger for the EMT has been related to a period of anomalously strong Aegean heat loss (Josey, 2003; Josey et al., 2011).

The EMT also affected the properties of outflow from the eastern into the western Mediterranean. Given that the base of LIW in the open eastern Mediterranean lies at 500–600 m depth, the underlying deeper waters remain considerably below the maximum depth of the Strait of Sicily (deepest channels at ~430 m and ~360 m; Garzoli and Maillard, 1979; Astraldi et al., 2001; Stansfield et al., 2003; Béranger et al., 2004). Outflow through the strait from the eastern to the western Mediterranean is restricted to levels below roughly 200 m, at a rate of ~1 Sv and mean velocities of ~0.2 m s^{-1} (Stansfield et al., 2003; Béranger et al., 2004, 2005). Such low velocities do not generate much Bernoulli aspiration over the sill(s).

Stommel et al. (1973) argue that, for the Strait of Gibraltar, a maximum aspiration depth of ~1400 m would apply if outflow velocities were ~0.2 m s^{-1} (but note that observed velocities are much higher in that strait; see Sections 3.2 and 5). Density stratification below sill depth is stronger in the eastern Mediterranean (~0.03 kg m^{-3}) than in the western basin (~0.02 kg m^{-3}) (Astraldi et al., 1999, 2001), so that ~1000 m may be a decent first estimate for the maximum Bernoulli aspiration depth for the Strait of Sicily, in agreement with findings that the 'upper layer pressure gradients … raise the [deeper-water] vein from ~800 m depth' (Astraldi et al., 2001). In addition, sloping of isopycnals along the basin margins, associated with large-scale circulation, brought deep water in closer proximity to the sill depth (Gasparini et al., 2005). Combined, these effects provided a mechanism for escape of deeper waters from the eastern Mediterranean, but only for those 'uplifted' or gradually mixed to depths close to ~800 m. Emplacement of dense, new deep/bottom waters (AeDW) lifted the core of old, pre-EMT, Adriatic deep water up to 800–1200 m (Theocharis, 2009), from where it could feed the EMDW vein that became aspired over the sill in the Strait of Sicily, and which upon its exit into the western Mediterranean basin fed a deep-water cascade in the Tyrrhenian Sea (e.g., Astraldi et al., 2001; Gasparini et al., 2005; Schröder et al., 2006). Thus, the EMT signal reached the Tyrrhenian entrance from April–May 1992, and its impact on the western basin peaked in 1992–1994, when a great proportion of strait outflow sank into the deep Tyrrhenian basin, until a 'recovery' to pre-transient conditions in 2001 (Gasparini et al., 2005)

3.3.2. Western Mediterranean Deep Water (WMDW)

The Gulf of Lions is the key area for winter-time (January/February) WMDW formation, initiated by outbreaks of the cold and relatively dry Mistral. Deep convection within the western Mediterranean is intermittent and may not occur every year (Marshall and Schott, 1999; Smith et al., 2008). Some studies have also reported WMDW formation under extreme climate forcing outside the Gulf of Lions (Smith et al., 2008). Generally, three phases are distinguished in the formation of WMDW: (1) a preconditioning phase, (2) a violent mixing phase and (3) a sinking and spreading phase (e.g., MEDOC-group, 1970; Send et al., 1999; Smith et al., 2008. For schematic diagrams, see Rohling et al., 1998, 2009).

The preconditioning phase comprises reduction in the water-column stability due to winter cooling, which generates surface waters of low temperatures (10–12 °C) at salinities of ~38.40 (Wüst, 1961; MEDOC-group, 1970; Leaman and Schott, 1991). The vertical hydrographic profile remains organised in three layers: (1) a relatively fresh and cold surface layer, (2) a warm and saline intermediate layer and (3) a cold and medium-saline deep layer. The onset of strong north-westerly 'Mistral' winds intensifies cyclonic circulation (MEDOC-group, 1970; Smith et al., 2008), and associated Ekman pumping drives a shallowing of the pycnocline between surface and intermediate waters, from its usual depth of approximately 200–250 m (Perkins and Pistek, 1990) to <100 m (see Rohling et al., 1995).

Then follows a violent mixing phase. Cooling and intense evaporation (2 cm day^{-1}; MEDOC-group, 1970) throughout February eliminate the gradient between surface and intermediate waters. This creates favourable conditions for development of 'chimneys' or 'plumes' of convective mixing within the gyre centre, which reach throughout the water column to great depths (>2000 m) (MEDOC-group, 1970; Leaman and Schott, 1991; Marshall and Schott, 1999; Smith et al., 2008). Although vertical velocities in these 'plumes' are high (up to 10 cm s^{-1}), there is zero net vertical transport, so that these areas act more like strong mixing elements (Schott and Leaman, 1991; Marshall and Schott, 1999; Smith et al., 2008).

The final phase commences as the stormy period ceases. It is marked by rapid sinking of the mixed water to form WMDW, which spreads horizontally between ~1500 and ~3000 m into the Balearic basin and Tyrrhenian Sea, with a relatively high oxygen content of 4.4–4.7 ml l^{-1} and seasonally even higher (e.g., Wüst, 1961; Béthoux, 1989). Once in the Alboran Sea, WMDW forms a narrow (~20 km) westward flowing boundary current along the Moroccan coast. Between the 'proper' WMDW and the base of LIW, the TDW has been recognised (see Section 3.2) (Send et al., 1999). TDW is thought to form a major portion of the densest waters involved in Mediterranean Outflow through the Strait of Gibraltar, which consequently – because of the Tyrrhenian cascade involving deep outflow from the Strait of Sicily – has a more 'eastern Mediterranean' origin than pure WMDW (e.g., Millot et al., 2006; Millot, 2009, 2014).

Deep-water formation in the northwestern Mediterranean was particularly active in the mid to late 2000s, and especially in the winters of 2004–05 and 2005–06 (Font et al., 2009). This resulted in the appearance and spreading of a new deep-water mass that was significantly warmer and saltier (and denser) than the older, resident deep waters, which it displaced upward throughout almost the entire western Mediterranean (e.g., Schröder et al., 2006, 2008; Smith et al., 2008; Bryden, 2009; Font et al., 2009; García Lafuente et al., 2009). This caused marked acceleration of an underlying, weaker, long-term trend towards warmer and more saline WMDW conditions (e.g., Béthoux et al., 1990; Leaman and Schott, 1991; Rohling and Bryden, 1992; Krahmann and Schott, 1998; Gasparini et al., 2005; Schröder et al., 2006). Some have ascribed the underlying long-term trend to progressive damming of major river inputs into the eastern Mediterranean (Rohling and Bryden, 1992; Boscolo and Bryden, 2001; Skliris and Lascaratos, 2004; Skliris et al., 2007), but – as with the EMT – the accelerated change in deep-water properties cannot be readily explained by just the long-term salinification trend. Conversely, accelerated eastern Mediterranean salt import due to the EMT would suffice (Schröder et al., 2006), possibly in combination with salinification of Atlantic inflow (Millot, 2007). Superimposed severe winter heat losses in 2004–05 and 2005–06 (Josey et al., 2011) then triggered formation of warmer and saltier WMDW, a change known as the Western Mediterranean Transient (WMT) (Font et al., 2009). At a mean of ~2.4 Sv for 2005 and 2006, formation rates of this new WMDW were almost an order of magnitude higher than formation rates in the 1990s (Schröder et al., 2008; García Lafuente et al., 2009). García Lafuente et al. (2007, 2009) noted impacts of this strong new WMDW formation in Mediterranean outflow through the Strait of Gibraltar, due to uplifting of older, cooler WMDW (also Bryden, 2009; Font et al., 2009) — cool pulses in the outflow were observed a few months after the deep-water formation events of 2005 and 2006.

With the base of LIW in the western Mediterranean at ~700 m, underlying TDW/WMDW (note that, from here on, we capture both under the WMDW label) remains well below the depth of the Camarinal Sill of the Strait of Gibraltar (284 m). Its contribution to Mediterranean Outflow therefore relies on a balance between Bernoulli aspiration over the sill and distributed vertical advection throughout the western Mediterranean into the overlying Intermediate Water (the main outflow component) (Stommel et al., 1973; Kinder and Parrilla, 1987; Bryden, 2009). Routines to quantify the maximum depth affected by Bernoulli aspiration have been presented by Stommel et al. (1973) and Seim and Gregg (1997); below this depth, no velocity is imparted on WMDW by aspiration and it has consequently become known as the 'stagnation depth'. In Section 5, we assess the implications of changes in this stagnation depth for preconditioning basins to sapropel formation, which highlights notable differences between the western and eastern Mediterranean basins.

4. Sapropels

4.1. Appearance, alterations, and duration

In marine cores, sapropels (cf., Kullenberg, 1952; Olausson, 1961; Cita et al., 1977; Ryan and Cita, 1977; Vergnaud-Grazzini et al., 1977; Kidd et al., 1978; Calvert, 1983; Vergnaud-Grazzini, 1985; Murat and Got, 1987) are recognisable as beds ranging in colour from dark grey to olive green and black (Fig. 5a). In land-sections, sapropels display notably darker shades of grey than surrounding beige to blueish clays when excavated, but their common appearance in the field is affected by weathering into distinct reddish-brown hues (Fig. 5b). When fresh, sapropels contain elevated organic carbon concentrations (C_{org}) relative to surrounding sediments (e.g., Emeis et al., 1998) and modern surface sediments (Möbius et al., 2010), which are poor in C_{org}. C_{org} levels in sapropels typically range between 1 and 10%. Kidd et al. (1978) argued that a 'sapropel' *sensu stricto* should contain >2%, while the term 'sapropelic' should be used for sediments featuring lower C_{org} values (also Cramp and O'Sullivan, 1999), while others have proposed a cut-off of >1% C_{org} (Murat and Got, 2000). However, 'definitions' based on C_{org} contents are rather artificial and strongly dependent on sediment mass accumulation rates; in consequence, they are only loosely interpreted by most of today's researchers. Extreme C_{org} contents of up to 30% have been reported for certain Pliocene sapropels (Emeis

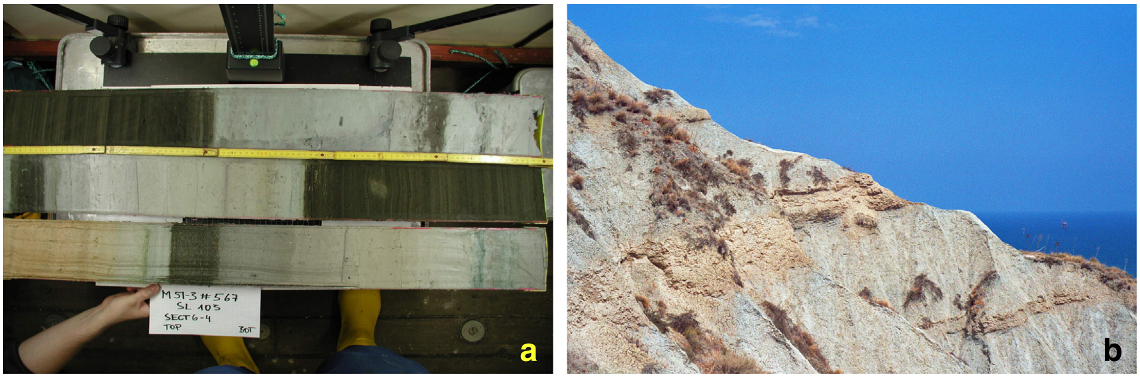

Fig. 5. Sapropel photos. a. Sapropels within a sediment core recovered in 2001 during *RV Meteor* cruise M51-3 (Hemleben et al., 2003) (photograph by EJR and K.C. Emeis). b. Sapropels as exposed in the Vrica section, southern Italy (photograph by EJR).

et al., 1998; Passier et al., 1999a; Nijenhuis and De Lange, 2000). Sapropel S5, deposited during the last interglacial northern hemisphere insolation maximum between 128.34 and 120.97 ka (in southeastern Aegean Sea core LC21; Grant et al., 2012) is one of the most intensely developed sapropels of the Late Quaternary, with C_{org} concentrations commonly around 7 or 8% and exceptionally reaching 15% (e.g., Struck et al., 2001; Rohling et al., 2006; Marino et al., 2007).

Sapropels are more common in the eastern Mediterranean (east of the Strait of Sicily) than in the western Mediterranean, where they are also known as Organic Rich Layers (ORLs) (e.g., Emeis et al., 1991; Cramp and O'Sullivan, 1999; De Kaenel et al., 1999; Meyers and Doose, 1999; Murat, 1999; Meyers, 2006; Rogerson et al., 2008). Plio-Pleistocene sapropels in the Tyrrhenian Sea (western Mediterranean) reach C_{org} contents up to 6% (Emeis et al., 1991; Meyers and Doose, 1999; Murat, 1999). Outside the Tyrrhenian Sea, western Mediterranean Plio-Pleistocene sapropels generally have low C_{org} contents, up to at most 3% (Murat, 1999). Murat (1999) argues that western Mediterranean sapropels generally correlate well with eastern Mediterranean sapropels, but that notable exceptions occur where correlation is not straightforward.

The conventional identification scheme for late Pleistocene sapropels counts them downward, starting with early-mid Holocene sapropel S1 (McCoy, 1974). For records into deeper geological time (Pliocene, Miocene), the accepted sapropel numbering relates to the downward-counted sequential number of the orbital insolation maximum that they are associated with, using 'i-' numbers (Lourens et al., 1996; De Kaenel et al., 1999; Emeis et al., 2000a).

In the open eastern Mediterranean, the shallowest water depth in which the four most recent obvious sapropels S1, S3, S4, and S5 have been found is ~300 m (Rohling and Gieskes, 1989; Rohling et al., 1993a). This broadly supports earlier reports of S1 at ~400 m in the northern Levantine Sea (Shaw and Evans, 1984). In the Adriatic Sea, sapropel S1 is know from depths >400 m (Jorissen et al., 1993). However, in the Aegean Sea, S1 is found at (modern) water depths as shallow as 120 m (Perissoratis and Piper, 1992), which implies only about 80–110 m water depth at the onset of deposition (e.g., Siddall et al., 2003; Stanford et al., 2011). Observations for S3 to S8 in the open eastern Mediterranean suggest deposition at depths greater than 390 ± 130 m below present sea level (Murat, 1991; Murat and Got, 2000).

Sapropels often display obvious sub-millimetre to millimetre-scale lamination (e.g., Fig. 5a). This is especially the case in sapropels from areas with enhanced sediment accumulation rates, such as occasional ones in marine cores (e.g., Moller et al., 2012, who argue that the high accumulation rates are – in part – due to sediment fabric variations associated with the laminations) and in many that are exposed in land-sections. This lamination may represent preserved original sedimentary lamination, due to a lack of bioturbation. This agrees with observations that sapropels are commonly marked by an absence of benthic foraminifera, which suggests persistent sea-floor anoxia, while several are preceded by a short interval containing benthic faunas indicative of severe bottom-water oxygen depletion (such faunas sometimes return within, or can persist into/through, the sapropel) (e.g., Van Straaten, 1972; Nolet and Corliss, 1990; Verhallen, 1991; Rohling et al., 1993b; Nijenhuis et al., 1996; Rohling et al., 1997; Jorissen, 1999; Mercone et al., 2001; Casford et al., 2003; Schmiedl et al., 2003; Kuhnt et al., 2007; Abu-Zied et al., 2008; Schmiedl et al., 2010).

Sapropels in land-sections commonly show remarkably sharp transitions between non-laminated and distinctly laminated sediments, which coincide with the (near) disappearance of benthic faunas from the sediments (e.g., Rohling et al., 1993b). Well-preserved diatom floras in a laminated, high accumulation-rate, sapropel S5 from the last interglacial period (Eemian) in ODP Hole 971C suggest that the original lamination may reflect seasonal variability (Pearce et al., 1998; Kemp et al., 1999, 2000). Scanning electron microscopy studies of this S5 identified a number of intervals with clear lamina couplets that comprise laminae of rhizosolenid diatoms alternating with laminae of mixed assemblages, which are interpreted to represent annual deposition or 'varves' on the basis of correlation with the seasonal succession of diatom floras in the Mediterranean (Pearce et al., 1998; Kemp et al., 1999, 2000). The average varve thickness for all the coherent laminated intervals, which comprise only 15% of S5 in Hole 971C, is 623 ± 482 μm. Extrapolating this to the entire thickness of the sapropel would suggest a duration of deposition of just over 1 kyr. Moller et al. (2012) discuss other laminated S5 sapropels. They confirm the presence of diatom frustules, and also infer that it is the presence of these frustules that yields an 'open sediment fabric', which causes increased thickness of S5 sapropels in which opal is preserved, relative to those without opal. Moller et al. (2012) suggest that the laminations relate to complex interactions between productivity and/or terrestrial input and/or redox conditions, rather than to straightforward seasonal productivity cycles. This might explain why the extrapolated age for S5 based on varve thickness differs so remarkably from other independent sapropel duration estimates, such as: an ~4 kyr duration for S1 (e.g., Mercone et al., 2000; Casford et al., 2002; Rohling et al., 2002a; Casford et al., 2007; De Lange et al., 2008); an ~6 kyr duration for S5 obtained from comparison of its thickness with that of the complete precession cycle in which it is embedded (using Fig. 4 of Lourens et al., 1996), which is supported by similar estimates for well-developed Pliocene sapropels (Wehausen and Brumsack, 1999); durations of ~4.4, ~4.0, ~6.2, and ~7.4 kyr for S1, S3, S4, and S5, respectively, in a speleothem-U/Th based age assessment (Grant et al., 2012); and an ~2.5 kyr estimate by Cane et al. (2002) on the basis of an average ~0.5 mm thickness of beige-brown lamina couplets in the macroscopically well-laminated 128 cm thick Pliocene sapropel i-182 from the terrestrially-influenced Vrica section in southern Italy. Overall, it appears that intervals of sapropel deposition were of variable duration, but typically lasted between ~3 and ~8 kyrs.

The original C_{org} content of sapropel deposits can undergo post-depositional oxidation (burn-down). This causes chemical fronts, creating sharp apparent tops to sapropels that are not representative of the actual tops, which may have been more gradual (e.g., De Lange et al., 1989; Higgs et al., 1994; Thomson et al., 1995, 1999; De Lange et al., 2008). Weakly developed sapropels may become completely oxidised after the return of oxygenated bottom-water conditions. Sediment colour and C_{org} records are then no longer useful to detect the (original) presence of a sapropel. When it can be identified by other methods that a sapropel was originally present, for example using chemical tracers (especially sedimentary Ba/Al records) or absence of benthic faunas, such entirely oxidised sapropels are coined 'ghosts' (e.g., Emeis et al, 2000a). Studies have also identified 'missing' sapropels. Although the terms were initially used interchangeably (e.g., Van Santvoort et al., 1997), we assert that a 'ghost' sapropel differs from a 'missing' sapropel in that the latter represents a total absence of sapropel-specific signals (and hence of the environmental conditions that cause their formation) in an interval where a sapropel would be expected on the basis of their relationship to the astronomical cycle of precession. The Ba/Al ratio is a particularly useful proxy for the original extent of sapropels, since these beds contain distinctly higher Ba/Al ratios than the sediments above and below, while Ba is not easily mobilised once deposited (in contrast to easily oxidised C_{org}). Ba/Al profiles show striking similarity to C_{org} profiles in sapropels from high accumulation rate sequences, where post-depositional oxidation ('burn-down') hardly occurs (Mercone et al., 2000, 2001). This justifies the use of Ba/Al records to approximate original C_{org} levels in partially reoxidised sapropels (cf. Higgs et al., 1994; Thomson et al., 1995; Van Santvoort et al., 1996, 1997; De Lange et al., 2008). Larrasoaña et al. (2006) propose further criteria, elaborating on the problem of 'ghost' versus 'missing' sapropels on the basis of their environmental palaeomagnetic signatures.

Passier et al. (1996) demonstrate how the presence of reduced (sapropel) sediments on top of oxidised sediments triggers downward sulphidisation, which causes formation of a dark grey, sulphur-enriched reduction halo below the sapropels. Based on colour alone, these haloes had initially been interpreted as early onsets of the processes of sapropel formation (sometimes called 'protosapropels') (cf. Stanley et al., 1975; Maldonado and Stanley, 1976; Stanley and Maldonado, 1977, 1979; Anastasakis and Stanley, 1984; Murat and Got, 1987). Although the dark haloes were thus re-interpreted by Passier et al. (1996), this by no means excludes the potential existence of longer-term developments that culminated in sapropel formation (see Section 4.4).

4.2. Timing and climatic conditions

There is strong evidence for enhanced freshwater influx into the eastern Mediterranean at sapropel times, from negative anomalies in stable oxygen isotope ratios ($\delta^{18}O$) measured on the calcium-carbonate shells of planktonic foraminifera that live in near-surface habitats. Freshwater has distinctly low $\delta^{18}O$ compared with seawater, and especially the fresh waters derived from heavy (monsoon-type) rainfalls are isotopically very light (Sonntag et al., 1979; Rozanski, 1985; McKenzie, 1993; Abell and Hoelzmann, 2000; Gasse, 2000; Hoelzmann et al., 2000; Rodrigues et al., 2000; Beuning et al., 2002). Admixture of freshwater floods to the Mediterranean surface waters therefore causes low $\delta^{18}O$ anomalies in surface-dwelling foraminifera (e.g., Vergnaud-Grazzini et al., 1977; Thunell and Williams, 1983; Jenkins and Williams, 1984; Ganssen and Troelstra, 1987; Thunell and Williams, 1989; Tang and Stott, 1993; Fontugne et al., 1994; Kallel et al., 1997a,b; Emeis et al., 1998; Rohling and De Rijk, 1999a,b; Emeis et al., 2000b; Rohling et al., 2002b; Emeis et al., 2003; Rohling et al., 2004). Note that it is not straightforward to deconvolve the calcification temperature and seawater $\delta^{18}O$ contributions to foraminiferal $\delta^{18}O$ signatures in the (eastern) Mediterranean (Boussetta et al., 2011) because diagenetic precipitation of $CaCO_3$ precludes the use of established shell-chemistry-based 'palaeothermometers' (e.g., Mg/Ca; Hoogakker et al., 2009). However, available temperature-corrected $\delta^{18}O$ data, based on transfer function techniques or alkenone unsaturation ratios, confirm that intervals of sapropel deposition were coincident with major influx of low-$\delta^{18}O$ freshwater into the eastern Mediterranean (e.g., Kallel et al., 2000; Emeis et al., 2000a,b, 2003; Marino et al., 2009). Geochemical, environmental magnetic, and clay mineralogical data confirm that times of sapropel deposition were characterised by high runoff into the basin, whereas intervening times saw reduced riverine and enhanced wind-blown sediment supply (e.g., Krom et al., 1999; Wehausen and Brumsack, 1999; Foucault and Mélières, 2000; Wehausen and Brumsack, 2000; Lourens et al., 2001; Larrasoaña et al., 2003; Scrivner et al., 2004; Osborne et al., 2008, 2010; Revel et al., 2010; Box et al., 2011; Zhao et al., 2012; Ehrmann et al., 2013; Hennekam et al., 2014; Weldeab et al., 2014). Freshwater flooding into the basin has been ascribed to monsoon-fuelled flooding, Black Sea flooding, and/or runoff from more local precipitation around the basin. These are reviewed in turn in Sections 4.2.1–4.2.3.

4.2.1. Monsoon-fuelled freshwater

Intensification of northern hemisphere monsoon precipitation over North Africa is generally viewed as a key source for extra freshwater delivery into the Mediterranean basin during sapropel times. Temporal coincidence between sapropel occurrences and insolation-driven monsoon maxima, affecting the eastern Mediterranean via changes in Nile discharge, was first described by Rossignol-Strick et al. (1982) and Rossignol-Strick (1983, 1985). They specified an index for monsoon intensity ('monsoon index') as a function of two parameters: *(i)* insolation at the (north) Tropic of Cancer; and *(ii)* the insolation difference between the Tropic of Cancer and the equator. The pioneering studies of Rossignol-Strick and co-workers led to further assessments of the timing of sapropel formation over their full range from the Present back into the Miocene (e.g., Kidd et al., 1978; Van der Zwaan and Gudjonsson, 1986; Hilgen et al., 1995; Krijgsman et al., 1995; Santarelli et al., 1998; Schenau et al., 1999; Sierro et al., 1999). This confirmed that sapropels (especially in the central and eastern Mediterranean) were commonly formed at times when perihelion falls in northern hemisphere summer ('precession minima', relative to 'maxima' that represent the present configuration with perihelion in northern winter). A precession minimum is characterised by maximised summer insolation on the northern hemisphere, and reduced winter insolation, which increases the seasonal contrast and enhances summer monsoon intensity. Other studies emphasised that not all precession minima have sapropels, but that they instead occur in discrete clusters. Each cluster was found to represent times of maximum orbital eccentricity, in agreement with eccentricity modulation of the impact of precession, so that sapropels commonly coincide with high-amplitude precession minima (insolation maxima) (Hilgen, 1991a,b; Hilgen et al., 1993, 1995; Lourens et al., 1996, 2001). Numerical climate models have corroborated the impact of precession and eccentricity on monsoon intensity (e.g., Kutzbach, 1985; Kutzbach and Guetter, 1986; COHMAP, 1988). Finally, observation of a subdued but clear obliquity/tilt component in the variability of Mediterranean climate/sapropel sequences (Lourens et al., 1996) suggests that the simple 'monsoon index' may be improved by including the insolation contrast between the tropic of Capricorn and the tropic of Cancer, to incorporate cross-equatorial influences (Lourens and Reichart, 1997). Fig. 6, from Larrasoaña et al. (2013), shows the sapropel record of the past 8 million years within a context of insolation changes, African and wider Northern Hemisphere climate developments, which they relate to key stages in hominin evolution.

The close correspondence between times of sapropel formation and insolation maxima has led to their application, combined with other cyclic features in Mediterranean sedimentary sequences such as lithological alternations and oxygen isotope variations, in exercises to astronomically 'tune' the age models for these sequences, and so of the geomagnetic polarity timescale (Hilgen, 1991a,b; Hilgen et al., 1993, 1995; Lourens et al., 1996, 2001; Lourens, 2004). Such work uses a relationship in which the sapropel midpoint is taken to lag the northern hemisphere insolation maximum by 3 kyr, based on comparison of astronomical solutions with ^{14}C datings of S1 (Lourens et al., 1996). Timing of S1 and, thus, the lag of its midpoint with respect to the insolation maximum, were corroborated by extensive dating of several S1 sections across the eastern Mediterranean basin (de Lange et al., 2008). However, application of the concept beyond sapropel S1 remains a matter of debate. Ziegler et al. (2010) propose an independent (radiometric) chronology for eastern Mediterranean ODP Site 968 over the last 350,000 years, based on correlations with Chinese speleothem records (Wang et al., 2008) and a global benthic $\delta^{18}O$ stack (Lisiecki and Raymo, 2005), and infer that the 3 kyr lag behind the northern hemisphere insolation maximum is a recurring feature of sapropel deposition. However, a precise radiometric chronology for the last 150,000 years for southeastern Aegean core LC21, using process-based correlation of its surface foraminiferal $\delta^{18}O$ signal with the Soreq Cave $\delta^{18}O$ record (Grant et al., 2012), shows that this generalised concept may be applied only within broad tolerances of several thousands of years to sapropels older than S1.

Orbitally controlled intensity variations of the monsoon-fuelled runoff from North Africa definitely affected the Mediterranean by means of changes in Nile river discharge (e.g., Rossignol-Strick et al., 1982; Rossignol-Strick, 1985; Rohling and De Rijk, 1999a,b; Scrivner et al., 2004; Revel et al., 2010; Box et al., 2011; Hennekam et al., 2014; Weldeab et al., 2014). This is best illustrated using the most recent northern hemisphere summer insolation maximum, which was reached at ~11 ka (Berger and Loutre, 1991). Records of change in eastern Mediterranean surface waters document a shift towards enhanced influx of monsoon-fuelled freshwater with a characteristic geochemical fingerprint (low $\delta^{18}O$, high dissolved Ba) between ~10.8 and ~9.7 ka (e.g., Marino et al., 2009; Weldeab et al., 2014). Several lines of evidence

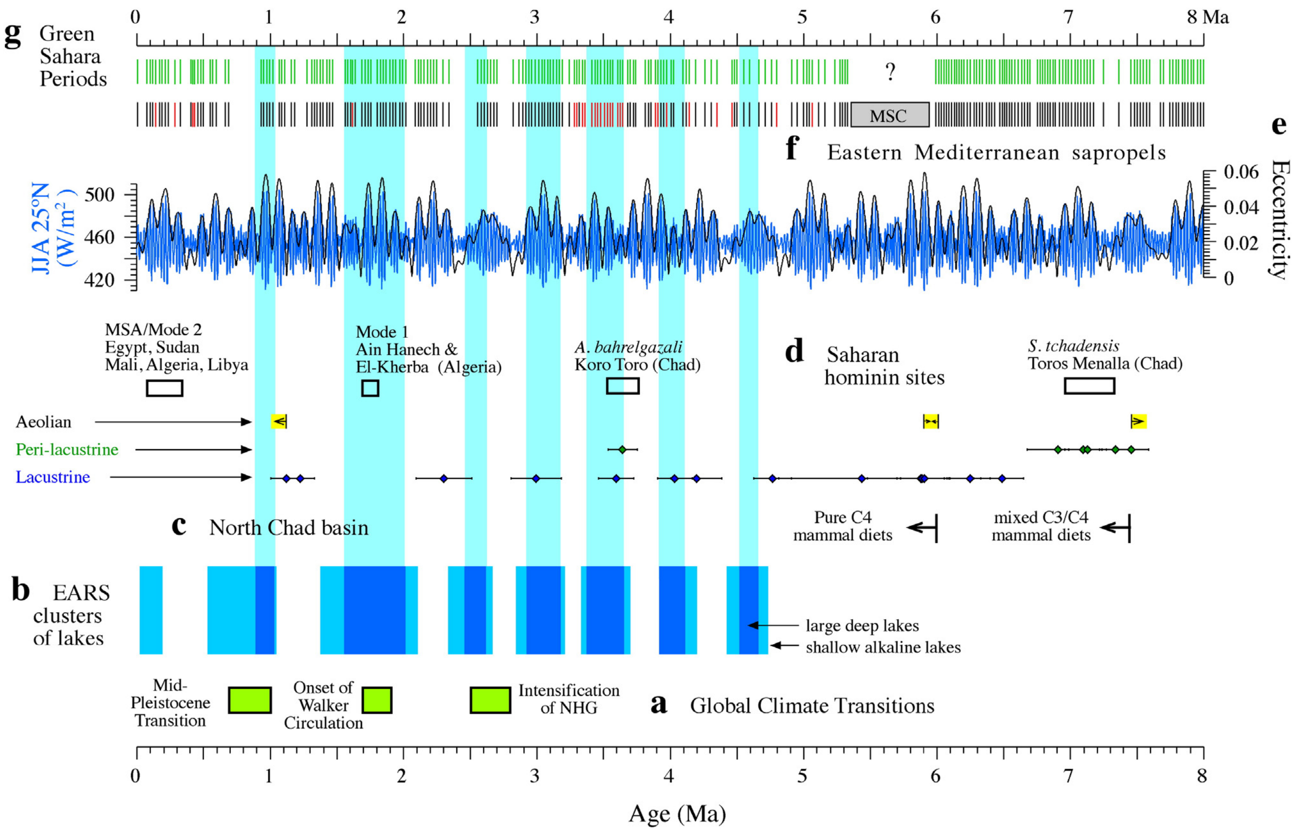

Fig. 6. Saharan climate and hominin occupation 8 Ma to present. a. Chronology of global climate transitions (NHG: northern hemisphere glaciation). b. Chronology of East Africa Rift System (EARS) lake periods. Formation of large lakes was prevented by the lack of full-graben basin morphologies before 5 Ma. Vertical shaded bars indicate periods with large, deep, freshwater lakes. c. Chronology of lacustrine, peri-lacustrine and eolian sediments in the North Chad Basin plotted with earliest evidence for mixed C3/C4 and pure C4 mammal diets in the basin. d. Chronology of Saharan hominin occupation sites. e. Variations in summer insolation (June, July, August; JJA) at 25°N and eccentricity back to 8 Ma. f. Composite eastern Mediterranean sapropel record from ODP Leg 160 sites and land sections at Gibliscemi, Metochia, Kastelli and Faneromeni (red bars indicate oxidised sapropels). g. Green Sahara periods back to 8 Ma inferred from the eastern Mediterranean sapropel record. From Larrasoaña et al. (2013) — we refer to that study for in-depth discussion of all original data sources, with references.

attribute these changes to enhanced Nile River discharge, due to a shift to wetter conditions over subtropical North Africa. First, the largest injection of Ba-enriched freshwater was noted at a location in the direct path of Nile River discharge (Weldeab et al., 2014). Second, at approximately the same time, accumulation rates and sedimentary ^{87}Sr/^{86}Sr signatures in Levantine sites near the suspended sediment plume of the Nile imply a decrease in the discharge of Blue Nile sediments and an increase in White Nile sediments (Box et al., 2011). Although the Blue Nile accounts for most of the (pre-Aswan) Nile discharge (see Section 2.2), enhanced monsoon precipitation in the Blue Nile catchment (Ethiopian Highlands, subtropical East Africa) would reduce soil erosion due to an increase in vegetation cover (Box et al., 2011). Enhanced precipitation in the Blue Nile catchment is supported by a negative anomaly in the δD of leaf waxes from Lake Tana (Costa et al., 2014). Third, the transport of wind-blown Saharan dust into the eastern Mediterranean dropped during the earliest Holocene, testifying to the establishment of more humid conditions, with increased vegetation cover and soil cohesion, over large parts of subtropical North Africa (Box et al., 2011; Hennekam et al., 2014). These results corroborate previous inferences for the Nile and the Sahara since the Last Glacial Maximum (LGM) (summarised after Adamson et al., 1980; Williams et al., 2000) that suggest very low Nile discharge until roughly 12.5 ka, at which time the White Nile was seasonal and intermittent, until Lake Victoria overflow developed and the 'buffering' Sudd swamps in Sudan became established at ~12.5 ka, which ensured more regular, perennial discharge from the White Nile. Note that recent high-resolution work on the chemical signature of (total integrated) Nile discharge into the eastern Mediterranean suggests a slightly different timeline (Revel et al., 2010). That work documents an earlier onset of the humid regime at ~14 ka, followed by an arid interlude from ~12.5 to ~12 ka, which gave way to intense humid conditions from ~12 ka until ~8 ka, and then a weakening of rainfall over the Ethiopian Highlands (Blue Nile source region) until a return of widespread aridification over subtropical Africa by ~5 ka.

Evidently, the Nile maximum coincided closely with the deposition of sapropel S1 in the eastern Mediterranean, between ~10.5 and ~6 ka (e.g., Mercone et al., 2000; Rohling et al., 2002a; Casford et al., 2007; De Lange et al., 2008; Marino et al., 2009; Hennekam et al., 2014; Weldeab et al., 2014). However, it has also been widely documented that, in addition to the Nile impact, the (African) monsoon had a more widespread influence on the Mediterranean; that is, not only the intensity of the monsoon was enhanced during insolation maxima, but also its spatial extent over North Africa. This caused strong reductions in the size of the Sahara desert by northward migration of its southern margin due to enhanced moisture advection from the Atlantic Ocean (Bosmans et al., 2012), and such expansions of the monsoon domain over North Africa during northern hemisphere insolation maxima caused pronounced 'green Sahara' events (see synthesis in Larrasoaña et al., 2013; Fig. 6). Greening of the Sahara is indisputable from a wide variety of field observations: rock-art and animal, human and vegetation remains in the central Sahara; massive expansion of Lake Chad; presence of substantial palaeolakes in currently hyperarid areas such as the Oyo depression of NW Sudan; and activation of large-scale systems of presently inactive wadis (among many others, Pachur and Braun, 1980; Gaven et al., 1981; Ritchie et al., 1985; McKenzie, 1993; Szabo et al., 1995; Petit-Maire and Guo, 1997; Gasse, 2000; Hoelzmann et al., 2000; Williams et al., 2000; Mandel and Simmons, 2001; Pachur, 2001; Hassan, 2002 (edited volume); Smith et al., 2004; Armitagea et al., 2007; Drake et al, 2011; Whiting-Blome et al., 2012; Coulthard et al., 2013; Larrasoaña et al., 2013; and references therein). Greening of the Sahara may in part have been a self-reinforcing process, through vegetation-climate feedbacks (Kutzbach et al., 1996; Brovkin et al., 1998; Claussen et al., 1998; Irizarry-Ortiz et al., 2003; Bosmans et al., 2012), but this feedback is not without debate between numerical climate models (Bosmans et al., 2012) or even in observation-based reconstructions (Weldeab et al., 2014).

Eastern Mediterranean stable oxygen isotope ($\delta^{18}O$) data suggest that the monsoon front penetrated sufficiently far northwards during the insolation maximum of the last interglacial to have caused significant runoff to the North of the central Saharan watershed (~21°N) (Rohling et al., 2002b, 2004). Thus, runoff not only reached the eastern Mediterranean via the Nile River, but also along the wider North African margin. This notion was supported by a study of Nd isotopes, which demonstrated considerable runoff from the central Saharan mountains towards the Gulf of Sirte (Lybia) (Osborne et al., 2008), and by orbital imaging radar observations of major palaeo-riverchannels along that pathway (Paillou et al., 2009, 2012). Aeolian dust variations over the last 3 million years in combination with a wide variety of other Saharan data also support this scenario, and extend it to all substantial insolation maxima (Larrasoaña et al., 2003, 2013). Archaeological observations around exclusively rain-fed depressions on the Lybian Plateau suggest that summer rains of central Africa may have periodically penetrated at least as far north as Kharga (roughly 25°N) during the early-mid Holocene, even though conditions during that pluvial phase seem to have remained drier than during earlier Quaternary pluvial phases (Mandel and Simmons, 2001). The observation of Mandel and Simmons (2001), that the Holocene monsoon maximum was of relatively low intensity compared with previous Quaternary monsoon maxima, agrees with quantifications of Holocene and last interglacial monsoon impacts on the freshwater budget of the eastern Mediterranean (Rohling, 1999; Rohling et al., 2004). These suggest that the Holocene monsoon maximum was considerably weaker than the last interglacial monsoon maximum (see also Section 4.3).

Finally, there remains debate about the source of the monsoon rain over North Africa during sapropel times (insolation maxima). A general circulation model for the last interglacial infers prominent strengthening of the zonal transport of Atlantic-sourced moisture across Africa, which results in strong ^{18}O depletion in precipitation towards northeast Africa (Herold and Lohmann, 2009). Similarly, Lake Tana leaf-wax δD data would be consistent with enhanced transport of moisture over the Congo Basin, linked to an eastward shift of the Congo Air Boundary across Africa (Costa et al., 2014). On the other hand, it appears that early to middle Holocene freshening of the eastern Mediterranean (Marino et al., 2009; Hennekam et al., 2014; Weldeab et al., 2014) and intensification of the Indian Summer Monsoon (ISM, Fleitmann et al., 2003; Gupta et al., 2003, 2005; Fleitmann et al., 2007) were (nearly) synchronous. This may imply either some direct influence of ISM rainfall on Northeast Africa (as inferred also for the present; Tierney and DeMenocal, 2013; Costa et al., 2014), or (nearly) simultaneous evolution of the North-East African monsoon and ISM during precession minima (e.g., Marino et al., 2009; Bosmans et al., 2012).

4.2.2. Black Sea

Olausson (1991) drew attention to the potential importance to sapropel formation of enhanced freshwater flow from the Black Sea into the eastern Mediterranean. He considered the effects of reconnections of the glacial, virtually fresh “Black Lake” with the Aegean Sea (via the Sea of Marmara), due to global sea-level rise above the Bosphorus sill depth of ~35 m below present sea level. Invasion of saline Mediterranean waters into Black Lake (settling at depth because of the density difference) then might force a surface flow of fresh Black Lake water out into the Mediterranean. Lane-Serff et al. (1997) used hydraulic control modelling to modify this concept, in that outflow from the Black Sea would start only after sea level had risen at least ~10 m above the sill, since Mediterranean inflow into Black Lake would block the potential for any outflow at lower sea levels.

Global sea level reached −35 m at ~9.7 cal. ka, and −25 m at ~9.0 cal. ka (Stanford et al., 2011), but note that for the Bosphorus these threshold timings are approximate because precise assessment would require careful inclusion of local isostacy and erosion. The first impacts of Mediterranean water inside Black Lake were noted at ~9.5 to 9.3 cal. ka (Major et al., 2006; Bahr et al., 2008). Then followed a period of salinification, resulting eventually in a modern-type stratified Black Sea configuration (and onset of anoxic conditions) by ~8 cal. ka (Bahr et al., 2006). This delay agrees with model-based estimates of a millennial time-scale for significant salinity (hence stratification) build-up in the Black Sea (Lane-Serff et al., 1997; Myers et al., 2003).

Given that sapropel S1 formation in the eastern Mediterranean started at ~10.5 cal. ka, some 1000 years before the earliest reconnection signals (see Section 4.2.1), Black Sea flooding can be excluded as a trigger for S1 deposition. Indeed, Sperling et al. (2003) demonstrate: (*i*) that there was no low-salinity water in the Sea of Marmara during the deposition of S1; (*ii*) that there were ‘gradients of freshening in the eastern Mediterranean Sea … [which indicate that] … the major sources of freshwater were closer to the Levantine Basin’; and (*iii*) that ‘the Black Sea was not a major freshwater source contributing to formation of S1’. For last interglacial sapropel S5, things are less well documented and dated, but the earliest signals of reconnection are suggested at ~128.1 ± 0.7 ka (Wegwerth et al., 2014), which is within uncertainties the same as the onset of S5 deposition in southeastern Aegean core LC21 (Grant et al., 2012; Section 4.1).

In summary, a Black-Sea outflow contribution cannot be excluded for S5, but for S1 all evidence is stacked against an important role for Black Sea outflow. There are also issues with considering Black Sea reconnection scenarios for so-called “glacial” sapropels S6 and S8, when sea level was well below the Bosphorus sill depth. We infer that there is no evident (essential) causal link between sapropel formation and the expelling of fresh water from the Black Sea due to reconnection with the Mediterranean. But it cannot be excluded that, in some cases, Black Sea fresh water contributed somewhat to the maintenance of enhanced surface buoyancy in the eastern Mediterranean (similar to a riverine freshwater influx).

4.2.3. Other freshwater sources

In addition to monsoon flooding from the North African margin at times of sapropel formation, records of pollen abundances from terrestrial vegetation around the Northern Borderlands of the Eastern Mediterranean (NBEM) show high abundances of deciduous arboreal taxa (especially deciduous oak) and low abundances of steppe elements, which were initially interpreted to indicate increased summer rainfall/moisture availability (e.g., Rossignol-Strick, 1987; Wijmstra et al., 1990; Rohling and Hilgen, 1991; Tzedakis, 1993; Mommersteeg et al., 1995; Rossignol-Strick, 1995; Frogley et al., 1999; Rossignol-Strick, 1999; Rossignol-Strick and Paterne, 1999). Tzedakis (2007) questioned this interpretation and pointed out – among other issues – that the amount of annual rainfall commonly invoked for the flourishing of deciduous oak (800–1200 mm yr^{-1}; Rossignol-Strick, 1999; Rossignol-Strick and Paterne, 1999) might be achieved in winter only. Palynological studies (Wijmstra et al., 1990; Kotthoff et al., 2008; Tzedakis, 2009; Peyron et al., 2011; Milner et al., 2012) have also inferred increases in NBEM winter precipitation at times of sapropel formation (see also Roberts et al., 2011). For example, Kotthoff et al. (2008) combined detailed taxonomic distinction between evergreen (*Quercus ilex*, *Quercus coccifera*) and deciduous oak (*Quercus pubescens*, *Quercus robur*) with pollen-based transfer function techniques (cf., Peyron et al., 1998) to document a ~50% winter precipitation increase in the borderlands of the Aegean Sea during S1. This might relate to increased wintertime storm-track precipitation over the NBEM, as suggested by some numerical models for periods of precession minima (Brayshaw et al., 2010, 2011; Kutzbach et al., 2014).

Further insight into the seasonal nature of NBEM precipitation is provided by the expansion of sclerophyllous vegetation (*Olea*, *Pistacea*, *Phyllyrea*, evergreen *Quercus*) during the first halves of interglacial sapropels, which has been attributed to severe summer aridity (Tzedakis, 2007; Milner et al., 2012). A mechanism was proposed to explain this NBEM summer aridity, based on close temporal coupling between sapropel intervals and ISM maxima (Tzedakis, 2007) (see Section 4.2.1), and building on the notion that adiabatic descent in the upper troposphere of the Levant is reinforced by ISM strengthening (Rodwell and Hoskins, 1996; Raicich et al., 2003; Ziv et al., 2004). However, there is a clear complication to this, namely an apparent mismatch between the duration of NBEM summer aridity episodes (~2.5 kyr; Brauer et al., 2007; Tzedakis, 2007; Milner et al., 2012) and that of ISM maxima (~5 and ~7 kyr; Fleitmann et al., 2003; Gupta et al., 2003, 2005; Fleitmann et al., 2011) during (at least) the last two interglacials.

To support the inferred increase in precipitation in the NBEM and in northern sectors of the Mediterranean Sea in general, a wealth of stable isotope studies on speleothems has been used (Bar-Matthews et al., 1999, 2000; Matthews et al., 2000; Bard et al., 2002; Bar-Matthews et al., 2003; Frisia et al., 2006; Zanchetta et al., 2007; Spötl et al., 2010; Göktürk et al., 2011), as have elevated lake levels (e.g., Digerfeldt et al., 2000), and combinations (e.g., Roberts et al., 2011). Such archives, however, do not give straightforward information. The δ^{18}O record of Soreq Cave, Israel, is dominated by a source-water effect, whereby (likely monsoon-flooding related) changes in eastern Mediterranean surface-water δ^{18}O caused similar changes in δ^{18}O in Soreq Cave, because the eastern Mediterranean is the evaporative source region for moisture that precipitates over the Levant (Matthews et al., 2000; Bar-Matthews et al., 2003; Kolodny et al., 2005; Marino et al., 2009; Grant et al., 2012). After accounting for the source-water effect, sapropels S1, S3, and S4 reveal no systematic deviation to wetter/warmer conditions at Soreq Cave (Israel), relative to the present, whereas S5 suggests a weak and variable deviation to wetter conditions (Fig. 7). If anything, temporary increases in regional humidity were more pronounced in the latter portions of S1, S4, and S5, while the earlier portions were characterised by enhanced regional aridity (Fig. 7), which would support aforementioned inferences from pollen data (Tzedakis, 2007; Milner et al., 2012). Other cave records also seem to be strongly affected by the source-water effect. For example, a considerable part of the δ^{18}O changes through the interval corresponding to sapropel S6 (between ~180 and ~170 ka) in Argenterola Cave (Italy) may be attributed to a source-water effect (Bard et al., 2002), and a source-water effect (in this case from the Black Sea) also dominates the record of Sofular Cave in northeastern Turkey (Badertscher et al., 2011). Given that source-water effects have not (yet) been fully accounted for in all Mediterranean cave records, the environmental conclusions drawn from them may be biassed.

Lake-level data cannot be taken at face value either, because these depend on a complex integration of changes in evaporation and precipitation (e.g., Giraudi et al., 2011), and are also sensitive to issues such as changes in the ratio between the areas of the lake surface and its wider catchment basin, and in the rate of transfer of runoff/groundwater flow from the catchment into the lake. For example, Lake Lisan (the palaeo-Dead Sea) experienced a pronounced lowstand phase during the time of S1 deposition, but this does not mean that precipitation (P) was the same or lower than today. Instead, it merely means that – with increased evaporation (E) under warmer conditions during the most recent insolation maximum – any precipitation increase was insufficient to prevent P–E over the lake catchment from becoming slightly negative (e.g., even a full 100% increase of mean P over the Dead Sea catchment from 110 to 220 mm y^{-1} would be more than offset by only 5% increase in the mean pan-evaporation rate, which typically is ~2500 mm y^{-1}; Rohling, 2013, and references therein). Note that the fact that the lake was reduced in size but did not disappear completely implies that $P > P_{present}$ because any notable deviation from approximate balance between evaporation change and precipitation change would have caused not just shrinkage, but rapid dessication of the lake. Lakes in the Konya Basin, Anatolian Plateau, seem to show similar patterns to Lake Lisan, with high levels during cold periods, and low levels (to complete disappearance) in warm periods (Naruse et al., 1997). However, the crater-lake interpretation of Roberts et al. (2001) for Eski Acıgöl, central Turkey, does not show the same relationship on shorter timescales;

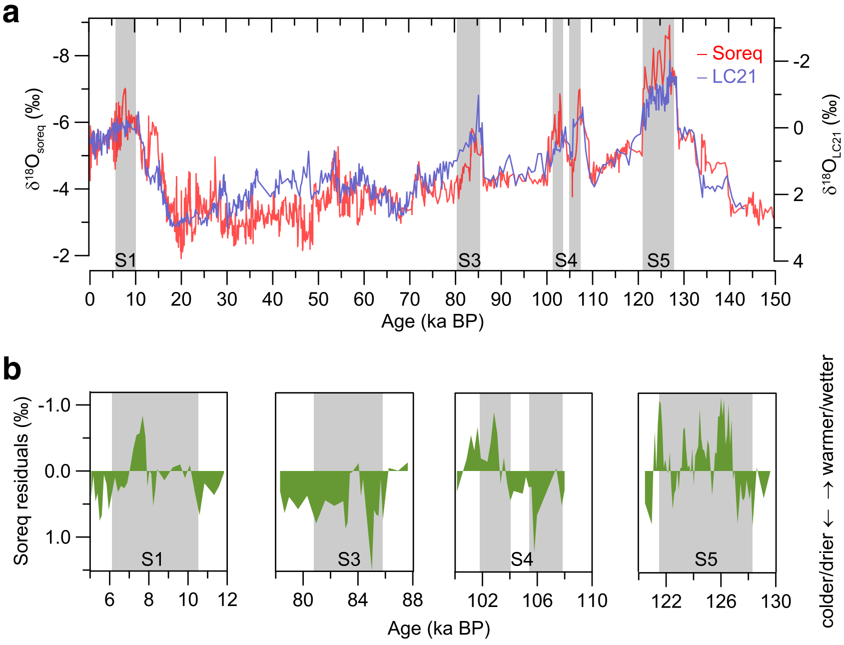

Fig. 7. Oxygen isotope ratio comparison between southeastern Aegean Sea core LC21 and Soreq Cave (Israel) speleothems (after Grant et al., 2012). a. Comparison of records on a common timescale (see Grant et al., 2012). b. Residuals, i.e., difference between Soreq Cave values and LC21 values, for each of the well-expressed sapropels. Negative offsets (up) broadly indicate warmer/wetter conditions at Soreq Cave, and positive offsets (down) colder/drier conditions at Soreq Cave, relative to the mean of the past 3000 years (to which the records were normalised).

instead it seems to suggest net humidity during the early Holocene and net aridity conditions during the late Holocene. Lake conditions are notoriously local/regional in nature, which may explain the contrasting reconstructions; in addition, different responses may reflect different forcings on different timescales (centennial-millennial versus orbital).

Combined reconstruction of pollen and lake level data for the middle Holocene (6 ka, approximately coincident with the end of S1 deposition) suggests positive P–E anomalies of 50 (west) to 200 (east) mm y^{-1} around the NBEM, relative to the present (Cheddadi et al., 1997). However, Tzedakis (2007) emphasises the need for accurate dating in making such comparisons, because – for example – he argues that the main 'LGM' highstand phase in many lakes predates the actual LGM by a couple of thousand years (so that the actual LGM coincides with dropping lake levels, hence net aridity), and that pollen data around the Mediterranean for the actual LGM indicate arid conditions. Tzedakis (2007) also argues that pollen data imply strong summer aridity at least during the first halves of the sapropels, but less arid conditions during their latter halves. Hence, comparison with Cheddadi et al. (1997) may be biassed because that study concerns a time-slice at the very end of S1 deposition. Evidently, much additional work is needed before a comprehensive E–P interpretation can be formed that is coherent between both pollen data and other terrestrial archives, such as lake-level and speleothem records.

Support for enhanced NBEM river runoff at sapropel times comes from mixing arguments based on strontium isotope and major element ratios for the Holocene (Krom et al., 1999), and from clay mineralogy in the Aegean Sea (Ehrmann et al., 2007). In western Mediterranean Pleistocene sapropels, NBEM runoff is indicated by light (organic) δ^2H and (carbonate) δ^{18}O values (Bernasconi and Pika-Biolzi, 2000; Krishnamurthy et al., 2000). Given the mounting arguments against precipitation increase in summer (Tzedakis, 2007, 2009; Roberts et al., 2011; Milner et al., 2012), enhanced NBEM river runoff may imply amplification of the Mediterranean winter-wet conditions, and potential drivers should be considered. Penetration of direct precipitation from the African or Indian monsoon systems into the Mediterranean basin has been excluded (Goodfriend, 1991; Arz et al., 2003; Vaks et al., 2003, 2006, 2007, 2010; Brayshaw et al., 2011), and – if any had occurred – would have been concentrated in (late) summer, not in winter. Instead, enhanced winter-time NBEM moisture availability likely reflects increased Mediterranean depression activity due to enhanced cyclogenesis over the basin (see Rohling and Hilgen (1991), but then for winter, rather than summer as suggested by those authors, possibly as part of an enhanced winter depression track activity; Kutzbach et al., 2014). In addition, precipitation may have resulted from persistent low-level convective activity (Bosmans et al., submitted for publication). As discussed in Section 2.1, such Mediterranean sourcing of the moisture is corroborated by isotopic characteristics of speleothems and their fluid inclusions.

In summary, the exact E–P developments around the Mediterranean during sapropel formation remain unclear, as do changes in these conditions through the several thousands of years spanned by sapropel episodes. But we know that any moisture increase was predominantly sourced from the Mediterranean Sea itself, and that any extra precipitation likely fell in winter. Finally, an enhanced Mediterranean moisture flux at times of insolation maxima, observed at the northernmost tip of the Red Sea (Arz et al., 2003), has a potentially important implication. Such a process would at best have affected the overall Mediterranean hydrological budget by very little, since any runoff it caused into the basin would have originated from evaporative loss out of the same basin. At worst, however, it may have shifted the Mediterranean hydrological budget into a net 'drier' direction, since any net moisture export into watershed areas of other basins (e.g., Jordan Valley and Dead Sea rift, Red Sea, or Tigris/Euphrates and Persian Gulf) would represent an increase in net evaporative loss from the Mediterranean Sea.

Perhaps the most important consequence of enhanced Mediterranean cyclogenesis would be a generally eastward freshwater redistribution within the Mediterranean basin. Thus, the hydrological budget may have been substantially affected on local scales and in terms of regional gradients, even if the basin-wide budget was not much affected or even shifted into a net 'arid' direction. Consequent reduction of the Mediterranean west-to-east salinity gradient could help to curtail convective, salt-driven overturning (intermediate water formation) in the NE Levantine sector. Such 'flattening' of the west-east gradient has been inferred from surface-water δ^{18}O data (Fontugne et al., 1994; Rohling and De Rijk, 1999a,b; Emeis et al., 2000b) (see Section 4.3). A more even distribution of surface salinities would amplify the influence of local cooling processes in determining where overturning might take place. Similar effects were observed in numerical circulation experiments for the time of S1 deposition; overturn in the Levantine sector became inhibited, and convective overturn became restricted to the relatively cool Adriatic region (Myers et al., 1998).

4.2.4. Impacts of sea-level rise

During deglaciations, melt-water addition into the world ocean (especially into the North Atlantic, due to reduction of Eurasian and North American ice sheets) causes reduction in North Atlantic surface-water salinities, as well as global sea-level rise (which opened up the cross-sectional areas of the Straits of Gibraltar and Sicily). Both processes would drive progressive surface-water buoyancy gain in the Mediterranean, and thus a strong increase in stratification potential. Using simple conceptual arguments, based on salinity calculations with a simple hydraulic control model over the last deglaciation (Rohling, 1991a,b; Rohling and Bryden, 1994; Rohling, 1994) argues that this would have caused progressive pre-conditioning of the Mediterranean, from ~14.5 ka, towards a stratification event (possibly interrupted by renewed deep-water formation during the cool Younger Dryas).

Béthoux and Pierre (1999) included intermediate water changes in the concept, and similarly find that deglaciations would precondition the basin for stratification. Next, Rogerson et al. (2008, 2012a) investigate the issue in terms of changes to Bernoulli suction of deep waters over the sill in the Strait of Gibraltar; this work is evaluated in detail in Section 5. Finally, focussing specifically on the eastern Mediterranean, Grimm et al. (submitted for publication) use a numerical circulation model that includes biogeochemical assessment of carbon burial over the last deglaciation, and find that S1 formed after 6000 years of deglaciation-driven build-up of limited deep-water circulation. Grimm et al. (submitted for publication) argue that the deglaciation effect was dominant in the development of S1.

Combined, these studies suggest that sapropels deposited within several thousand years of a deglaciation are likely to have a strong generic relationship with that deglaciation. If not the dominant cause, any preceding and substantial phase of deglaciation will at least have strongly preconditioned the eastern Mediterranean for sapropel deposition. However, it cannot be seen as a ubiquitous mechanism, since not all eastern Mediterranean sapropels follow deglaciations, and since western Mediterranean sapropels may require a more complex set of circumstances (Section 5).

4.3. Changes in surface buoyancy loss

To date, the spatially best-characterised quantitative estimates for the magnitude of the buoyancy-forcing changes associated with periods of sapropel formation are available for S1, from δ^{18}O mapping and modelling. Thunell and Williams (1989) presented a first reconstruction, combining data from various planktonic foraminiferal species and using a fixed S:δ^{18}O gradient through time. They inferred that the W–E surface-water salinity gradient had been reversed, relative to the present, which was taken as evidence that the vertical overturning circulation had reversed to an estuarine type (as hypothesised previously by Stanley et al., 1975). Kallel et al. (1997a) added more sites, still including a variety of species. They employed two different S:δ^{18}O relationships, one for $S > 37.5$ and one for $S < 38$, and concluded that the

W–E salinity gradient had virtually vanished (flat field), but not reversed. Rohling and De Rijk (1999a,b) added yet more records, and demonstrated that comparisons should be made only on the basis of single-species records, since inter-species differences in isotopic change would adversely affect reconstructed spatial gradients. Allowing for non-conservative behaviour of oxygen isotope ratios, in contrast to salinity, Rohling and De Rijk (1999a,b) concluded that the W–E Mediterranean salinity gradient during formation of Holocene sapropel S1 was of similar sign as today, but weakened to ~75% of its modern magnitude. This estimate was corroborated with a box model to simulate the main Mediterranean salinity and δ^{18}O changes over the last 20,000 years (Rohling, 1999), which suggests that the salinity gradient during S1 deposition remained near ~80% of its present-day value, in response to a reduction in the excess of evaporation over total freshwater input (X) to ~65% of its present value. Note that this was not a constant condition throughout the period of S1 formation; some records of surface-water δ^{18}O from the open eastern Mediterranean through S1 suggest a sharp monsoon 'decline/interruption' at ~8 ka BP (Emeis et al., 2000b, 2003), and African lake levels suggest a similar arid interlude between ~8.5 and ~7.8 ka BP (e.g., Gasse, 2000) (see also Section 4.6).

In spite of a general consensus that the Nile reached its most recent period of peak discharge during the monsoon maximum that coincided with S1 deposition, mapping of surface-water δ^{18}O anomalies failed to identify a single point-source around the Nile delta. Instead, a widely distributed depletion is found throughout the Levantine Sea, resulting in a general weakening of the west–east gradient (Rohling and De Rijk, 1999a,b). This was corroborated by a transect study of Holocene sapropel S1, which includes δ^{18}O corrections for spatial and temporal changes in sea surface temperature (Emeis et al., 2000b). The weakened W–E salinity gradient during times of sapropel deposition may partly reflect an increase in circum-Mediterranean humidity, but also partly (at least during many sapropels, if not all) reflects monsoon-sourced runoff along the wider N African margin, into the central Mediterranean (Fontugne et al., 1994; Rohling et al., 2002b; Larrasoaña et al., 2003; Rohling et al., 2004; Osborne et al., 2008). Evidence for these inputs was discussed in Section 4.2.1.

In short, three different interpretations exist for the W–E surface-water salinity gradient at the time of Holocene S1 deposition: one argues for a reversed condition, one for a flat field, and one for a weakened present-day gradient. In-depth discussion of these hypotheses can be found in Emeis et al. (2000b). Myers et al. (1998) employed the intermediate reconstruction to define a main S1-run for their numerical Mediterranean circulation experiments, and the other two options to define sensitivity tests. The model of Myers et al. (1998), which used restoring boundary conditions, was later upgraded to include more realistic forcing by surface heat and freshwater fluxes (Myers, 2002). The latter model shows development of deep-water stagnation when X is reduced to less than 80% of the present-day value. The best-fit solution of Myers (2002) suggests that the net evaporative flux from the Mediterranean during S1 formation was around 20–40% of the present-day value.

The next-best-studied sapropel is S5 from the last interglacial (~128–121 ka; Grant et al., 2012). Eastern Mediterranean surface-water δ^{18}O data for S5 show two distinct 'peaks', separated by an 'interruption' with a duration initially estimated at 800 year (Cane et al., 2002; Rohling et al., 2002b, 2004), but which more likely spans 1100–1500 years (revised chronology of Grant et al., 2012). A δ^{18}O box model to quantify freshwater flooding during the two monsoon peaks suggests that basin-averaged Mediterranean X was reduced to 5–45% (older peak) and 35–60% (younger peak), relative to the present (Rohling et al., 2004). It also suggests that the 'interruption' between the two peaks was characterised by X levels close to the present value. The notion of monsoon maximum interruptions within both S5 and S1 has been corroborated by anomalies in neodymium isotope data for planktonic foraminifera (Scrivner et al., 2004; Osborne et al., 2008, 2010).

It is obvious from the above that quantifying the net evaporative flux at times of sapropel deposition remains considerably model-dependent, and there is no model (yet) for the Mediterranean that resolves the general circulation as well as mixed-layer variability and δ^{18}O. Those would be essential requirements for a more detailed approach to past δ^{18}O distributions. At the same time, more observational data are required. Ganssen and Troelstra (1987) pioneered the use of δ^{18}O signatures of multiple planktonic foraminiferal species from different depth-habitats to discuss changes in Mediterranean surface-water stratification. Using this approach, Tang and Stott (1993) inferred that freshwater discharge into the eastern Mediterranean at the time of S1 occurred in the form of discrete, probably season-bound lenses, rather than as a 'lid' over the basin. Using a δ^{18}O box model for the seasonal cycle as recorded by a variety of planktonic foraminiferal species through S5, Rohling et al. (2004) found that maps of δ^{18}O anomalies as measured in the planktonic foraminiferal species *Globigerinoides ruber* (white) – the most commonly used species – are likely to overestimate freshwater influxes because this particular species appears to record freshwater impacts in a concentrated form, probably within or close to freshwater lenses near the very surface (similar to the conclusion for S1 by Tang and Stott, 1993). These studies illustrate that a whole-fauna perspective of isotope anomalies in sapropels is essential to avoid bias in interpretations, which greatly enhances the analytical effort and costs involved.

Finally, new methods are emerging for gauging past sea-surface salinities. For example, alkenone δ^{2}H changes through S5 in the northeastern Mediterranean have been used to suggest a strong (6 psu) surface salinity reduction (Van der Meer et al., 2007). However, combined interpretation with δ^{18}O, and inclusion of complete error propagation, yielded a somewhat smaller anomaly, and revealed that uncertainties are larger than the signal (-4.9 ± 6.9 psu at 1σ; Rohling, 2007). Hence, these methods are promising additions to the proxy-base for investigation of buoyancy changes associated with sapropel formation, but as yet remain insufficiently constrained and lacking in spatial coverage.

4.4. Vertical extent of anoxia, and organic δ^{15}N and δ^{13}C

Although more independent data are needed on the vertical extent of persistently anoxic/euxinic conditions from benthic foraminiferal and chemical analyses of sapropels in newly cored shallow-water settings (0–600 m), organic geochemical records of isorenieratene and its derivatives have already offered intriguing new insight. Isorenieratene is a specific aromatic carotenoid of anaerobic, photolithotrophic green sulphur bacteria (Chlorobiaceae), which require both sulphide and light, albeit at very low intensity. It thus constitutes a proxy for shoaling of the chemocline, which marks the top of euxinic waters, towards the surface where sufficient light is available, in analogy with present conditions in the Black Sea (Repeta et al., 1989; Koopmans et al., 1996; Passier et al., 1999b). This configuration was also inferred from trace metal studies (Passier et al., 1999b), and is colloquially referred to as 'photic layer euxinia' (e.g., Bosch et al., 1998; Passier et al., 1999b; Nijenhuis and De Lange, 2000; Menzel et al., 2002). Rohling et al. (2006) and Marino et al. (2007) reported isorenieratene derivatives in S5 samples of ODP Site 971A (South of Crete), and southeastern Aegean Sea core LC21, which needed to be reconciled with the apparently contradicting abundance of deep-dwelling planktonic foraminifera in the same samples, and with stable oxygen and carbon isotope records for various planktonic foraminiferal species that imply a mixed-layer system of considerable depth (~100 m) (Rohling et al., 2004). Rohling et al. (2006) explain this discrepancy by noting that the 'base of the photic layer' cited in papers concerning the habitat of Chlorobiaceae refers to a level of much lower irradiance than the conventional 1% irradiance level, causing the vertical expansion of anoxia during sapropel formation to be overestimated. Overmann et al. (1992) determined that irradiance at the Black Sea chemocline, where Chlorobiaceae are present, may be as low as 0.0005% of surface values. In the present-day western

Mediterranean, the 1% irradiance level occurs at up to 80 m depth (Algarra et al., 1988), and in the eastern basin it reaches up to 125 m (Berman et al., 1984; Abdel-Moati, 1990). The much lower irradiance levels required by Chlorobiaceae will be found considerably deeper.

Based on e-folding light attenuation with depth, an irradiance level ~4 orders of magnitude below 1% occurs around 300–375 m in the eastern basin, or 200–240 m in the western basin. Enhanced productivity at times of sapropel deposition may have caused stronger light attenuation than today. However, microfossil (foraminiferal, coccolith, diatom) and stable isotope records indicate that this productivity was focused in a deep chlorophyll maximum (DCM) below an oligotrophic mixed layer, which implies that deep light penetration remained important (cf. Rohling and Gieskes, 1989; Castradori, 1993; Kemp et al., 1999; Sachs and Repeta, 1999; Struck et al., 2001; Cane et al., 2002; Corselli et al., 2002; Rohling et al., 2004, 2006). This suggests a considerable thickness of habitable, oxygenated water above the chemocline. A first useful comparison would be the 150–200 m thick system above the Oxygen Minimum Zone in the Arabian Sea (cf. Ivanova, 1999; Peeters, 2000). A second constraint can be derived from glacial faunas from closely spaced cores SL-11 and SL-21 in the Aegean Sea (Casford et al., 2002, 2003). These differ in that the deepest-dwelling species *Globorotalia scitula* is absent in SL-11 (palaeo-water depth of 140 m) and continues in SL-21 (200 m), which suggests that a presence of *G. scitula* requires a water depth in excess of 140 m. Third, the rate at which climatically imposed δ^{18}O anomalies reduce with depth in a box-model representation of the mixed layer for S5 time-intervals suggests that *Neogloboquadrina pachyderma* (right coiling) and especially *G. scitula* lived at 100 m depth or more (Rohling et al., 2004). Finally, S5 sapropels from the South Cretan slope show complete absence of benthic foraminifera at and below 600 m (reflecting persistent anoxia), while persistence of benthics at 300 m depth (Rohling and Gieskes, 1989; Rohling et al., 1993a) suggests regular – if perhaps intermittent – oxygenation at that depth throughout S5. Taken together, these results suggest that the chemocline resided within a depth range of 150–300 m in the open eastern Mediterranean during the deposition of S5. Much of the range would be due to temporal (seasonal?) and regional variability. A mean value of ~200 m would imply that eastern Mediterranean light attenuation during S5 deposition was enhanced to values comparable to those observed today in the western Mediterranean.

Sedimentary nitrogen isotope ratios (δ^{15}N) show strong shifts to low values in sapropels, compared with non-sapropelic sediments (e.g., Calvert et al., 1992; Sachs and Repeta, 1999; Struck et al., 2001; Higgins et al., 2010; Möbius et al., 2010). Calvert et al. (1992) suggest that this results from different isotope fractionations during nitrate uptake under nutrient-rich and nutrient-poor conditions, so that the low δ^{15}N would reflect incomplete utilisation of dissolved nitrate during sapropel formation, due to enhanced near-surface nutrient concentrations. The authors allow for a change in their interpretation should high abundances of diazotrophic phytoplankton have prevailed during sapropel formation, since atmospheric nitrogen fixation would also cause a shift to low δ^{15}N because the ^{15}N/^{14}N ratio is much lower in atmospheric N_2 than in dissolved inorganic nitrogen (also Hood et al., 2000). Bouloubassi et al. (1999) suggest that this alternative option of Calvert et al. (1992) would match with inferences of stratified surface waters and DCM development (Rohling and Gieskes, 1989; Castradori, 1993; Rohling, 1994; Kemp et al., 1999). Mat-forming rhizosolenid diatom species, which were found to be especially abundant within S5, have active buoyancy control that allows them to migrate vertically through the photic layer (Corselli et al., 2002, and references therein), and are known to host abundant nitrogen-fixing symbionts (Zehr et al., 2000; Wilson, 2003).

Sachs and Repeta (1999) provide further evidence to the nitrogen fixation argument with δ^{15}N analyses of fossil chlorophyll (chlorins) in sapropel samples. They argue that the low δ^{15}N signals in sapropels reflect new production with an important component of atmospheric nitrogen fixation. From low δ^{15}N data in the modern Mediterranean, Sachs and Repeta (1999) infer that nitrogen fixation also occurred during non-sapropel times, and that high (bulk) δ^{15}N in non-sapropelic marls therefore reflects extensive diagenetic alteration of nitrogen isotope ratios in the presence of oxygen (a similar mechanism to that suggested for phases of "burn-down" of uppermost sapropel sections after the return of oxygenated bottom waters; Moodley et al., 2005). However, Higgins et al. (2010) managed to analyse chlorins from both sapropels and oxidised marls, and disagree about the proposed diagenetic alteration in the presence of oxygen. They find that modern conditions cannot be used in analogy of past oxidised marl deposition because modern conditions are anomalously biassed towards low δ^{15}N signatures due to anthropogenic aerosol N input (modern fixation rates are too low to invoke diazotrophy as the main source of fixed nitrogen; Bar Zeev et al., 2008). Higgins et al. (2010) conclude that high δ^{15}N in non-sapropelic marls reflects the isotopic composition of nitrogen used by surface water biomass at those times, where the nitrogen ultimately was supplied from the North Atlantic.

Sachs and Repeta (1999) consider that their findings support sapropel formation under stratified surface water conditions with a subsurface algal community (among which mat-forming diatoms with diazotrophic symbionts) above anoxic deep waters, but they do not infer any major change in the export productivity flux. Higgins et al. (2010) instead attribute low δ^{15}N values in sapropels to runoff-enhanced productivity, where phosphorus excess related to enhanced river flow would have caused a predominance of atmospheric nitrogen fixation. Möbius et al. (2010) also think (following a different line of argument) that N_2 fixation is a likely cause of low δ^{15}N in sapropels, but argue (in contrast to Higgins et al., 2010) that N_2 fixation equally prevailed in the eastern Mediterranean during non-sapropel times. For S5, Möbius et al. (2010) in addition consider that extremely low δ^{15}N values would be difficult to explain by either N_2-fixation from cyanobacteria or preferential uptake of $^{14}NO_3^-$ as a result of NO_3^- excess alone, but instead suggest a highly fractionating N-pathway such as chemoautotrophic NH_4^+ assimilation, which would agree with the aforementioned indications of a shallow chemocline during S5 deposition.

Studying S5, Struck et al. (2001) present a similar case in terms of nitrogen fixation (see also overview in Emeis and Weissert, 2009), but disagree with Sachs and Repeta (1999) about productivity during sapropel times, in a similar way as Higgins et al. (2010). Both Struck et al. (2001) and Higgins et al. (2010) infer that the total export flux had increased significantly during sapropel deposition, in contrast to Sachs and Repeta (1999) who considered that the Mediterranean remained a low nutrient and low flux environment. However, where Higgins et al. (2010) focus on enhanced river-flow for explaining the phosphorus excess that led to atmospheric nitrogen fixation, Struck et al. (2001) argue that an abundant supply of 'new' phosphorus was established by leakage from sediments overlain by anoxic waters. Struck et al. (2001) and Emeis and Weissert (2009) obtain their evidence for this phosphorus source from high C/P ratios in sapropels (Eijsink et al., 1997; Slomp et al., 2002). In the Struck et al. (2001) hypothesis, the subsequent mechanisms for nutrient advection from deep into surface waters are not explored in detail, but we infer that these may include both basin-scale and meso-scale circulation (e.g., Weldeab et al., 2003; Rohling et al., 2006), as well as 'uplifting' of old resident, anoxic deep waters due to injection of occasional pulses of new deep water (analogous to the effects of the EMT and WMT; see Sections 3.3.1 and 3.3.2), and subsequent 'erosion' of the nutricline by winter mixing (down to ~200 m in the Mediterranean). High initial abundances of reduced compounds within the ambient anoxic/euxinic water column during the deposition of the intense sapropel S5 may have 'titrated' out the oxygen from any newly injected waters, leaving little to no bio-available oxygen (e.g., Rohling et al., 2006). Hence, new deep-water pulses would be a viable mechanism to move nutrients from deep to shallow levels, without necessarily causing notable benthic repopulation. Regardless, some benthic repopulation potential has been demonstrated even within S5 (Schmiedl et al., 2003; Capotondi et al., 2006; Morigi, 2009), which indicates that – at least occasionally – some bio-available oxygen remained.

Another open issue concerns the interpretation of stable carbon isotope variations through sapropels. Krishnamurthy et al. (2000) report that $\delta^{13}C_{organic}$ in Pleistocene sapropels from the Tyrrhenian Sea (western Mediterranean) is higher than in non-sapropelic marls. They relate this shift to elevated algal production and accompanying decrease in the availability of dissolved CO_2 for subsequent production. An interruption within one of their sapropels displays a $\delta^{13}C_{organic}$ shift towards non-sapropelic values, interpreted as a temporary reduction of productivity (Krishnamurthy et al., 2000). In the eastern Mediterranean, Fontugne and Calvert (1992) and Nijenhuis and De Lange (2000) observe a reverse situation, where sapropels display lower $\delta^{13}C_{organic}$ values than non-sapropelic sediments. Fontugne and Calvert (1992) ascribe this to lowering of the $\delta^{13}C$ values of CO_2 used in photosynthesis due to increased freshwater flow into the eastern Mediterranean during sapropel formation, since freshwater not only contains dissolved inorganic carbon (DIC) with $\delta^{13}C$ of −5 to −10‰, but in addition carries dissolved and suspended organic carbon (e.g. humics) with $\delta^{13}C$ as low as −27‰. Nijenhuis and De Lange (2000) contest this view based on their observations that the depletions do not increase towards the Nile, but instead show an opposite trend. They favour an explanation that centres on selective preservation of isotopically light organic compounds during anoxic diagenesis. However, this test is imperfect because it has since been demonstrated that the Nile was not the only (or even the most important) route for monsoon floods (e.g., Rohling et al., 2002b, 2004; Osborne et al., 2008). In addition, diagenetic effects might perhaps explain part of the anomalies, but certainly not all, given that $\delta^{13}C_{carbonate}$ through sapropels in both the eastern (e.g., Tang and Stott, 1993; Rohling et al., 2004, 2006) and western Mediterranean (Bernasconi and Pika-Biolzi, 2000) is also lower than in non-sapropelic sediments. For the central Aegean Sea, Aksu et al. (1999) highlight yet another type of signal in the $\delta^{13}C_{organic}$ record through S1, namely one that fluctuates very little around an overall increasing trend from 11 to 2 ka BP. However, their compound-specific $\delta^{13}C_{16}$ and $\delta^{13}C_{18}$ records do show considerable depletions within the sapropel.

Overall, it appears that – whatever the direction of change – there often (but not always; Aksu et al., 1999; Struck et al., 2001) are notable shifts between sapropelic and non-sapropelic $\delta^{13}C_{organic}$. Influences of algal production rates and of freshwater input and diagenesis may be working in opposite directions. Compound-specific analyses may provide better insight into fluctuations in autochtonous components alone, compared with analyses that combine autochtonous and allochtonous organic-matter pools (Aksu et al., 1999). Clearly, more work is needed to clarify and validate the various alternative interpretations of $\delta^{13}C_{organic}$ changes through sapropels, and these interpretations must be tested against, and be consistent with, concomitant changes in $\delta^{13}C_{carbonate}$.

4.5. Productivity and preservation

Reported $\delta^{18}O$ ‘anomalies’ relative to background can differ greatly between sapropels (see Rohling et al., 2014, their Extended Data Fig. 1). This suggests variable buoyancy forcing between sapropels, due to freshwater input and temperature differences, but there is no straightforward proportionality between the severity of buoyancy forcing and sapropel C_{org} content. For example, sapropels i282 and i292, which date to 2.943 and 3.058 million years ago (Emeis et al., 2000b), have high C_{org} contents in excess of 10% (Nijenhuis et al., 1999), but are not marked by extreme $\delta^{18}O$ anomalies (see Rohling et al., 2014, their Extended Data Fig. 1). The same is true for S5 in SE Aegean core LC21, where C_{org} levels reach 14%, relative to other S5 sapropels with lower C_{org} levels but stronger $\delta^{18}O$ anomalies (Marino et al., 2007). Such findings imply additional impacts on the C_{org} content, likely due to differences in the total mass accumulation rates, export production flux, depositional depth, and C_{org} preservation between sapropels. This includes an old debate with respect to sapropel/organic-rich sediment deposition, namely that of the relative importances of productivity and preservation (e.g., Demaison and Moore, 1980; Cheddadi et al., 1991; Rohling, 1994; Cramp and O'Sullivan, 1999; Emeis and Weissert, 2009).

Ba/Al profiles through sapropels are generally considered to be among the most reliable information for palaeoproductivity reconstruction (e.g., Higgs et al., 1994; Thomson et al., 1995; Schenau et al., 1999; Thomson et al., 1999; Wehausen and Brumsack, 1999; Nijenhuis and De Lange, 2000; Mercone et al., 2001; Thomson et al., 2004; De Lange et al., 2008). Conditions that favour barite formation (decaying organic matter and silica) are especially found in recently dead siliceous plankton (Bishop, 1988). However, the Ba/Al peaks in sapropels reflect the Ba component that actually reached the sea floor with C_{org}, which suggests an implicit role of C_{org} preservation during settling through the water column and before burial. Addition of refractory organic matter into the deep sea can also affect the eventual ratio between C_{org} and biogenic Ba in sediments (Francois et al., 1995). Overall, Ba/Al data seem more closely related to the C_{org} burial flux than to palaeoproductivity levels, although post-depositional Ba loss from sediments cannot be excluded (Mercone et al., 2001), and these issues hinder efforts to obtain quantitative estimates of past C_{org} fluxes. Also, up to 5-fold differences between Ba/Al ratios in seven S1 sapropels show a systematic trend towards higher values with lower sediment accumulation rates, which indicates that these rates would need to be accounted for in detail (Mercone et al., 2000), which is not possible for most sapropels because of a lack of radiometric age control. Möbius et al. (2010) similarly argue against applicability of Ba/Al data to calculate primary productivity levels, and present a case based on $\delta^{15}N$ changes that no increase in export production (relative to the present) would be needed to explain formation of S1 (note that S1 is a low-C_{org} sapropel; De Lange et al. (2008) calculated a mean C burial flux of only 0.65 cm^{-2} kyr^{-1} for it).

Abundances of neogloboquadrinids are enhanced on a basin-wide scale in the planktonic foraminiferal faunas of most sapropels (but not S1), which qualitatively reflects the presence of a distinct DCM during their formation (Rohling and Gieskes, 1989; Corselli et al., 2002). This pattern is consistent throughout the Pliocene and Miocene (Schenau et al., 1999). An important portion of this taxon's diet consists of diatoms (Hemleben et al., 1989), suggesting a close relationship with abundance variations in diatoms and diatom-dependent dinoflagellates. Coccolith studies corroborated the hypothesis that a distinct basin-wide DCM was present during the deposition of most sapropels, with significantly elevated abundances of *Florisphaera profunda* relative to low abundances in non-sapropelic sediments (Castradori, 1993; Corselli et al., 2002; Thomson et al., 2004; Grelaud et al., 2012). Holocene sapropel S1 is exceptional in that it contains very few neogloboquadrinids, but *F. profunda* is abundantly present in S1 (Castradori, 1993; Thomson et al., 2004).

Organic-walled dinoflagellate cyst studies indicate elevated abundances of heterotrophic dinoflagellate taxa in sapropels (Targarona et al., 1997; Sangiorgi et al., 2003, 2006; Marino, 2008), mostly belonging to the genus *Protoperidinium* that by preference grazes on other microplankton, such as diatoms (Jacobson and Anderson, 1986). Whether this evidence can be ascribed to increased primary production during sapropels remains controversial, as there is no consensus on the relative importance of preservation versus productivity for the *Protoperidinium* cyst abundances in marine sediments (Zonneveld et al., 2001; Versteegh and Zonneveld, 2002; Reichart and Brinkhuis, 2003; Zonneveld et al., 2007). The opaline skeletons of the diatoms themselves would normally dissolve in the silica-undersaturated (eastern) Mediterranean (e.g., Ribera d'Alcalà et al., 2003), but may under exceptional circumstances be preserved (e.g., Kemp et al., 1999). Such conditions include a high flux of diatoms, so that bottom and pore water may temporarily become silica-saturated and (partial) preservation of opaline skeletons may ensue, and/or deposition in pockets of bottom water that have been isolated over long periods of time and become silica-saturated. Preservation of diatoms in sapropel S5 has been noted to the South and South-East of Crete, likely witnessing their important original contribution to the planktonic ecosystem during times of sapropel deposition (Schrader and Matherne, 1981; Corselli et al., 2002; Sangiorgi et al., 2006; Moller et al., 2012).

Sancetta (1994) speculated that fluxes of mat-forming diatoms may have been a driving factor of sapropel formation. Scanning Electron Microscope (SEM) investigation of high accumulation-rate sapropel S5 in ODP Hole 971C shows lamination that consists of seasonal diatom bloom deposits, with regular occurrence of mat-forming *Rhizosolenia* (also noted by Corselli et al., 2002; Moller et al., 2012), which was suggested to have inhabited a DCM setting (Pearce et al., 1998; Kemp et al., 1999). Assuming that the diatom biomass present within this S5 is representative of the original diatom flux during its formation throughout the eastern Mediterranean, Kemp et al. (1999) supported Sancetta's (1994) suggestion that diatom productivity may have accounted for a large proportion of the organic carbon present within S5. As noted before, Moller et al. (2012) argue that the open sediment fabric that results from deposition (and preservation) of large numbers of diatoms may account for the enlarged thickness of S5 in the region around Crete. It is not (yet) known whether the opal-rich versions of S5 represent the original nature of all S5 sapropels – in which case non-opal-rich S5 sapropels would represent remainder facies after opal dissolution – or whether there were strong regional differences in the original depositional environments. It also remains to be established whether abundant diatom deposition and/or enhanced preservation is specific only to S5, or whether (and to what extent) it applies also to other (strongly developed) sapropels.

Molecular (organic geochemical) compositions of sapropels in cores from the open eastern Mediterranean suggest that the major fraction of organic matter derives from marine algal sources, which corroborates similar conclusions based on organic carbon isotope analyses and organic petrographic studies (see overview in Bouloubassi et al., 1999). The sensitivity of biomarkers to oxidation has been used to infer that sapropels resulted not only from enhanced marine productivity, but that improved preservation played a crucial role as well (Bouloubassi et al., 1999). This supports previous inferences from marine pollen records that organic matter preservation was greatly improved during episodes of sapropel formation (Cheddadi et al., 1991). Comparing long-chain alkenone and C_{28} sterol data, Bouloubassi et al. (1999) infer that there are strong influences of diatoms in the organic matter of S5 and S7, and of prymnesiophytes in S6. On the basis of C_{30} sterols, they suggest that dinoflagellates dominated the production of organic matter incorporated in S7, while S5 appears to have received a dominant supply from diatoms. These findings, using established markers to distinguish between phytoplankton groups (Schubert et al., 1998), support the inferred importance of diatoms in S5 formation (see above), but also indicate that diatoms did not dominate the production of organic matter in all sapropels. Based on coccolith associations, Castradori (1993) also suggested a different mode of productivity for S6 than for other sapropels. Overall, there remains much uncertainty about the type, mechanism, and amount of primary/export production. Several lines of evidence indicate that some type of DCM was important during the formation of many sapropels, but as yet there are only broad suggestions concerning the dominant plankton groups in the various sapropels. Clearly, these need to be determined in more detail before proper ecological models for sapropel deposition can be developed and/or validated, and organic biomarker and possibly genetic assessments seem to be promising ways forward. In any case, it is already apparent that there is no 'one size fits all' solution — sapropels will need to be considered individually, or perhaps in 'families', for their ecological characteristics.

High abundances of chalcophilic and redox-sensitive elements in sapropels, and sulphur isotope indications of iron sulphide formation in the water column, suggest that the depositional environment was anoxic to anoxic-sulphidic (e.g., Calvert, 1983; Passier et al., 1996; Nijenhuis et al, 1998, 1999; Passier et al., 1999a,b; Nijenhuis and De Lange, 2000; Warning and Brumsack, 2000; Mercone et al., 2001). This corroborates the commonly observed benthic azoic conditions in sapropels. It is not clear whether these conditions developed abruptly, whether they represent the culmination of a slowly developing trend, or whether individual sapropels have different (rapid or slow) patterns of anoxia development. Elucidating these details will strongly advance understanding of the relative roles of C_{org} flux and reduced deep-water ventilation in driving deep-water oxygen depletion. Especially promising information comes from ecological studies of the deep-sea environment leading up to sapropel intervals. Even after almost 6 decades of study, only two sapropels have really been investigated in sufficient temporal and spatial resolution, and with sufficient (relative) age control, to allow specific assessments with validity over more than just a single site. These are Holocene S1 and last interglacial S5, and they are discussed below, including – where relevant – comments about other sapropels.

4.5.1. Sapropel S1

Benthic faunas in the Adriatic Sea suggest progressive eutrophication that started ~1000 years before the onset of S1, leading to severe low-oxygen stress ~200 years prior to the benthic azoic interval that marks the onset of true sapropel conditions in the Adriatic, with a radiocarbon convention age of ~8.3 ka (Rohling et al., 1997). Note that this S1 onset in the Adriatic is considerably later than the S1 onset in the open eastern Mediterranean (radiocarbon convention age of ~9.8 ka according to De Lange et al., 2008; i.e., ~10.5 cal. ka after Casford et al., 2002). Instead, the S1 onset in the open basin appears to be (approximately) coincident with the start of eutrophication in the Adriatic. Similar long-term development into sapropel conditions is typically found in benthic foraminiferal records through S1 from other relatively shallow settings, whereas the onset seems more abrupt in deeper settings (>2000 m) (Jorissen, 1999).

There are also indications that water-column stratification increased considerably before the S1 onset. Stable O and C isotope studies on sediment cores from the Aegean Sea suggest that enhanced water-column stratification especially developed from ~11.3 cal. ka (Casford et al., 2002), some 1500 years before the S1 onset in the Aegean Sea at ~10 cal. ka (Casford et al., 2002; Rohling et al., 2002a; Abu-Zied et al., 2008). The δ^{18}O change is also dated at ~11.5 cal. ka in the open eastern Mediterranean (De Lange et al., 2008), where the onset of S1 appears some 500 years earlier than in the Aegean Sea (~10.5 cal. ka, see above), making the offset there ~1000 years. Note that these δ^{18}O indications of stratification are not so much an abrupt shift, but more an acceleration upon a longer trend towards increasing stratification, which started as early as 17 cal. ka (Fig. 8).

Benthic foraminiferal faunas suggest that organic flux to the sea floor remained low in the interval prior to S1 deposition in the Aegean Sea, and only increased close to the S1 onset at ~10 cal. ka (Abu-Zied et al., 2008). Conversely, data for the Adriatic Sea (notably core IN68-9; Fig. 1) show a rapid increase in organic flux to the sea floor from ~9.8 cal. ka, over a period of 1000 years, prior to the S1 onset in that basin at ~8.8 cal. ka (Rohling et al., 1997). Again this suggests that the Adriatic simply had a delayed onset of benthic azoic S1 conditions, and that it experienced benthic eutrophication (while still oxygenated at the sea floor) when sapropel deposition had started already in the rest of the eastern Mediterranean. This suggests that some new subsurface water formation continued in the Adriatic during (at least) that early phase, providing enough to oxygenate its own sea floor but largely failing to accomplish that in the open eastern Mediterranean.

We infer the following qualitative sequence of events for S1 (Figs. 8, 9). Deglacial sea-level rise caused a progressive surface buoyancy increase within the Mediterranean, preconditioning the basin for a stratification episode. Superimposed, an accelerated shift in δ^{18}O-based stratification indications occurred at ~11.5 cal. ka, likely marking the onset of monsoon intensification. Conditions of increasing stratification and attendant decreasing deep-water oxygenation drove onset of sapropel deposition from ~10.5 cal. ka in the open eastern Mediterranean. Some differences in the onset timing from that date occur, which likely reflect regional differences in water depth, sediment accumulation rates, C_{org} fluxes, and/or vicinity to continuing (weakened) sources of deep/intermediate-water formation (Kuhnt et al., 2007). By ~10 cal. ka, the surviving benthic faunas in the Adriatic and Aegean sub-basins (where limited deep-water formation remained active enough to ensure some bottom oxygenation) record an increase in sea-floor eutrophication (Abu-Zied et al., 2008). The associated increase in biological oxygen demand soon (~10 cal. ka) overcame deep oxygenation in the Aegean (although not to fully azoic conditions; Kuhnt et al., 2007; Triantaphyllou et al., 2009), and after some more time (~8.8 cal. ka) also in the Adriatic. From then on, the Aegean and Adriatic Seas were marked by highly restricted benthic faunas (Casford et al., 2003; Kuhnt et al., 2007) and in some intervals reached azoic conditions. A widespread S1 'interruption' between ~8.5 and ~7.8 cal. ka (Rohling et al., 2002a) marks a return of significant deep-water oxygenation, down to at least 1500 m water depth (e.g., Mercone et al., 2001; Casford et al., 2003; Kuhnt et al., 2007; Abu-Zied et al., 2008). De Lange et al. (2008) infer from geochemical signatures that impacts of such reventilations were limited to the upper ~1800 m. Similar reventilation events are widespread in many sapropels, and even extend down to 2000 m waterdepth in the open eastern Mediterranean during S6 (Casford et al., 2003; Schmiedl et al., 2003). Apart from the distinct signature of the S1 'interruption', we note that oxygen-dependent benthic trace faunas continued throughout S1 in the Aegean (Casford et al., 2003; Kuhnt et al., 2007; Triantaphyllou et al., 2009) and on the Libyan margin down to 1400 m (Casford et al., 2003), which strongly suggests continuation of limited deep-water ventilation. Casford et al. (2003) suggest that, for sapropels containing these features, persistent anoxia may have been limited to depths below ~2000 m (*sensu* De Lange et al., 2008), while only a 'blanket' of anoxic conditions draped over the sea-floor topography existed at shallower levels (underneath a severely dysoxic water column). Occasional oxygenation of the blanket during a cooler spell over the basin then allowed re-establishment of benthic trace faunas. Potentially, the blanket was established and maintained due to fast-sinking organic-rich material, such as diatom mats and faecal pellets. Support for this concept came from a biogeochemical model of sapropel formation (Bianchi et al., 2006), in which such a blanket developed as a direct consequence of allowing a separation between slow and fast sinking organic matter. Note that for more conclusive results, such a sinking-rate concept needs to be viewed in a time-transient 3-dimensional context against potential remineralisation rates in the water column, including factors such as depth, temperature, oxygenation state, type of productivity (constant versus pulsed), etc.

4.5.2. Sapropel S5

Jorissen (1999) reports that depth-dependent trends in the onset of anoxic conditions for S6 seem roughly similar to those for S1. However, he also shows that the trends are different for the onset of S5, which seems relatively gradual regardless of depth. Schmiedl et al. (2003) corroborate this for S5, reporting that – even in their deepest (2158 m) site M40-4/67SL – there is a stepwise reduction of deep-water ventilation that started ~3000 years before the S5 onset. Cane et al. (2002) note considerable diachroneity for S5 in the onset of benthic azoic conditions, a key criterion for the presence of persistent sea-floor anoxia. They

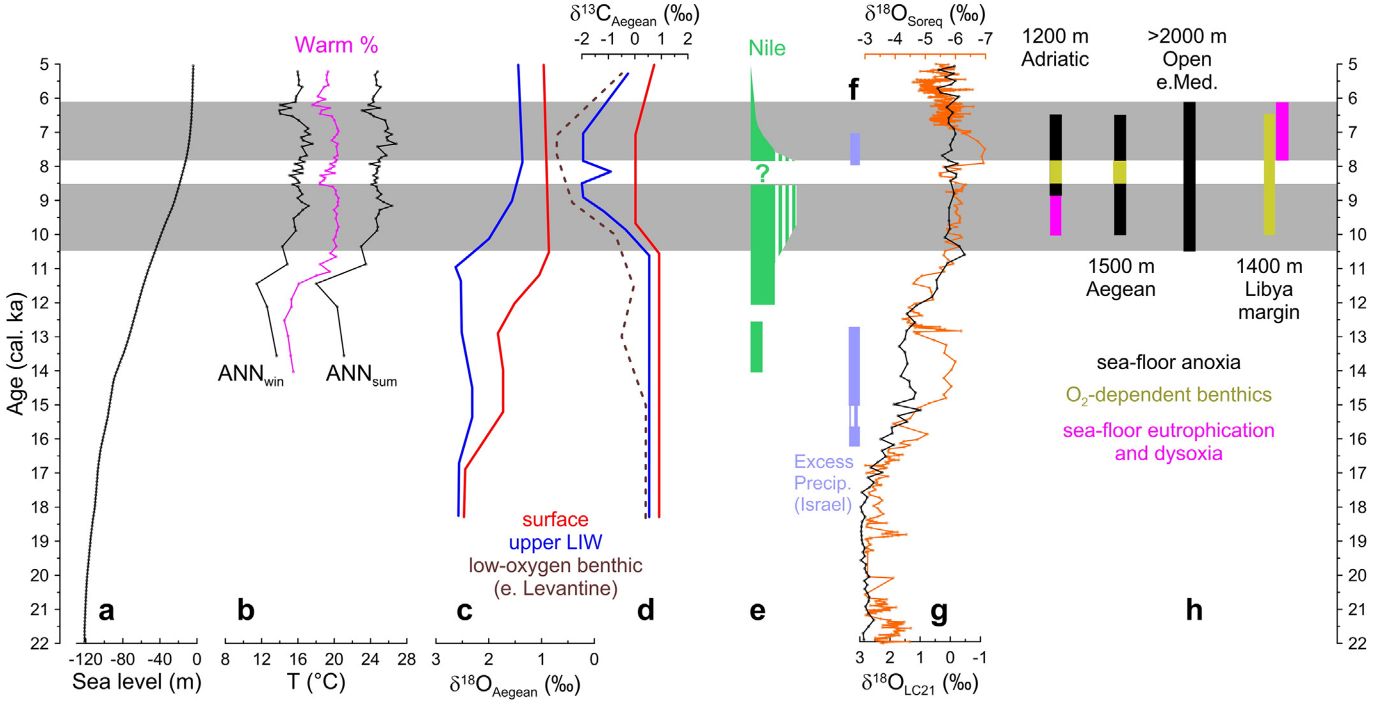

Fig. 8. Schematic sequence of events through the last deglaciation and sapropel S1. a. Sea-level change (median reconstruction of Stanford et al., 2011). b. Temperature reconstructions for southeastern Aegean core LC21. Artificial Neural Network, ANN, reconstructions for winter and summer (Marino et al., 2009) and warm planktonic formaniniferal species percentage (Rohling et al., 2002a). c. Schematic summary of oxygen isotope ratios for surface (*G. ruber* white), upper LIW (*N. pachyderma* dextral), and low-oxygen tolerant benthics (redrawn and modified after Casford et al., 2002; Grimm et al., submitted for publication). d. As c but for carbon isotope ratios. e. Intervals of intensified Nile discharge (solid green after Revel et al., 2010; hatched green after Marino et al., 2009; Weldeab et al., 2014). f. Potential increase in precipitation in Israel, deduced from g. g. Comparison on identical scales of oxygen isotope ratios in Soreq Cave speleothems (orange) and surface waters at northeastern Aegean core LC21 (black) (synchronised data after Grant et al., 2012). Where cave data are substantially more negative than surface-water data, fractionation likely occurred between the evaporative source and the cave-catchment waters, which may indicate enhanced precipitation via an amount–effect relationship. h. Key sea-floor observations through S1 (colours as explained in the legend; references as given in main text).

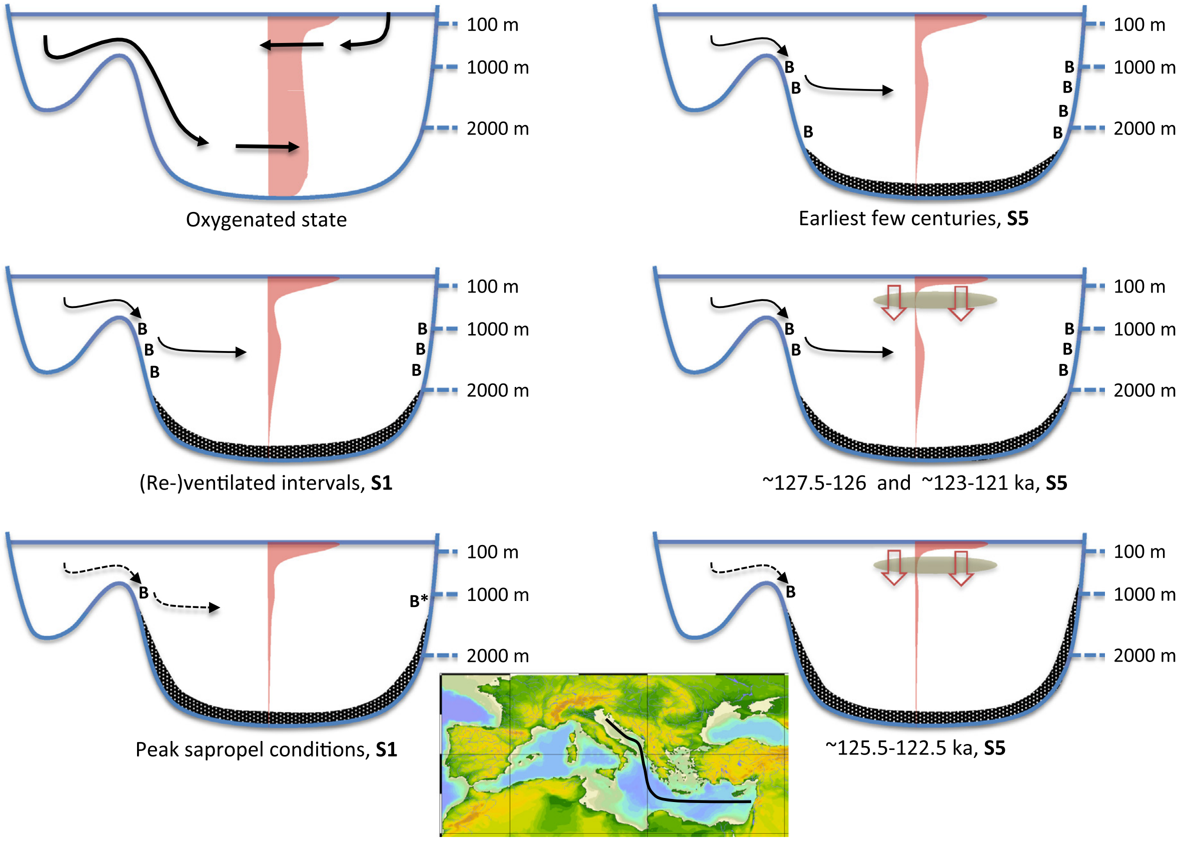

Fig. 9. Highly schematic and simplified interpretations of key observations within sapropel S1 and S5, along a transect shown in the inset (not to scale). The top-left panel shows a 'modern-type' oxygenated state. Below that, two 'ventilation states' are indicated for S1, which alternated with one another on a variety of timescales (see text). The three right-hand panels depict different stages of S5. 'B' implies presence of benthic faunas in the deep-sea during sapropel episodes (B* refers to an observation off the transect, of benthics on the Lybian margin; Casford et al., 2003). Dark hatching indicates anoxic sea-floor environments and pink profiles imply inferred water-column oxygenation levels. Black arrows represent rough estimates of subsurface circulation. Olive shading indicates presence of 'photic layer' euxinia (isorenieratene presence). Open arrows reflect inferred intensification of export productivity. This figure needs to be viewed in conjunction with discussion and references in the main text, as synthesised in Fig. 8 for S1, and Fig. 10 for S5.

inferred the offset from a multi-parameter correlation framework (as validated by Capotondi et al., 2006), and it is strongly corroborated by comparing the onset of benthic azoic conditions with the timing of the large drop in surface-water δ^{18}O, a virtually synchronous marker between all sites that is related to basin-wide change in hydrological forcing (Cane et al., 2002; Rohling et al., 2002b; Capotondi et al., 2006; Marino et al., 2007). The sea-floor anoxia associated with S5 deposition seems to have developed first in the western and central parts of the eastern Mediterranean, and only 400–600 years later in the easternmost sector (Cane et al., 2002).

Capotondi et al. (2006) quantified benthic assemblages in several additional S5 sapropels, over a water-column depth range from 3224 m to 933 m, and instead suggest that benthic populations 'crashed' due to the onset of persistent anoxia (or severe dysoxia in their shallowest core) approximately simultaneously in all their records, at about 200–300 years after the midpoint of the large surface-water δ^{18}O shift. Other studies, however, report an even closer association between onset of anoxic conditions and the surface-water δ^{18}O shift. These records with relatively early onsets in core M40-4/67SL (2158 m; S of Crete; Schmiedl et al., 2003) and BAN89-GC09 (2011 m; S of Crete; Morigi, 2009) complement similarly early onsets in nearby ODP Site 971A (2016 m; Cane et al., 2002) and core KS205 (2384 m, northern Ionian Sea; Cane et al., 2002). However, Schmiedl et al. (2003) show a distinctly late onset in their shallower site (GeoTüKL83, 1433 m; Israel margin), where anoxia is noted ~15 cm higher in the core (= roughly 2000 years later) than the surface-water δ^{18}O shift. Intriguingly, the δ^{18}O shift in that latter core coincides with an increase in C_{org} fluxes to the sea floor and an associated drop in sea-floor oxygenation. Hence, the shallow, eastern site of GeoTüKL83 seems to have 'immediately felt' the early change in conditions (which in the deep sites rapidly led to anoxia), but subsequent anoxia took time to develop in GeoTüKL83.

The observations can be compared with a concept of water-depth dependent 'expansion' of anoxia from intermediate depths down to the greatest depths (e.g., Strohle and Krom, 1997; Stratford et al., 2000). It is then found that such a concept cannot be reconciled with the delayed onset of S5 anoxia in ODP Site 967C (2554 m; South of Cyprus), relative to other sites at or below 2 km depth, nor with the rather early (only ~200–300 years after the δ^{18}O shift) 'crash', but low-level continuation, in benthic populations at 933 m depth in the northeastern Ionian Sea (Capotondi et al., 2006) and very late onset of anoxia in GeoTüKL83 (Schmiedl et al., 2003). Moreover it seems that expansion of euxinic conditions up to ~200 m water depth at ODP Site 971A, South of Crete (Rohling et al., 2006), must have been a regionally specific development, given that benthic faunas continued (in low numbers) throughout S5 at 933 m (Capotondi et al., 2006; Morigi, 2009). Moreover, sea-floor anoxia seems to have developed with a multi-century lag in 2470 m deep site BD02-GC01, relative to site BAN89-GC09 (2011 m; Morigi, 2009), ODP Site 971A (2016 m; Cane et al., 2002), core M40-4/67SL (2158 m; Schmiedl et al., 2003), and KS205 (2384 m; Cane et al., 2002), which also deviates from a concept of depth-dependence.

Another highly resolved S5 record, from the southeastern Aegean Sea (Marino et al., 2007), was correlated in detail (with a 1σ error of <1 cm) to the multi-proxy stratigraphy of Cane et al. (2002) and Capotondi et al. (2006). Marino et al. (2007) infer that the vast majority of freshwater forcing behind S5 deposition came from the North African margin (hence African monsoon); this is supported by neodymium

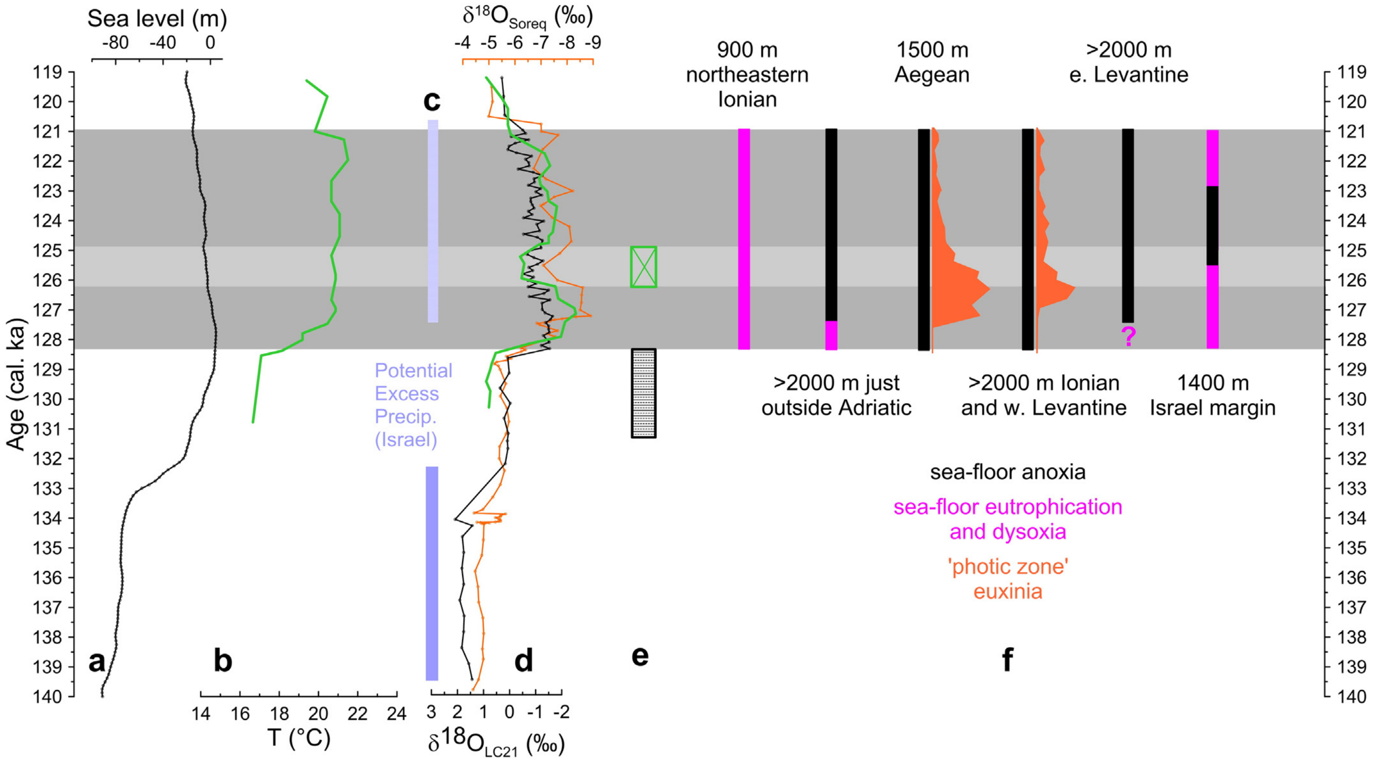

Fig. 10. Schematic sequence of events through the penultimate deglaciation and sapropel S5. a. Sea-level change (probability maximum of Grant et al., 2012, 2014). b. Temperature reconstruction for open eastern Mediterranean ODP Site 971A (Rohling et al., 2002b). c. Potential increase in precipitation in Israel, deduced from d. d. Comparison on identical scales of oxygen isotope ratios in Soreq Cave speleothems (orange) and surface waters at northeastern Aegean core LC21 (black) (synchronised data after Grant et al., 2012), and for ODP Site 971A (green; Rohling et al., 2002b). Where cave data are substantially more negative than surface-water data, fractionation likely occurred between the evaporative source and the cave-catchment waters, which may indicate enhanced precipitation via an amount-effect relationship. Given that the offsets differ when taken relative to LC21 or relative to Site 971A, the amount-effect contribution through S5 is debatable (hence, hatched). e. Indication of 3-kyr lead up to S5 of stepwise ventilation reduction (Schmiedl et al., 2003; black hatched), and of monsoon interruption during S5 deposition (Rohling et al., 2002b, 2004; Osborne et al., 2008) (green crossed box). f. Key observations through S5 (colours as explained in the legend; references as given in main text).

evidence for a lack of substantial northern freshwater inputs at that time (Osborne et al., 2010). Marino et al. (2007) also found that this surface-freshening influence affected the southeastern Aegean in less than ~40 years, where it instantly resulted in a collapse of Aegean deep-water ventilation. Within ~650 years, euxinic conditions had then expanded to ~200 m water depth in the Aegean, which predates a similar development in the open eastern Mediterranean (ODP Site 971A) by several centuries (Marino et al., 2007).

We infer the following sequence of events for the onset of S5 (Figs. 9, 10). First, a step-wise reduction in deep-water formation started ~3000 years prior to S5 deposition (Schmiedl et al., 2003), probably in response to gradual freshening of the basin due to sea-level rise (cf. Rohling, 1994) after the Marine Isotope Stage (MIS) 6 glaciation (for sea level see Grant et al., 2012; Rohling et al., 2014). Then followed a major reduction in deep-water ventilation, which affected all sites at about the same time, in direct response to the abrupt onset of North African monsoon flooding. Sea-floor anoxia developed with different timings at different locations: (a) virtually immediately after the monsoon onset at ~1500 m in the SE Aegean and at sites between 2000 and 2400 m in the central and western sectors of the eastern Mediterranean; (b) ~500 years later at ~2500 m depth South of Cyprus and just south of the Adriatic Sea; and (c) another ~2000 years later at 1433 m on the Israel margin (all timings based on the S5 from Grant et al., 2012). At 933 m depth in the northeastern Ionian Sea (core SIN97-GC01), just outside the Aegean Sea, bio-available oxygen availability persisted throughout the deposition of S5, in stark contrast with persistently anoxic/euxinic conditions up to ~200 m depth within the Levantine Sea and southeastern Aegean Sea. We propose that the spatially differentiated timings for the start of sea-floor anoxia likely reflect spatial differences in C_{org} flux to the sea floor, in response to spatial (export) productivity gradients and/or spatial ecosystem differences that affected the 'packaging' of sinking matter in different proportions of fast- versus slow-sinking particles (e.g., Kemp et al., 1999; Casford et al., 2003; Schmiedl et al., 2003; Weldeab et al., 2003; Bianchi et al., 2006; Rohling et al., 2006), and/or any regionally persistent new subsurface water formation, likely in the Adriatic since Aegean overturn seems to have ceased very rapidly (Marino et al., 2007).

The very rapid onset of sea-floor anoxia in the southeastern Aegean Sea (Marino et al., 2007) suggests that it did not develop due to oxygen depletion of the entire water column (which would take some 500–600 years; Béthoux, 1993; Rohling, 1994), but that it instead occurred via development of an anoxic 'blanket' that was draped over the sea-floor topography (and which reached fully anoxic states most rapidly under the most productive areas; cf. dynamic concept of Casford et al., 2003). Bianchi et al. (2006) suggest that this may be indicative of ecological changes that favour a fast-sinking export productivity flux (see also Kemp et al., 1999). Next, S5 developed into a more extreme mode than S1, in that indications of euxinic conditions at ~200 m depth, near the base of the photic layer (see Section 4.4), appeared in the Aegean Sea some 650 years after the onset of monsoon flooding, and a few centuries later also in the open eastern Mediterranean (Rohling et al., 2006; Marino et al., 2007). This expansion of euxinic conditions may have started at a mid-depth maximum of biological oxygen demand (an Oxygen Minimum Zone; OMZ), rather than all the way up from the sea floor, so that a certain amount of bio-available oxygen may have persisted for hundreds to 1000+ years in between the OMZ and an abyssal anoxic layer (see Bianchi et al., 2006). Support for such a 'split anoxia' concept for S5 comes from continuation of benthic faunas for about 2000 years at 1433 m depth on the Israel margin (Schmiedl et al., 2003), from some minor benthic repopulation potential within S5 even at abyssal sites (Schmiedl et al., 2003), and from continuation of benthic faunas throughout S5 at 933 m depth in the north-eastern Ionian Sea (Capotondi et al., 2006; Morigi, 2009). Finally, we note that the inference of Strohle and Krom (1997), that anoxia first developed in an OMZ and then progressively expanded downward, seems at odds with the information summarised here for both S1 and S5, unless it is meant that this progressive expansion occurred over such a short period of time (a century or so) that it is undetectable in the records.

4.6. Internal variability

Although surface-water δ^{18}O records through many sapropels show a generally light anomaly with lowest values in the bottom one-third section of the sapropel, these curves are not smooth in detail. Instead, they contain distinct internal variability with sharp transitions, which has since been supported by high-resolution studies using a variety of proxies (among many others, Rohling et al., 1993b, 1997; Emeis et al., 2000b; Mercone et al., 2000, 2001; Corselli et al., 2002; Rohling et al., 2002a,b; Casford et al., 2003; Emeis et al., 2003; Schmiedl et al., 2003; Sperling et al., 2003; Rohling et al., 2004; Scrivner et al., 2004; Capotondi et al., 2006; Rohling et al., 2006; Sangiorgi et al., 2006; Marino et al., 2007; Abu-Zied et al., 2008; De Lange et al., 2008; Kotthoff et al., 2008; Osborne et al., 2008; Marino et al., 2009; Jilbert et al., 2010; Ní Fhlaithearta et al., 2010). These studies reveal two main types of variability within periods of sapropel deposition; one concerns variability in African monsoon flooding, and the other concerns variability in northerly climatic influences on the Mediterranean (notably, cooling). Responses within the basin commonly included intermittent weakening, or even interruption, of sapropel formation (often with benthic repopulations in between azoic intervals). In particular cases, enough intermittent deep-water oxygenation persisted to sustain a low-level benthic fauna throughout (large parts of) the sapropels (e.g., Rohling et al., 1997; Casford et al., 2003; Schmiedl et al., 2003; Capotondi et al., 2006; Morigi, 2009; Triantaphyllou et al., 2009).

Neodymium isotope data from planktonic foraminifera indicate that monsoon-related flooding from the Blue Nile and Atbara – which drain the Ethiopian highlands that consist of relatively young, radiogenic volcanics – was marked by two discrete maxima within both S1 and S5, separated by an interruption of the monsoon maximum (Scrivner et al., 2004). Recent work suggests that the ‘interruption’ of S1 marks the onset of a (stepwise) decline in monsoon flooding (Revel et al., 2010; Weldeab et al., 2014). Interruption of the freshwater dilution in the middle of S1, around 8 cal. ka BP, has also been inferred from δ^{18}O residuals calculated for several S1 sapropels by correction for ice-volume effects and (alkenone-based) SST variations (Emeis et al., 2000b). At around the same time, a pronounced (2–3 °C) cooling event occurred with a focus on the Adriatic and Aegean Seas (Rohling et al., 1997; De Rijk et al., 1999; Hayes et al., 1999; Geraga et al., 2000; Mercone et al., 2000, 2001; Rohling et al., 2002a; Casford et al., 2003), which also had wide-ranging regional impacts in terrestrial palaeoclimate and archaeological archives (e.g., Ariztegui et al., 2000; Clare et al., 2008; Pross et al., 2009; Weninger et al., 2009; Peyron et al., 2011). A coeval cool/arid event has also been identified in marine records for the western Mediterranean (Cacho et al., 2001, 2002). Emeis et al. (2000b) observe little cooling around 8 ka in S1 from the open eastern Mediterranean, which suggests that cooling was predominantly registered in regions directly influenced by Atlantic/high-latitude continental air masses (Rohling et al., 2002a; Casford et al., 2003; Marino et al., 2009; Weninger et al., 2009) and left insignificant mean SST signals over the open eastern Mediterranean. The concomitant aridity signal seems more widespread, mostly between about 8.5 and 7.8 ka, and is registered both in the Mediterranean borderlands (Hassan, 1998; Bar-Matthews et al., 1999; Ariztegui et al., 2000; Casford et al., 2001; Kotthoff et al., 2008; Peyron et al., 2011), and in the North African monsoon region (e.g., Gasse, 2000; Mayewski et al., 2004; Rohling and Pälike, 2005). The notion (De Rijk et al., 1999; Revel et al., 2010; Weldeab et al., 2014) that this episode marked the onset of climate deterioration, following the peak (early S1) of the Holocene interglacial, was corroborated by Jilbert et al. (2010), who found less frequent (300–600 year) ventilation variability during early S1, and more frequent (100–300 year) variability during late S1.

Coincidence between cooling and enhanced aridity around the Mediterranean and interruption of the insolation-driven monsoon maximum was also noted for a millennial-scale episode within last interglacial sapropel S5 (cf., Frogley et al., 1999; Rohling et al., 2002b; Schmiedl et al., 2003; Rohling et al., 2004; Scrivner et al., 2004; Capotondi et al., 2006; Sprovieri et al., 2006). Schmiedl et al. (2003) argue that this episode marked the onset of regional climate deterioration following the peak (early S5) of the last interglacial. In that case – using S5 start and end dates of 128.34 and 120.97 ka (Grant et al., 2012) and an assumed linear sedimentation rate through S5 (as in Rohling et al., 2002b) – this regional climate deterioration began at ~126 ka, soon after the ~127.5 ka onset of negative (dropping) rates of sea-level change after the last interglacial maximum (Grant et al., 2012).

In terms of circulation response to these events, it has been noted in records from the Adriatic and Aegean Seas that the cool/arid episode within S1 at ~8 ka saw temporary repopulation by benthic molluscs and foraminifera, which attests to improved ventilation and sea-floor oxygenation, in agreement with geochemical data (e.g., Van Straaten, 1966, 1972; Rohling et al., 1997; Mercone et al., 2001; Casford et al., 2003; Abu-Zied et al., 2008; Jilbert et al., 2010). Repopulation events are not unique to S1, but are known also from Pliocene sapropel C2 from the Monte Singa section (Rohling et al., 1993b), S6 (e.g., Casford et al., 2003; Schmiedl et al., 2003), and S5 (e.g., Schmiedl et al., 2003; Capotondi et al., 2006; Morigi, 2009), while other sapropels have distinctly ‘split’ appearances (e.g., S4; Grant et al., 2012) or contain intervals with deep-dwelling planktonic faunas (S7 and S8; Casford et al., 2003), which also suggest episodic re-ventilation. The inferred link between temporarily increased buoyancy loss (cooling and aridity) and increased deep-water ventilation was supported by numerical modelling experiments (Myers and Rohling, 2000), which showed that the Myers et al. (1998) sapropel mode of circulation would show immediate ventilation responses in the Adriatic and Aegean Seas when 2–3 °C cooling was imposed over those regions. Hennekam et al. (2014) infer that, at their site close to the Nile outflow, deep-water oxygenation (inferred from C_{org} and V/Al changes) improved within S1 at ~8 ka despite an absence of change in export production (inferred from Ba/Al), strengthening the case that this event was primarily driven by increased deep-water ventilation.

Even today, cooling over the northern sectors of the Mediterranean is strongly related to short and intense episodes of cold continental air outbreaks in winter that are orographically channelled towards the Mediterranean, and the frequency of such events shows considerable inter-annual variability (see Section 2.1). Moreover, historical data support the existence of distinct multi-century ‘clusterings’ of such episodes of more intense/frequent winter cooling (Yavuz et al., 2007). A stable O and C isotope study of several planktonic and benthic foraminiferal species through S1 in the Aegean Sea revealed that occasional ventilation occurred down to the sea floor even within the ‘peaks’ of S1 development, and that such ‘ventilation bursts’ occurred at least once – probably more often – within the interval of time covered by each sample (~50 years) (Casford et al., 2003). Jilbert et al. (2010) corroborate such variability on inter-decadal to inter-centennial timescales. Casford et al. (2003) propose that there were certain years or decades that were characterised by more frequent and/or intense cold outbreaks over the basin, leading to more frequent and/or intense deep ventilation bursts. The longer-term aliasing of such interannual/-decadal variability imposed by the ~50-year sampling interval would then generate the appearance of an extended episode that was on the whole colder and better ventilated.

4.7. Termination

Termination of sapropel deposition is difficult to discuss, as it strongly depends on how 'sapropel' is defined. If done on the basis of C_{org} concentrations or colour, then post-depositional processes (downward sulphidisation at the base, and especially 'burn-down' at the top) may cause spurious temporal offsets between sites, masking any real regional temporal differences due to different sea-floor oxygenation, export productivity fluxes, water-depth, etc. If done on the basis of Ba/Al anomalies, then the 'sapropel' may contain (intervals with) considerable abundances of benthic fauna, and thus mask spatial and depth-dependent complexities of sea-floor oxygenation. If done on the basis of benthic azoic conditions, then many 'sapropels' would not be sapropels at all because they contain benthic foraminifera throughout; e.g., the S5 interval of Capotondi et al. (2006) and Morigi (2009) at 933 m depth in the northeastern Ionian Sea would not be a 'sapropel' at all in that definition, even though it coincided in time with other, intensely developed S5 intervals with azoic sea-floor conditions and even water-column euxinia. If done on the basis of the surface-water $\delta^{18}O$ anomaly, then regional differences in its expression and amplitude (e.g., Marino et al., 2007) would potentially bias comparisons between sites, and also the $\delta^{18}O$ anomaly occupies a wider depth-range than other sapropel criteria within individual sediment cores (De Lange et al., 2008). For sake of comparisons between sites and studies, however, some level of agreement is needed. Following arguments presented for S1 by De Lange et al. (2008), a Ba/Al anomaly seems one of the best, easy-to-apply criteria, as long as care is taken not to impose it too rigidly between locations, depth zones, and sedimentary environments (see also Mercone et al., 2001). Extra care is needed in low accumulation-rate settings, where 'burn-down' is especially prominent. In high-accumulation sites, with limited 'burn-down', C_{org} levels (and, secondarily, sediment colour) may provide reasonable (but not perfect) approximations of the 'Ba/Al-based sapropel'. On that basis, some generalised statements can be made about 'sapropel terminations' and the processes leading up to those, as listed in the following.

Recolonisation of the sea floor by benthic faunas was distinctly diachronous between sites. In the northeastern Ionian Sea at 933 m depth, the sea floor never seems to have reached a persistently azoic state during S5 (Capotondi et al., 2006), suggesting some possible continuation of deep-water outflow from the Adriatic (Section 4.5.2). On the Israel margin at 1433 m depth, benthic recolonisation of S5 occurred early, within its upper 1/3 portion (Schmiedl et al., 2003). At deep (~2000 m or more) sites in the open eastern Mediterranean, the sea floor seems to have been (predominantly) azoic throughout virtually all of S5 (Schmiedl et al., 2003; Capotondi et al., 2006). Regardless of these regional differences in when the first benthic faunas became re-established, and of any short-term repopulation events within sapropels, there appears to be a remarkable increase in benthic populations and diversity at the very end of S5, which from comparison with surface-water $\delta^{18}O$ changes appears to closely coincide with the termination of monsoon flooding (Schmiedl et al., 2003; Capotondi et al., 2006). This change seems to mark a sharp and widespread (basinwide) onset of deep-water oxygenation due to resumption of strong convective deep-water formation.

Similar cases can be formulated for the basin-wide ending of S1. Benthic foraminiferal faunas in two Aegean cores at ~700 and ~1000 m depth strongly imply continuation of some deep-water formation in the North Aegean throughout S1 (Kuhnt et al., 2007), supporting similar inferences based on stable isotope data from that region (Casford et al., 2003). Also, a major benthic repopulation event is found within S1 (e.g., Rohling et al., 1997; Mercone et al., 2001; Kuhnt et al., 2007; Abu-Zied et al., 2008; Schmiedl et al., 2010). Geochemical signals in S1 suggest persistent changes in ventilation intensity in 300–600 to 100–300 year cycles (Jilbert et al., 2010). However, no matter whether some benthic faunas continued through all, part, or hardly any portion of S1, the faunas that indicate resumption of strong reoxygenation at the top of S1 are recognisably distinct from those 'survivor faunas' (e.g., Mercone et al., 2001; Casford et al., 2003; Kuhnt et al., 2007; Abu-Zied et al., 2008). Again similar impressions can be gleaned from S6 (Schmiedl et al., 2003).

Overall, the 'terminal' benthic repopulations commonly start within the uppermost portions of the visual sapropels, and then show a remarkable succession of faunas as repopulation and ecosystem recovery progress over hundreds to thousands of years above the sapropels (cf., references in the paragraphs above). Note that all individual sapropels show their own specific benthic faunal succession, and that the above descriptions represent a strongly generalised view of the sea-floor ecosystem changes. For more complete descriptions, we refer to Jorissen (1999) and references listed in this section.

5. Deep-water renewal and implications for western versus eastern Mediterranean sapropel formation

In the western Mediterranean, Plio-Pleistocene sapropels have been most notably deposited in the Tyrrhenian Sea (Emeis et al., 1991; De Kaenel et al., 1999; Murat, 1999), although they also exist in other parts (De Kaenel et al., 1999; Murat, 1999). Older sapropels are well known from the pre-Messinian Betic strait region, southern Spain (Krijgsman et al., 1999; Sierro et al., 1999; Krijgsman et al., 2001). Emeis et al. (1991) propose that Tyrrhenian sapropels, with C_{org} levels up to ~6%, likely formed because of impeded WMDW ventilation below about 2000 m depth; that is, at levels below Tyrrhenian Deep Water (TDW). Thus, it is not directly relevant to focus on changes in the exchange through the Strait of Sicily and their impacts on TDW formation. Instead, we need to compare and contrast conditions of true deep-water (WMDW and EMDW) renewal between the western and eastern Mediterranean basins.

As outlined above, deep water is today formed in both the eastern and western Mediterranean basins, as a result of strong buoyancy loss by evaporation and cooling. Stommel et al. (1973) argued that there are two main ways for deep water to 'escape' from below the sills in the Straits of Sicily and Gibraltar. One is through upward advection and admixture into the outflowing intermediate water, and the other is through Bernouilli aspiration from deeper layers up and over the sill. Upward advection and admixture into outflowing layers is greatly assisted by injection of new deep water into the deep basins, which 'lifts up' existing water masses (e.g., Bryden, 2009; and direct EMT and WMT observations reviewed above). This route of deep-water removal dwindles to insignificance when deep-water formation becomes inhibited (as during periods of sapropel formation). Bernoulli aspiration of water from below sill depth up and over the sill depends, in essence, on the velocity of the outflow and the density gradient below sill depth.

Rogerson et al. (2008, 2012a) were the first to quantitatively assess deep-water aspiration changes in palaeo-scenarios, based on a formulation from Seim and Gregg (1997). However, results need to be reconsidered because both studies (Rogerson et al., 2008, 2012a) erroneously refer the ratio of vertical density gradient over surface layer density ($\Delta\rho/\rho_0$) to the inflowing Atlantic water density. Instead, it should refer to LIW, the main outflowing water mass, which significantly affects the interpretations. In the following, we evaluate the implications of this correction, which will help foster a better understanding of the processes (and their sensitivities) behind western versus eastern Mediterranean sapropel formation.

As reviewed above, outflow velocity is high (order 1 m s^{-1}) in the Strait of Gibraltar and low (order 0.2 m s^{-1}) in the Strait of Sicily, while density stratification below sill depth is stronger in the eastern Mediterranean (~0.03 kg m^{-3}) than in the western basin (~0.02 kg m^{-3}). These numbers can be used in the formulation of

Seim and Gregg (1997) to estimate the maximum Bernoulli aspiration depth, or 'stagnation depth' (d):

$$d = -\left(0.5H_2 + \left[0.25H_2^2 + \frac{u^2}{g\frac{\Delta\rho_v}{\rho_0 H_1}}\right]^{0.5}\right) \tag{1}$$

where H_1 is the scale depth in the open basin (set to 2000 m as the depth below which deep waters are virtually homogenous), H_2 is the depth of the sill in the strait (present-day values of 284 m and 440 m for the Straits of Gibraltar and Sicily, respectively), u is mean outflow velocity (in m s^{-1}), g is the acceleration due to gravity (9.81 m s^{-2}), ρ_0 is density of the outflowing layer at the sill (~1027 kg m^{-3}), and $\Delta\rho_v$ is the vertical density gradient below sill depth, on the interior (Mediterranean) side.

We calculate that Bernoulli aspiration in the western Mediterranean today reaches mean depths in excess of 2500 m (well within the, in terms of density, virtually homogenous WMDW). We thus agree with Stommel et al. (1973) that – at current outflow velocities – Bernoulli aspiration can remove waters from the entire deep western Mediterranean, so that there are two feasible mechanisms for removal of that deep water. In contrast, use of the eastern Mediterranean values in Eq. (1) highlights that Bernoulli aspiration over the Strait of Sicily only reaches as deep as ~800 m. Hence, Bernoulli aspiration by itself cannot account for the removal of all deep water from today's eastern Mediterranean; in that basin, full deep-water removal critically depends on injection of new deep waters.

These findings clarify why – in a marginal sea with the same overall climatic forcing – sapropel formation would be more prevalent in the eastern basin than in the western basin. That contrast is especially intriguing because – today – surface primary productivity and organic export flux to the sea floor are considerably lower in the eastern basin than in the western basin (Antoine et al., 1995; De Rijk et al., 2000). Rather than attributing the contrast to such things as focussing of freshwater inputs (via the Nile and/or wider North African margin), or intensification of West to East moisture distribution by Mediterranean depressions, we here propose that it simply results from different controls on deep-water removal between the two basins. In the eastern basin this removal is critically dependent on formation of new deep water with the same or higher density than existing waters. In contrast, the western basin also has strong Bernoulli aspiration, which helps to remove old deep waters even during times of reduced/inhibited new deep-water formation.

The more efficient mode of western Mediterranean deep-water renewal will have implications for organic-rich layer (ORL) development in that basin. Rohling (1994) qualitatively suggested that, behind the Strait of Gibraltar, a Mediterranean 'deep-water stagnation potential' may develop during deglaciations, because sea-level rise would cause: (a) continuous freshening of Atlantic inflow, which together with climatic warming would make it harder for surface waters to reach the high densities of existing deep waters (a pre-requisite for deep-water injection); and (b) an opening up of the Strait profile area, reducing density contrasts across it and thus potentially the exchange velocities, while at the same time freshening and warming of surface waters would increase the vertical density gradient below sill depth. These combined influences would impose progressive surface buoyancy gain, and thus reduce potential for new deep-water formation, and in addition cause reduction of Bernoulli aspiration. Grimm et al. (submitted for publication) use a numerical model to argue that progressive deglacial buoyancy gain may be critical for (deglacial) sapropel formation in the eastern Mediterranean (but note that, there, Bernoulli aspiration is weak even today). To assess impacts on the western Mediterranean, we here use Eq. (1) following Rogerson et al. (2008, 2012a), with corrected interpretation of the $\Delta\rho/\rho_0$ term.

Note that we are not attempting to simulate reality, but instead aim to reasonably approximate changes in the parameters that govern exchange through the strait, to see whether and how these would affect Bernoulli aspiration and the potential for convective deep-water renewal in the western Mediterranean. This allows us to investigate the sensitivity of Bernoulli aspiration to a range of idealised forcing scenarios, which will distinguish the more important controls, which in turn may guide further interpretations about deep-water renewal potential.

We approximate changes in Atlantic inflow salinity (S_{in}) with sea level/ice volume based on ~1 unit mean ocean salinity change for ~120 m sea-level lowering, starting at a present-day $S_{in.p} = 36.2$, with a modern $T_{in.p} = 16$ °C (Bryden and Kinder, 1991), where the subscript marker p stands for present-day. Changes in exchange transport due to strait profile reduction with sea level are approximated (Rohling, 1991a, 1994; Rohling and Bryden, 1994) using a scale factor $\Phi = 1 - 0.5(z_{sl} / -120)$, where z_{sl} is sea level relative to the present (negative for a drop), based on median values from Stanford et al. (2011). Scaling present-day values so that the net excess of evaporation over total freshwater input (X_p) is 1, Atlantic inflow through the Strait of Gibraltar is $Q_{in.p} = 17.692$, and outflow is $Q_{out.p} = Q_{in.p} - 1$ (proportions after Bryden et al., 1994). Conservation of salt dictates that the salinity of outflow is $S_{out} = (Q_{in} / Q_{out})S_{in}$. Thus, we find $S_{out.p} = 38.4$, close to observations, which also show that $T_{out.p} = 13.15$ °C (Kinder and Parrilla, 1987). Considering palaeo-scenarios, we follow Rogerson et al. (2008) in scaling u-variations proportionally to $\Delta\rho_{out-in}/\Delta\rho_{out-in.p}$, but we additionally impose that the absolute glacial-interglacial range of u-changes must be consistent with passage of our reconstructed Q_{out} fluxes through the (sea-level dependent) depth and width (and thus area) of the outflow-occupied portion of the strait, following Bryden and Kinder (1991), Rohling and Bryden (1994) and Rohling (1994, 1999). For modern conditions, this gives $u_p = 1$ m s^{-1}, consistent with observations (see Section 3.2). For the last glacial maximum, we find u values of ~1.4 m s^{-1}. Changes in density and density gradients are considered in simple linear relationships relative to changes in salinity and temperature, using approximate coefficients for haline contraction $\beta = 0.77$ kg m^{-3} psu^{-1} and thermal expansion $\alpha = -0.2$ kg m^{-3} $°C^{-1}$. Thus, we specify that $\Delta\rho_v = \alpha\Delta T_v + \beta\Delta S_v$.

We solve Eq. (1) for records of change in the input parameters that schematically approximate reconstructed changes over the last 22 ky, as summarised in Rogerson et al. (2008). Estimated records for the input parameters are shown in Fig. 11. Changes in ΔT_v are approximated as $\Delta T_v = \Delta T_{v.p}\,(1 - kT_{\mathrm{history}})$, where $\Delta T_{v.p}$ is the modern temperature gradient between deep water and outflowing intermediate water (−0.4 °C; Kinder and Parrilla, 1987), and T_{history} is a non-dimensional scale factor with a range from 0 for the present to −1 for the coldest period, with temporal variations based on the temperature history of Martrat et al. (2004) over the past 22 ky. This calculation is set up with $k = 0$, 1, or 2, so that ΔT_v in the coldest period reaches 1×, 2×, or 3× the modern value $\Delta T_{v.p}$, respectively. This parameter is found to be a key control on the reconstructed results; we use the intermediate scenario with $k = 1$ as our 'main case' and the others as sensitivity tests.

We impose idealised, asymmetric, surface-water salinity anomalies with an amplitude of −2 in the Atlantic inflow during Heinrich event 1 (17.5–16.5 ka) and melt-water pulse 1a (14.7–14.3 ka) (after Rogerson et al., 2008) (Fig. 11a). Note that these anomalies have attenuated impacts on LIW (the main contributor to outflow); we use a simple constant volumetric attenuation factor $f = 1/5$ because an inflowing anomaly will – at most – occupy the upper 100 m in the basin (the inflowing layer), while LIW occupies a depth range of 200–700 m, which is 5× more voluminous. Temperature changes in LIW are similarly set using $f = 1/5$ relative to temperature changes at the surface (with the latter variations set after Martrat et al., 2004). This yields variations in $T_{\mathrm{out}} - T_{\mathrm{in}}$ as portrayed in Fig. 11b. We also impose an idealised, asymmetric, surface-water salinity anomaly during sapropel formation (10.5–6.0 ka), interrupted by an event with a salinity anomaly of 0

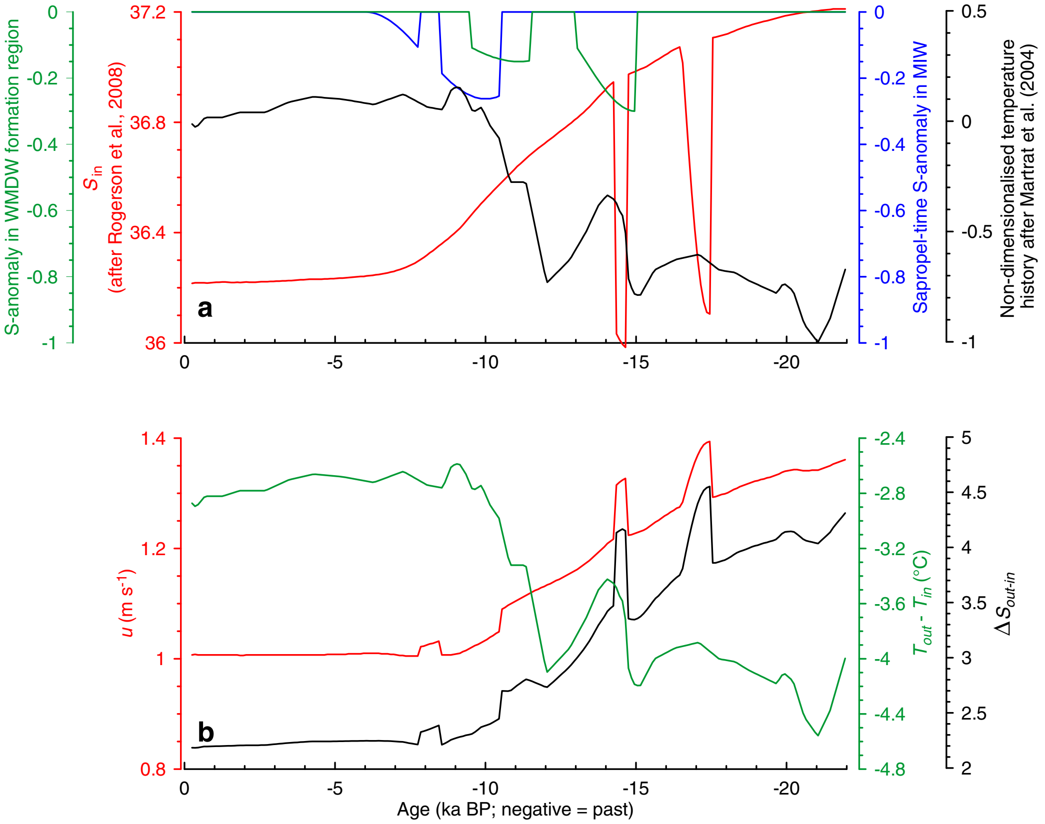

Fig. 11. Parameter variations used in the calculations, and as explained in the Section 5. a. Schematically prescribed surface salinity changes in the WMDW formation area (green); changes in inflowing Atlantic surface-water salinity (red; after Rogerson et al., 2008); schematically prescribed MIW salinity anomalies due to monsoon flooding into the eastern Mediterranean at times of sapropel deposition (blue); and non-dimensionalised variability in temperature after Martrat et al. (2004), relative to the range between the minimum and 0 ka (black). b. Calculated changes in the velocity of subsurface outflow through the Strait of Gibraltar (red); calculated changes in the temperature contrast between outflow and inflow in the Strait of Gibraltar (green); calculated changes in the salinity contrast between outflow and inflow in the Strait of Gibraltar (black).

(giving a density change nearly equivalent to 1 °C cooling; 8.5–7.8 ka) (Fig. 11a). When we impose salinity anomalies to the Mediterranean due to monsoon flooding during sapropel (S1) formation, we use a mean surface-water salinity anomaly of -0.7 (Rohling, 1999), and a volumetric attenuation factor $\zeta = 1.5/4$ for LIW property change (Rohling et al., 2004). In addition to the salinity anomalies that are explicitly imposed, we consider a reduction in evaporation due to cooling, following the 20% reduction for full glacial times calculated by Rohling (1999), and linearly scaled according to the temperature variability of Martrat et al. (2004) (Fig. 11a).

In times when newly formed deep water – according to the imposed forcing of each time-step's ΔT_v along with a deep water salinity that is 0.06 (Kinder and Parrilla, 1987) lower than intermediate water salinity – reaches a sufficient density to replace existing deep water, we impose that deep-water properties fully adjust within each 100 y calculation time-step, to a temperature ΔT_v cooler than intermediate-water temperature, and a salinity 0.06 lower than intermediate-water salinity. Conversely, when the combined salinity and temperature (ΔT_v) forcings are not conducive to transformation of surface waters into waters with a density higher than existing deep waters, we allow only diffusive mixing to alter the properties of deep water, using an e-folding timescale for deep-water property changes of $\tau = 500$ y (Casford et al., 2002). A sensitivity test is done for the impact of deviation from this value to 1000 y.

In the 'best-estimate' experiment ($k = 1$ and $\tau = 500$ y; Fig. 12b,b′), Bernoulli aspiration through the Strait of Gibraltar (red line) reached down to 2000 m most of the time between 22 and 10.5 ka, and below 2500 m between 6.5 and 0 ka. The meltwater influences of H1 and mwp-1a caused brief shoaling events in the Bernoulli aspiration depth, up to ~1500 m. The (interrupted) monsoon flooding of S1 caused a longer-term shoaling to ~1250 m between 10.5 and 8.3 ka, then a rapid deepening during the S1 interruption event, and finally a brief shoaling event to ~1500 m between 7.8 and 6.5 ka. The period of ORL1, which formed in the Alboran Sea with a C_{org} content up to ~1% between ~14.5 and ~8.2 ka (Martinez-Ruiz et al., 2003; Rogerson et al., 2008), does not stand out as a special period in terms of changes in the Bernoulli aspiration depth. Although the general longer-term underlying shape of the calculated d record is highly sensitive to the selected value of k, the sensitivity experiments with $k = 2$ and $k = 0$ do not offer any help to better understand the timing of ORL1 (Figs. 12a,a′ and 8c,c′). Further sensitivity experiments (with $k = 1$), in which we switch off any reduction in evaporation due to cooling over the entire experiment (Fig. 12d,d′), or we increase τ to 1000 y rather than 500 y (Fig. 12e,e′), do not help to form a better understanding of the timing of ORL1 either. If anything, the combined experiments would suggest that – in terms of Bernoulli aspiration – ORL1 would most likely have coincided with the initial phase of S1 (10.5–8.3 ka), or at most a somewhat extended interval up to 10.5–5.65 ka (i.e., comparable to eastern Mediterranean S1). It appears, therefore, that for the combined forcings considered here, the timing of ORL1 cannot be viewed as a straightforward consequence of (only) changes in the Bernoulli aspiration depth. This contrasts with inferences made by Rogerson et al. (2008, 2012a), due to our corrected use of the $\Delta\rho/\rho_0$ term.

Our calculations also allow some basic insight into the potential for new formation of WMDW of sufficient density to replace existing 'old' WMDW. For the main experiment ($k = 1$ and $\tau = 500$ y; Fig. 12b,b′), shifts of the blue line to values greater than -0.06 indicate that new WMDW formation was briefly inhibited during both H1 and mwp-1a,

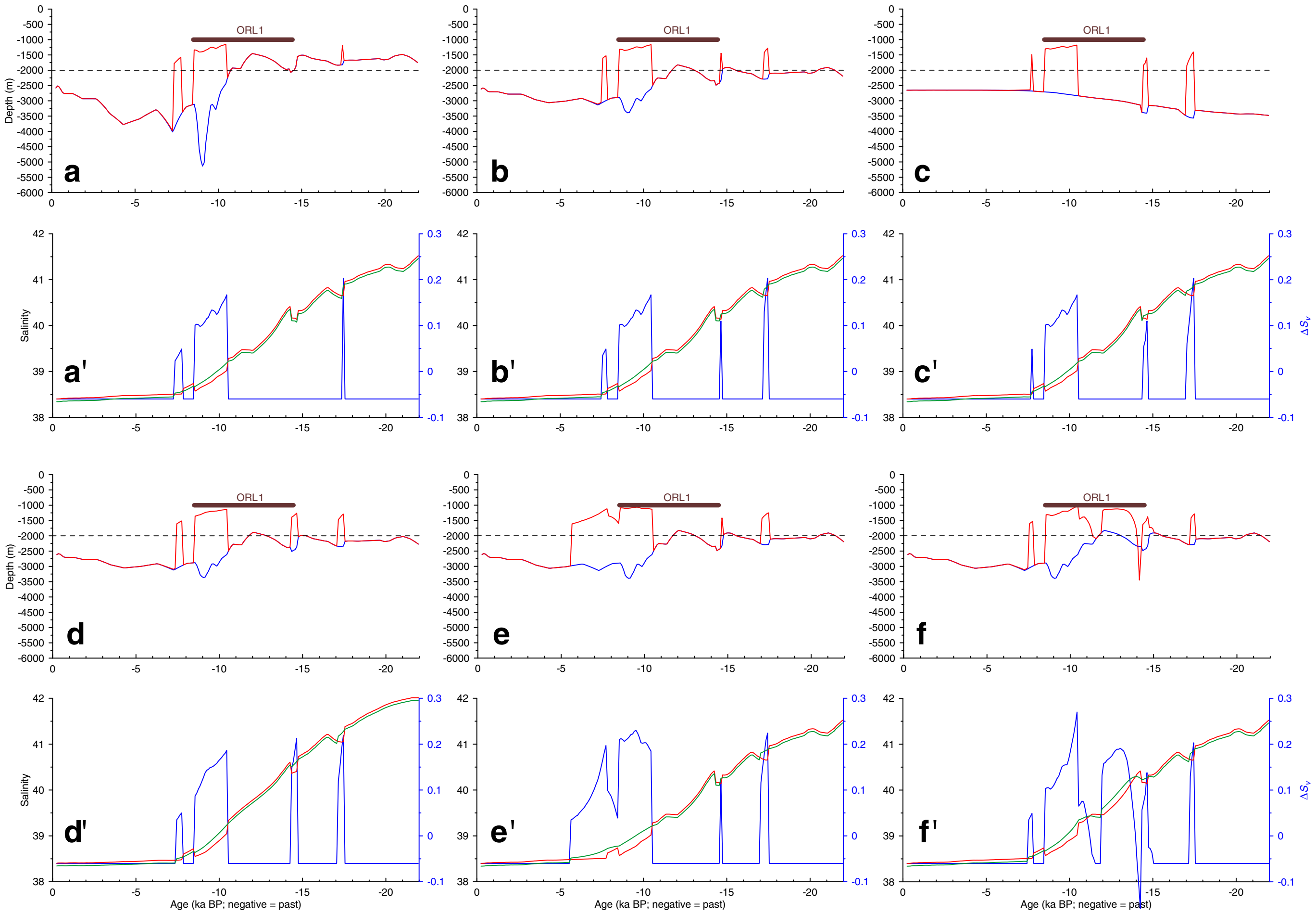

Fig. 12. Results of our experiments for different scenarios, where each scenario is represented by a pair of plots, e.g., a-a′, b-b′, etc. Panels a–f show calculated history of the maximum depth of Bernoulli aspiration from the western Mediterranean, for a case without (red) and with (blue) salinity anomalies during Heinrich Event, mwp-1a, and sapropel S1. Also indicated is the duration of ORL1 after Martinez-Ruiz et al. (2003) and Rogerson et al. (2008) (brown bar). Panels a′–f′ show reconstructed salinities of MIW (red) and WMDW (green), along with the offset between these (blue). During periods with convective overturn, $S_{WMDW} = S_{MIW} - 0.06$ (see text). During other times, WMDW properties change only due to diffusion (then, $S_{WMDW} > S_{MIW} - 0.06$; i.e., the blue line goes up). Panels b–b′ present results for the experiment of our 'best-estimate' scenario ($\tau = 500$ y; $k = 1$; 20% evaporation reduction due to cooling). All other panel sets represent the same scenario, but with change in one parameter. Panels a–a′ and c–c′ assess the impact of $k = 2$ and $k = 0$, respectively. Panels d–d′ include no evaporation reduction due to cooling relative to the present. Panels e–e′ consider $\tau = 1000$ y. Panels f–f′ present a scenario identical to the 'best estimate' case, but include direct salinity reductions of 0.3 and 0.15 at the WMDW formation region in two 2-ky events between 15 and 13 ka and between 11.5 and 9.5 ka, respectively (see text), to assess the impacts of likely Alpine melt-water routing at the time via – especially – the Rhone river.

and for more extend periods between 10.5 and 8.3 ka, and 7.8 and 6.5 ka (i.e., the period of eastern Mediterranean S1 deposition). Sensitivity experiments with $k = 2$ and $k = 0$ are rather similar (Fig. 12a,a′ and c,c′). The same is true for the sensitivity experiments (with $k = 1$) in which we switch off any reduction in evaporation due to cooling over the record (Fig. 12d,d′), or we increase τ to 1000 y rather than 500 y (Fig. 12e,e′). Only the sensitivity experiment with $\tau = 1000$ y shows a significant difference, in that the period with reduced WMDW formation potential due S1 monsoon flooding extends all the way from the onset of the flooding at 10.5 ka to 5.5 ka, which is a full 1 ky after the ending of monsoon flooding (Fig. 12e,e′). Regardless, none of the inferred intervals of WMDW inhibition seems to approximate the observed timing of ORL1.

It appears from these calculations that the observed timing of western Mediterranean ORL1 cannot be (fully) explained by changes in either Bernoulli aspiration and/or temporary inhibitions of new WMDW formation due to only sea-level rise, melt-water pulses into the Atlantic, and monsoon flooding into the eastern Mediterranean. Consequently, we investigate whether superimposed effects of Alpine melt-water input, via major southwestern European rivers (notably the Rhone) into the WMDW formation region, may have been important (see Rogerson et al., 2008). To test this, we impose such changes in two 2-ky events between 15 and 13 ka and between 11.5 and 9.5 ka (to span the key intervals of global sea-level rise; Rogerson et al., 2008; Stanford et al., 2011). We find that imposed salinity anomalies of as little as −0.30 and −0.15, respectively (Fig. 11), suffice to cause a remarkable change in both the Bernoulli aspiration depth and new WMDW formation potential (Fig. 12f,f′), and that the duration of the simulated period with shallow Bernoulli aspiration and inhibited WMDW formation becomes comparable with the timing of ORL1. Thus, we infer that ORL1 likely resulted from a complex interaction between the effects of sea-level rise, melt-water pulses into the Atlantic, monsoon flooding, and Alpine melt-water routing into the NW Mediterranean during the main phases of deglaciation.

Note that, in the absence of 'complications' such as Alpine melt-water routing into the NW Mediterranean, our calculations suggest that western Mediterranean sapropel deposition would be rather similarly timed to eastern Mediterranean sapropel deposition. This is mainly because LIW is an effective means for transporting (eastern Mediterranean) impacts of monsoon flooding – notably salinity reduction – into the western Mediterranean, where they then adversely affect convective WMDW formation. We therefore agree with Emeis et al. (1991) that this seems to be the most likely trigger for sapropel deposition in the deep Tyrrhenian Sea, which would explain why western Mediterranean sapropels commonly appear to correlate well with those in the eastern Mediterranean (De Kaenel et al., 1999; Murat, 1999). Especially during Alpine deglaciations, however, this correlation may be perturbed, as in the case of ORL1 (Martinez-Ruiz et al., 2003; Rogerson et al., 2008).

6. Conclusions

Strong hydrological forcing of the Mediterranean occurs at times of sapropel formation due to astronomically induced monsoon flooding from North Africa into the (eastern) Mediterranean Sea. For sapropels associated with a deglaciation, progressive buoyancy gain due to the deglaciation likely causes long-term preconditioning towards a stagnation event. The contribution of E–P developments around the Mediterranean borderlands remains unclear, as do the changes in these conditions through the several thousands of years spanned by sapropel periods. But it is apparent that any regional moisture increases derive predominantly from the Mediterranean Sea itself, with any excess precipitation on the Mediterranean borderlands most likely focussed on winter.

Any enhanced Mediterranean moisture flux during times of sapropel formation (likely related to Mediterranean depression activity) would – at best – not affect the Mediterranean Sea's overall hydrological budget by much, since any runoff from it into the basin would originate from evaporative loss out of the same basin. At worst, it may shift the Mediterranean hydrological budget into a net ‘drier’ direction, since net moisture export into other basins' watershed areas (e.g., the Jordan Valley and Dead Sea rift, the Red Sea, or the Tigris/Euphrates and Persian Gulf) would represent a potential increase in net evaporative loss from the Mediterranean Sea. The most important influence of enhanced Mediterranean depression activity during times of sapropel deposition likely was a contribution to ‘flattening’ of W–E salinity gradients within the basin.

Alpine meltwater contributions may be essential for early onsets of western Mediterranean sapropel (or organic-rich layer; ORL) deposition during deglaciations. Outside deglaciations, western Mediterranean sapropels likely are mechanistically related (and thus broadly coeval) to eastern Mediterranean sapropels. However, this opens the question why sapropels occur more frequently in the eastern basin than in the western basin. We propose that the eastern Mediterranean is more sensitive to development of deep-sea anoxia than the western Mediterranean, because of differences in the efficiency of deep-water renewal. In the eastern basin, deep-water renewal is essentially governed by a single process, namely formation of new deep water of sufficient density. In the western basin, however, two major processes are at play, namely both injection of new deep waters of sufficient density, and effective Bernoulli aspiration of deep waters into outflow from the basin through the Strait of Gibraltar.

We find extensive evidence of spatial and depth-dependent gradients, as well as major temporal variability, in all key environmental parameters within individual sapropel episodes, including physical changes, ecosystem responses, intensity and extent of oxygen depletion, carbon burial, etc. This applies to all sapropels considered, despite differences between separate sapropel episodes. Note also that the various responses are relative to time-integrated forcings over centuries to millennia, rather than instantaneously coeval with forcing changes. This complicates the search for cause-and-effect relationships relating to the processes behind sapropel formation (a good example is the likely long-term impact of deglaciations on basin preconditioning).

Overall, it is well established that sapropel formation occurs within broader episodes, associated with monsoon maxima, during which strong surface buoyancy gain (with or without the additional influence of deglaciations) sets up a deep-water ventilation crisis. However, superimposed site-specific, depth-dependent, and temporal variabilities within each episode clearly indicate that actual sapropel deposition during such episodes of is governed by a remarkably dynamic system with constraints from – and interactions between – physiography, physics of circulation, ecology, (bio-)geochemistry, etc. As a consequence, general patterns and event sequences may be found to agree between individual sapropels from the same episode (say, last interglacial S5), but specific details match only over relatively small spatial and depth scales. We anticipate that the strongest potential for deconvolving the exact mechanisms behind sapropel deposition lies in improved documentation and understanding of their regional variability.

Acknowledgements

We dedicate this review to our friend, student, and colleague James S.L. Casford, who passed away much too early in 2014. In Casford et al. (2003), James presented the first outline of a dynamical system concept for times of sapropel deposition. We thank the editor and two reviewers for support and suggestions. This study contributes to Australian Laureate Fellowship FL120100050.

References

Abdel-Moati, A.R., 1990. Particulate organic matter in the subsurface chlorophyll maximum layer of the southeastern Mediterranean. Oceanol. Acta 13, 307–315.

Abell, P.I., Hoelzmann, P., 2000. Holocene palaeoclimates in northwestern Sudan: stable isotope studies on molluscs. Glob. Planet. Chang. 26, 1–12.

Abu-Zied, R.H., Rohling, E.J., Jorissen, F.J., Fontanier, C., Casford, J.S.L., Cooke, S., 2008. Benthic foraminiferal response to changes in bottom water oxygenation and organic carbon flux in the eastern Mediterranean during LGM to Recent times. Mar. Micropaleontol. 67, 46–68.

Adamson, D.A., Gasse, F., Street, F.A., Williams, M.A.J., 1980. Late Quaternary history of the Nile. Nature 288, 50–55.

Adloff, F., Mikolajewicz, U., Kucera, M., Grimm, R., Maier-Reimer, E., Schmiedl, G., Emeis, K.-C., 2011. Upper ocean climate of the Eastern Mediterranean Sea during the Holocene Insolation Maximum — a model study. Clim. Past 7, 1103–1122.

Aksu, A.E., Abrajano, T., Mudie, P.J., Yaşar, D., 1999. Organic geochemical and palynological evidence for terrigenous origin of the organic matter in Aegean Sea sapropel S1. Mar. Geol. 153, 303–318.

Algarra, P., Estrada, M., Niell, F.X., 1988. Phycobiliprotein distribution across the western Mediterranean divergence. Deep-Sea Res. 35, 1425–1430.

Alhammoud, B., Béranger, K., Mortier, L., Crépon, M., 2005. Surface circulation of the Levantine Basin: comparison of model results with observations. Prog. Oceanogr. 66, 299–320.

Anastasakis, G.C., Stanley, D.J., 1984. Sapropels and organic-rich variants in the Mediterranean: sequence development and classification. In: Stow, D.A.W., Piper, D.J.W. (Eds.), Fine-grained Sediments: Deep-water Processes and Facies. Geological Society of London, pp. 497–510.

Antoine, D., Morel, A., André, J.M., 1995. Algal pigment distribution and primary production in the eastern Mediterranean as derived from coastal zone scanner observations. J. Geophys. Res. 100, 16.193–16.209.

Antonov, J.I., Seidov, D., Boyer, T.P., Locarnini, R.A., Mishonov, A.V., Garcia, H.E., 2010. World Ocean Atlas 2009 Volume 2: Salinity. In: Levitus, S. (Ed.), NOAA Atlas NESDIS 69. U.S. Government Printing Office, Washington, D.C. (184 pp.).

Ariztegui, D., Asioli, A., Lowe, J.J., Trincardi, F., Vigliotti, L., Tamburini, F., Chondrogianni, C., Accorsi, C.A., Bandini Mazzanti, M., Mercuri, A.M., Van der Kaars, S., McKenzie, J.A., Oldfield, F., 2000. Palaeoclimate and the formation of sapropel S1: inferences from Late Quaternary lacustrine and marine sequences in the central Mediterranean region. Palaeogeogr. Palaeoclimatol. Palaeoecol. 158, 215–240.

Armitagea, S.J., Drake, N.A., Stokes, S., El-Hawat, A., Salem, M.J., Whitee, K., Turnerf, P., McLaren, S.J., 2007. Multiple phases of north African humidity recorded in lacustrine sediments from the Fazzan basin, Libyan Sahara. Quat. Geochronol. 2, 181–186.

Arnone, R.A., Wiesenburg, D.A., Saunders, K., 1990. The origin and characteristics of the Algerian current. J. Geophys. Res. 95, 1587–1598.

Arz, H.W., Lamy, F., Pätzold, J., Müller, P.J., Prins, M., 2003. Mediterranean moisture source for an early-Holocene humid period in the Northern Red Sea. Science 300, 118–121.

Astraldi, M., Balopoulos, S., Candela, J., Font, J., Gacic, M., Gasparini, G.P., Manca, B., Theocharis, A., Tintore, J., 1999. The role of straits and channels in understanding the characteristics of Mediterranean circulation. Prog. Oceanogr. 44, 65–108.

Astraldi, M., Gasparini, G.P., Gervasio, L., Salusti, E., 2001. Dense water dynamics along the Strait of Sicily (Mediterranean Sea). J. Phys. Oceanogr. 44, 3457–3475.

Badertscher, S., Fleitmann, D., Cheng, H., Edwards, R.L., Goturk, O.M., Zumbuhl, A., Leuenberger, M., Tuysuz, O., 2011. Pleistocene water intrusions from the Mediterranean and Caspian seas into the Black Sea. Nat. Geosci. 4, 236–239.

Bahr, A., Arz, H.W., Lamy, F., Wefer, G., 2006. Late glacial to Holocene paleoenvironmental evolution of the Black Sea, reconstructed with stable oxygen isotope records obtained on ostracod shells. Earth Planet. Sci. Lett. 241, 863–875.

Bahr, A., Lamy, F., Arz, H.W., Major, C., Kwiecien, O., Wefer, G., 2008. Abrupt changes of temperature and water chemistry in the late Pleistocene and early Holocene Black

Sea. Geochem. Geophys. Geosyst. 9, Q01004. http://dx.doi.org/10.1029/2007GC001683.

Bar Zeev, E., Yogev, T., Man-Aharonovich, D., Kress, N., Herut, B., Béjà, O., Berman-Frank, I., 2008. Seasonal dynamics of the endosymbiontic, nitrogen-fixing cyanobacterium *Richella intracellularis* in the eastern Mediterranean. Int. Soc. Microb. Ecol. J. 2, 911–923.

Bard, E., Delaygue, G., Rostek, F., Antonioli, F., Silenzi, S., Schrag, D.P., 2002. Hydrological conditions over the western Mediterranean basin during the deposition of the cold Sapropel 6 (ca. 175 kyr BP). Earth Planet. Sci. Lett. 202, 481–494.

Bar-Matthews, M., Ayalon, A., Kaufman, A., Wasserburg, G.J., 1999. The Eastern Mediterranean paleoclimate as a reflection of regional events: Soreq cave, Israel. Earth Planet. Sci. Lett. 166, 85–95.

Bar-Matthews, M., Ayalon, A., Kaufman, A., 2000. Timing and hydrological conditions of Sapropel events in the Eastern Mediterranean, as evident from speleothems, Soreq cave, Israel. Chem. Geol. 169, 145–156.

Bar-Matthews, M., Ayalon, A., Gilmour, M., Matthews, A., Hawksesworth, C., 2003. Sea–land oxygen isotopic relationships from planktonic foraminifera and speleothems in the Eastern Mediterranean region and their implication for paleorainfall during interglacial intervals. Geochim. Cosmochim. Acta 67, 3181–3199.

Béranger, K., Mortier, L., Gasparini, G.-P., Gervasio, L., Astraldi, M., Crépon, M., 2004. The dynamics of the Sicily Strait: a comprehensive study from observations and models. Deep-Sea Res. II 51, 411–440.

Béranger, K., Mortier, L., Crépon, M., 2005. Seasonal variability of water transports through the Straits of Gibraltar, Sicily and Corsica, derived from a high resolution model of the Mediterranean circulation. Prog. Oceanogr. 66, 341–364.

Béranger, K., Drillet, Y., Houssais, M.-N., Testor, P., Bourdallé-Badie, R., Alhammoud, B., Bozec, A., Mortier, L., Bouruet-Aubertot, P., Crépon, M., 2010. Impact of the spatial distribution of the atmospheric forcing on water mass formation in the Mediterranean Sea. J. Geophys. Res. 115, C12041. http://dx.doi.org/10.1029/2009JC005648.

Berenger, M., 1955. Essai d'étude météorologique du Bassin Méditerranéen. Mem. Météorol. Natl. 40 (42 pp.).

Berger, A., Loutre, M.F., 1991. Insolation values for the climate of the last 10 million years. Quat. Sci. Rev. 10, 297–317.

Berman, T., Townsend, D.W., El Sayed, S.Z., Trees, C.C., Azov, Y., 1984. Optical transparency, chlorophyll and primary productivity in the eastern Mediterranean near the Israeli coast. Oceanol. Acta 7, 367–372.

Bernasconi, S.M., Pika-Biolzi, M., 2000. A stable isotope study of multiple species of planktonic foraminifera across sapropels of the Tyrrhenian Sea, ODP Site 974. Palaeogeogr. Palaeoclimatol. Palaeoecol. 158, 281–292.

Béthoux, J.P., 1984. Paleo-hydrologie de la Mer Méditerranée au cours des derniers 20 000 ans. Oceanol. Acta 7, 43–48.

Béthoux, J.P., 1989. Oxygen consumption, new production, vertical advection and environmental evolution in the Mediterranean Sea. Deep-Sea Res. 36, 769–781.

Béthoux, J.P., 1993. Mediterranean sapropel formation, dynamic and climatic viewpoints. Oceanol. Acta 16, 127–133.

Béthoux, J.P., Gentili, B., 1994. The Mediterranean Sea, a test area for marine and climatic interactions. In: Malanotte-Rizzoli, P., Robinson, A.R. (Eds.), Ocean Processes in Climate Dynamics: Global and Mediterranean Examples. Kluwer Academic Publishers, Netherlands, pp. 239–254.

Béthoux, J.P., Pierre, C., 1999. Mediterranean functioning and sapropel formation: respective influences of climate and hydrological changes in the Atlantic and the Mediterranean. Mar. Geol. 153, 29–39.

Béthoux, J.P., Gentili, B., Raunet, J., Tailliez, D., 1990. Warming trend in the western Mediterranean deep water. Nature 347, 660–662.

Béthoux, J.P., Gentili, B., Morin, P., Nicolas, E., Pierre, C., Ruiz-Pino, D., 1999. The Mediterranean Sea: a miniature ocean for climatic and environmental studies and a key for the climatic functioning of the North Atlantic. Prog. Oceanogr. 44, 131–146.

Béthoux, J.P., El Boukhary, M.S., Ruiz-Pino, D., Morin, P., Copin-Montégut, C., 2005. Nutrients, oxygen and carbon ratios, CO_2 sequestration and anthropogenic forcing in the Mediterranean Sea. In: Saliot, A. (Ed.), The Mediterranean Sea. Handbook of Environmental Chemistry. Springer, Berlin, pp. 67–86.

Beuning, R.M., Kelts, R., Russell, J., Wolfe, B.B., 2002. Reassessment of Lake Victoria-Upper Nile River paleohydrology from oxygen isotope records of lake-sediment cellulose. Geology 30, 559–562.

Bianchi, D., Zavatarelli, M., Pinardi, N., Capozzi, R., Capotondi, L., Corselli, C., Masina, S., 2006. Simulations of ecosystem response during the sapropel S1 deposition event. Palaeogeogr. Palaeoclimatol. Palaeoecol. 235, 265–287.

Bishop, J.K., 1988. The barite-opal-organic carbon association in oceanic particulate matter. Nature 332, 341–343.

Bosch, H.-J., Sinninghe Damsté, J.S., De Leeuw, J.W., 1998. Molecular palaeontology of Eastern Mediterranean sapropels: evidence for photic zone euxinia. In: Robertson, A.H.F., Emeis, K.-C., Richter, C., Camerlenghi, A. (Eds.), Proceedings of the Ocean Drilling Program. Scientific Results 160. ODP, College Station, TX, pp. 285–295.

Boscolo, R., Bryden, H.L., 2001. Causes of long-term changes in Aegean Sea deep water. Oceanol. Acta 24, 519–527.

Bosmans, J.H.C., Drijfhout, S.S., Tuenter, E., Lourens, L.J., Hilgen, F.J., Weber, S.L., 2012. Monsoonal response to mid-holocene orbital forcing in a high resolution GCM. Clim. Past 8, 723–740.

Bosmans, J.H.C., Drijfhout, S.S., Tuenter, E., Hilgen, F.J., Lourens, L.J., Rohling, E.J., 2015. Precession and obliquity forcing of the freshwater budget over the Mediterranean. Quat. Sci. Rev. (submitted for publication).

Boucher, K., 1975. Global Climate. The English University Press Ltd., London (326 pp.).

Bouloubassi, I., Rullkötter, J., Meyers, P.A., 1999. Origin and transformation of organic matter in Pliocene–Pleistocene Mediterranean sapropels: organic geochemical evidence reviewed. Mar. Geol. 153, 177–197.

Boussetta, S., Kallel, N., Bassinot, F., Labeyrie, L., Duplessy, J.C., Caillon, N., Dewilde, F., Rebaubier, H., 2011. Mg/Ca-paleothermometry in the western Mediterranean Sea on planktonic foraminifer species *Globigerina bulloides*: constraints and implications. Compt. Rendus Geosci. 344, 267–276.

Box, M.R., Krom, M.D., Cliff, R.A., Bar-Matthews, M., Almogi-Labin, A., Ayalon, A., Paterne, M., 2011. Response of the Nile and its catchment to millennial-scale climatic change since the LGM from Sr isotopes and major elements of East Mediterranean sediments. Quat. Sci. Rev. 30, 431–442.

Brauer, A., Allen, J.R.M., Mingram, J., Dulski, P., Wulf, S., Huntley, B., 2007. Evidence for last interglacial chronology and environmental change from Southern Europe. Proc. Natl. Acad. Sci. U. S. A. 104, 450–455.

Brayshaw, D.J., Hoskins, B., Black, E., 2010. Some physical drivers of changes in the winter storm tracks over the North Atlantic and Mediterranean during the Holocene. Philos. Trans. R. Soc. A Math. Phys. Eng. Sci. 368, 5185–5223.

Brayshaw, D.J., Rambeau, C.M.C., Smith, S.J., 2011. Changes in the Mediterranean climate during the Holocene: insights from global and regional climate modelling. The Holocene 21, 15–31.

Brovkin, V., Claussen, M., Petoukhov, V., Ganopolski, A., 1998. On the stability of the atmosphere-vegetation system in the Sahara/Sahel region. J. Geophys. Res. 103, 31613–31624.

Bruce, J.G., Charnock, H., 1965. Studies of winter sinking of cold water in the Aegean Sea. Rapp. Com. Int. Mer Médit. 18, 773–778.

Bryden, H.L., 2009. Where does the new Mediterranean deep water go? In: Briand, F. (Ed.), CIESM, 2009, Dynamics of Mediterranean Deep Waters. CIESM Workshop Monographs 38, pp. 67–70 (Monaco)

Bryden, H.L., Kinder, T.H., 1991. Steady two-layer exchange through the Strait of Gibraltar. Deep-Sea Res. 38, S445–S463.

Bryden, H.L., Stommel, H.M., 1984. Limiting processes that determine basic features of the circulation in the Mediterranean Sea. Oceanol. Acta 7, 289–296.

Bryden, H.L., Candela, J., Kinder, T.H., 1994. Exchange through the Strait of Gibraltar. Prog. Oceanogr. 33, 201–248.

Burman, I., Oren, O.H., 1970. Water outflow close to the bottom from the Aegean. Cahiers Océanograph. 22, 775–780.

Cacho, I., Grimalt, J.O., Canals, M., Sbaffi, L., Shackleton, N.J., Schönfeld, J., Zahn, R., 2001. Variability of the western Mediterranean Sea surface temperatures during the last 25,000 years and its connection with the northern hemisphere climatic changes. Paleoceanography 16, 40–52.

Cacho, I., Grimalt, J.O., Canals, M., 2002. Response of the Western Mediterranean Sea to rapid climatic variability during the last 50,000 years: a molecular biomarker approach. J. Mar. Syst. 33–34, 253–272.

Calvert, S.E., 1983. Geochemistry of Pleistocene sapropels and associated sediments from the eastern Mediterranean. Oceanol. Acta 6, 255–267.

Calvert, S.E., Nielsen, B., Fontugne, M.R., 1992. Evidence from nitrogen isotope ratios for enhanced productivity during formation of eastern Mediterranean sapropels. Nature 359, 223–225.

Cane, T., Rohling, E.J., Kemp, A.E.S., Cooke, S., Pearce, R.B., 2002. High-resolution stratigraphic framework for Mediterranean sapropel S5: defining temporal relationships between records of Eemian climate variability. Palaeogeogr. Palaeoclimatol. Palaeoecol. 183, 87–101.

Cantu, V., 1977. The climate of Italy. In: Wallen, C.C. (Ed.), Climates of Central and Southern Europe — World survey of climatology 6. Elsevier, Amsterdam, pp. 127–183.

Capotondi, L., Principato, M.S., Morigi, C., Sangiorgi, F., Maffioli, P., Giunta, S., Negri, A., Corselli, C., 2006. Foraminiferal variations and stratigraphic implications to the deposition of sapropel S5 in the eastern Mediterranean. Palaeogeogr. Palaeoclimatol. Palaeoecol. 235, 48–65.

Casford, J.S.L., Abu-Zied, R., Rohling, E.J., Cooke, S., Boessenkool, K.P., Brinkhuis, H., De Vries, C., Wefer, G., Geraga, M., Papatheodorou, G., Croudace, I., Thomson, J., Wells, N.C., Lykousis, V., 2001. Mediterranean climate variability during the Holocene. Mediterr. Mar. Sci. 2, 45–55.

Casford, J.S.L., Rohling, E.J., Abu-Zied, R., Cooke, S., Fontanier, C., Leng, M., Lykousis, V., 2002. Circulation changes and nutrient concentrations in the Late Quaternary Aegean Sea: a non-steady state concept for sapropel formation. Paleoceanography 17 (2000PA000601).

Casford, J.S.L., Rohling, E.J., Abu-Zied, R.H., Jorissen, F.J., Leng, M., Thomson, J., 2003. A dynamic concept for eastern Mediterranean circulation and oxygenation during sapropel formation. Palaeogeogr. Palaeoclimatol. Palaeoecol. 190, 103–119.

Casford, J.S.L., Abu-Zied, R., Rohling, E.J., Cooke, S., Fontanier, Ch., Leng, M., Millard, A., Thomson, J., 2007. A stratigraphically controlled multi-proxy chronostratigraphy for the eastern Mediterranean. Paleoceanography 22, PA4215. http://dx.doi.org/10.1029/2007PA001422.

Castradori, D., 1993. Calcareous nannofossils and the origin of eastern Mediterranean sapropels. Paleoceanography 8, 459–471.

Cheddadi, R., Rossignol-Strick, M., Fontugne, M., 1991. Eastern Mediterranean palaeoclimates from 26 to 5 ka BP documented by pollen and isotopic analysis of a core in the anoxic Bannock Basin. Mar. Geol. 100, 53–66.

Cheddadi, R., Yu, G., Guiot, J., Harrison, S.P., Prentice, I.C., 1997. The climate of Europe 6000 years ago. Clim. Dyn. 13, 1–9.

Cheney, R.E., Doblar, R.A., 1982. Structure and variability of the Alboran Sea frontal system. J. Geophys. Res. 87, 585–594.

Cita, M.B., Grignani, D., 1982. Nature and origin of Late Neogene Mediterranean sapropels. In: Schlanger, S.O., Cita, M.B. (Eds.), Nature and Origin of Cretaceous Carbon-Rich Facies. Academic, San Diego, California, pp. 165–196.

Cita, M.B., Vergnaud-Grazzini, C., Robert, C., Chamley, H., Ciaranfi, N., d'Onofrio, S., 1977. Paleoclimatic record of a long deep sea core from the eastern Mediterranean. Quat. Res. 8, 205–235.

Clare, L., Rohling, E.J., Weninger, B., Hilpert, J., 2008. Warfare in Late Neolithic/Early Chalcolithic Pisidia, southwestern Turkey. Climate Induced Social Unrest in the Late 7th Millennium calBCDocumenta Praehistorica 35 (Neolithic Studies 15) pp. 65–92.

Claussen, M., Brovkin, V., Ganopolski, A., Kubatski, C., Petoukhov, V., 1998. Modelling global terrestrial vegetation–climate interaction. Philos. Trans. R. Soc. Lond. 353, 53–63.

COHMAP members, 1988. Climatic changes of the last 18,000 years: observations and model simulations. Science 241, 1043–1052.

Corselli, C., Principato, M.S., Maffioli, P., Crudelli, D., 2002. Changes in planktonic assemblages during sapropel S5 deposition: evidence from Urania Basin area, eastern Mediterranean. Paleoceanography 17. http://dx.doi.org/10.1029/2000PA000536.

Costa, K., Russell, J., Konecky, J., Lamb, H., 2014. Isotopic reconstruction of the African Humid Period and Congo Air Boundary migration at Lake Tana, Ethiopia. Quat. Sci. Rev. 83, 58–67.

Coulthard, T.J., Ramirez, J.A., Barton, N., Rogerson, M., Brücher, T., 2013. Were Rivers Flowing across the Sahara During the Last Interglacial? Implications for Human Migration through Africa. PLoS ONE 8, e74834. http://dx.doi.org/10.1371/journal.pone.0074834.

Cramp, A., O'Sullivan, G., 1999. Neogene sapropels in the Mediterranean: a review. Mar. Geol. 153, 11–28.

Criado-Aldeanueva, F., Soto-Navarro, F.J., García-Lafuente, J., 2012. Seasonal and interannual variability of surface heat and freshwater fluxes in the Mediterranean Sea: budgets and exchange through the Strait of Gibraltar. Int. J. Climatol. 32, 286–302.

De Kaenel, E., Siesser, W.G., Murat, A., 1999. Pleistocene calcareous nannofossil biostratigraphy and the western Mediterranean sapropels, sites 974 to 977 and 979. In: Zahn, R., Comas, M.C., Klaus, A. (Eds.), Proceedings of the Ocean Drilling Program. Scientific Results 161. ODP, College Station, TX, pp. 159–183.

De Lange, G.J., Middelburg, J.J., Pruysers, P.A., 1989. Discussion: Middle and Late Quaternary depositional sequences and cycles in the eastern Mediterranean. Sedimentology 36, 151–156.

De Lange, G.J., Thomson, J., Reitz, A., Slomp, C.P., Speranza Principato, M., Erba, E., Corselli, C., 2008. Synchronous basin-wide formation and redox-controlled preservation of a Mediterranean sapropel. Nat. Geosci. 1, 606–610.

De Rijk, S., Rohling, E.J., Hayes, A., 1999. Onset of climatic deterioration in the eastern Mediterranean around 7 ky BP; micropalaeontological data from Mediterranean sapropel interruptions. Mar. Geol. 153, 337–343.

De Rijk, S., Jorissen, F.J., Rohling, E.J., Troestra, S.R., 2000. Organic flux control on bathymetric zonation of Mediterranean benthic foraminifera. Mar. Micropaleontol. 40, 151–166.

Demaison, G.J., Moore, G.T., 1980. Anoxic environments and oil source bed genesis. Am. Assoc. Pet. Geol. Bull. 64, 1179–1209.

Digerfeldt, G., Olsson, S., Sandgren, P., 2000. Reconstruction of lake-level changes in lake Xinias, centrel Greece, during the last 40,000 years. Palaeogeogr. Palaeoclimatol. Palaeoecol. 158, 65–82.

Drake, N.A., Blench, R.M., Armitage, S.J., Bristow, C.S., White, K.H., 2011. Ancient watercourses and biogeography of the Sahara explain the peopling of the desert. Proc. Natl. Acad. Sci. U.S.A. 108, 458–462.

Dünkeloh, A., Jacobeit, J., 2003. Circulation dynamics of Mediterranean precipitation variability 1948-1998. Int. J. Climatol. 23, 1843–1866.

Ehrmann, W., Schmiedl, G., Hamanna, Y., Kuhnt, T., Hemleben, Ch., Siebel, W., 2007. Clay minerals in late glacial and Holocene sediments of the northern and southern Aegean Sea. Palaeogeogr. Palaeoclimatol. Palaeoecol. 249, 36–57.

Ehrmann, W., Seidel, M., Schmiedl, G., 2013. Dynamics of Late Quaternary North African humid periods documented in the clay mineral record of central Aegean Sea sediments. Glob. Planet. Chang. 107, 186–195.

Eijsink, L.M., Krom, M.D., De Lange, G.J., 1997. The use of sequential extraction techniques for sedimentary phosphorus in eastern Mediterranean sediments. Mar. Geol. 139, 147–155.

El Dardir, M., 1994. Sedimentation in the Nile High Dam reservoir, 1987–1992, and sedimentary futurologic aspects. Sedimentol. Egypt 2, 23–39.

Emeis, K.-C., Weissert, H., 2009. Tethyan-Mediterranean organic carbon-rich sediments from Mesozoic black shales to sapropels. Sedimentology 56, 247–266.

Emeis, K.C., Camerlenghi, A., McKenzie, J.A., Rio, D., Sprovieri, R., 1991. The occurrence and significance of Pleistocene and Upper Pliocene sapropels in the Tyrrhenian Sea. Mar. Geol. 100, 155–182.

Emeis, K.C., Schulz, H.M., Struck, U., Sakamoto, T., Doose, H., Erlenkeuser, H., Howell, M., Kroon, D., Paterne, M., 1998. Stable isotope and temperature records of sapropels from ODP Sites 964 and 967: constraining the physical environment of sapropel formation in the Eastern Mediterranean Sea. In: Robertson, A.H.F., Emeis, K.C., Richter, C., Camerlenghi, A. (Eds.), Proceedings of the Ocean Drilling Program. Scientific Results 160. ODP, College Station, TX, pp. 309–331.

Emeis, K.C., Sakamoto, T., Wehausen, R., Brumsack, H.J., 2000a. The sapropel record of the eastern Mediterranean Sea — results of Ocean Drilling Program Leg 160. Palaeogeogr. Palaeoclimatol. Palaeoecol. 158, 371–395.

Emeis, K.C., Struck, U., Schulz, H.M., Bernasconi, S., Sakamoto, T., Martinez-Ruiz, F., 2000b. Temperature and salinity of Mediterranean Sea surface waters over the last 16,000 years: constraints on the physical environment of S1 sapropel formation based on stable oxygen isotopes and alkenone unsaturation ratios. Palaeogeogr. Palaeoclimatol. Palaeoecol. 158, 259–280.

Emeis, K.C., Schulz, H., Struck, U., Rossignol-Strick, M., Erlenkeuser, H., Howell, M.W., Kroon, D., Mackensen, H., Ishizuka, S., Oba, T., Sakamoto, T., Koizumi, I., 2003. Eastern Mediterranean surface water temperatures and δ^{18}O composition during deposition of sapropels in the late Quaternary. Paleoceanography 18. http://dx.doi.org/10.1029/2000PA000617.

Farmer, P., Miller, D., Pieprzak, A., Rutledge, J., Woods, R., 1996. Exploring the subsalt. Oilfield Rev. 8, 50–64.

Fleitmann, D., Burns, S.J., Mudelsee, M., Neff, U., Kramers, J., Mangini, A., Matter, A., 2003. Holocene forcing of the Indian monsoon recorded in a stalagmite from Southern Oman. Science 300, 1737–1739.

Fleitmann, D., Burns, S.J., Mangini, A., Mudelsee, M., Kramers, J., Villa, I., Neff, U., Al-Subbary, A.A., Buettner, A., Hippler, D., Matter, A., 2007. Holocene ITCZ and Indian monsoon dynamics recorded in stalagmites from Oman and Yemen (Socotra). Quat. Sci. Rev. 26, 170–188.

Fleitmann, D., Burns, S.J., Pekala, M., Mangini, A., Al-Subbary, A., Al-Aowah, M., Kramers, J., Matter, A., 2011. Holocene and Pleistocene pluvial periods in Yemen, Southern Arabia. Quat. Sci. Rev. 30, 783–787.

Font, J., Béranger, K., Bryden, H., Budillon, G., Fuda, J.L., Gačić, M., Gascard, J.C., Packard, T., Puig, P., Roether, W., Salat, J., Salusti, E., Schroeder, K., Theocharis, A., van Haren, H., 2009. I — Executive summary of CIESM Workshop 38 "Dynamics of Mediterranean deep waters.". In: Briand, F. (Ed.), CIESM, 2009, Dynamics of Mediterranean Deep Waters. CIESM Workshop Monographs 38, pp. 5–17 (Monaco).

Fontugne, M.R., Calvert, S.E., 1992. Late Pleistocene variability of the carbon isotopic composition of organic matter in the eastern Mediterranean: monitor of changes in carbon sources and atmospheric CO_2 concentrations. Paleoceanography 7, 1–20.

Fontugne, M., Arnold, M., Labeyrie, L., Paterne, M., Calvert, S., Duplessy, J.-C., 1994. Paleoenvironment, sapropel chronology, and Nile river discharge during the last 20,000 years as indicated by deep-sea sediment records in the eastern Mediterranean. Radiocarbon 34, 75–88.

Foucault, A., Mélières, F., 2000. Palaeoclimatic cyclicity in central Mediterranean Pliocene sediments: the mineralogical signal. Palaeogeogr. Palaeoclimatol. Palaeoecol. 158, 311–323.

Francois, R., Honjo, S., Manganini, S.J., Ravizza, G.E., 1995. Biogenic barium fluxes to the deep sea: implications for paleoproductivity reconstruction. Glob. Biogeochem. Cycles 9, 289–303.

Frisia, S., Borsato, A., Mangini, A., Spoetl, C., Madonia, G., Sauro, U., 2006. Holocene climate variability in Sicily from a discontinuous stalagmite record and the Mesolithic to Neolithic transition. Quat. Res. 66, 388–400.

Frogley, M.R., Tzedakis, P.C., Heaton, T.H.E., 1999. Climate variability in Northwest Greece during the last interglacial. Science 285, 1886–1889.

Furlan, D., 1977. The climate of southeast Europe. In: Wallen, C.C. (Ed.), Climates of Central and Southern Europe. World survey of climatology 6. Elsevier, Amsterdam, pp. 185–235.

Ganssen, G., Troelstra, S.R., 1987. Palaeoenvironmental changes from stable isotopes in planktonic foraminifera from eastern Mediterranean sapropels. Mar. Geol. 75, 221–230.

García Lafuente, J., Sánchez Román, A., Díaz del Río, G., Sannino, G., Sánchez Garrido, J.C., 2007. Recent observations of seasonal variability of the Mediterranean outflow in the Strait of Gibraltar. J. Geophys. Res. 112, C10005. http://dx.doi.org/10.1029/2006JC003992.

García Lafuente, J., Delgado, J., Sánchez Román, A., Soto, J., Carracedo, L., Díaz del Río, G., 2009. Interannual variability of the Mediterranean Outflow observed in Espartel Sill, western Strait of Gibraltar. J. Geophys. Res. 114, C10018. http://dx.doi.org/10.1029/2009JC005496.

Garrett, C., 1994. The Mediterranean Sea as a climate test basin. In: Malanotte-Rizzoli, P., Robinson, A.R. (Eds.), Ocean Processes in Climate Dynamics: Global and Mediterranean Examples. Kluwer Academic Publishers, Netherlands, pp. 227–237.

Garrett, C., 1996. The role of the Strait of Gibraltar in the evolution of the Mediterranean water properties and circulation. In: Briand, F. (Ed.), Dynamics of Mediterranean Straits and Channels. CIESM Science Series.

Garzoli, S., Maillard, C., 1979. Winter circulation in the Sicily and Sardinia straits region. Deep-Sea Res. 26A, 933–954.

Gascard, J.C., 1978. Mediterranean deep water formation, baroclinic instability and oceanic eddies. Oceanol. Acta 1, 315–330.

Gascard, J.C., Richez, C., 1985. Water mass and circulation in the western Alboran Sea and in the Strait of Gibraltar. Prog. Oceanogr. 15, 157–216.

Gasparini, G.P., Ortona, A., Budillon, G., Astraldi, M., Sansone, E., 2005. The effect of the Eastern Mediterranean Transient on the hydrographic characteristics in the Strait of Sicily and the Tyrrhenian Sea. Deep-Sea Res. I 52, 915–935.

Gasse, F., 2000. Hydrological changes in the African tropics since the last glacial maximum. Quat. Sci. Rev. 19, 189–211.

Gat, J.R., Carmi, I., 1970. Evolution of the isotopic composition of atmospheric waters in the Mediterranean Sea area. J. Geophys. Res. 75, 3039–3048.

Gaven, C., Hillaire-Marcel, C., Petit-Maire, N., 1981. A Pleistocene lacustrine episode in southeastern Libya. Nature 290, 131–133.

Geraga, M., Tsaila-Monopolis, S., Ioakim, Chr., Papatheodorou, G., Ferentinos, G., 2000. Evaluation of palaeoenvironmental changes during the last 18,000 years in the Myrtoon basin, SW Aegean Sea. Palaeogeogr. Palaeoclimatol. Palaeoecol. 156, 1–17.

Gilman, C., Garrett, C., 1994. Heat flux parameterizations for the Mediterranean Sea: the role of atmospheric aerosols and constraints from the water budget. J. Geophys. Res. 99, 5119–5134.

Giraudi, C., Magny, M., Zanchetta, G., Drysdale, R.N., 2011. The Holocene climatic evolution of Mediterranean Italy: a review of the continental geological data. The Holocene 21, 105–115.

Göktürk, O.M., Fleitmann, D., Badertscher, S., Cheng, H., Edwards, R.L., Leuenberger, M., Frankhauser, A., Tüysüz, O., Kramers, J., 2011. Climate on the Southern Black Sea coast during the Holocene: implications from the Sofular Cave record. Quat. Sci. Rev. 30, 2433–2445.

Goldsmith, V., Sofer, S., 1983. Wave climatology of the southeastern Mediterranean: an integrated approach. Israel J. Earth Sci. 32, 1–51.

Goodfriend, G.A., 1991. Holocene trends in ^{18}O in land snail shells from the Negev Desert and their implications for changes in rainfall source areas. Quat. Res. 35, 417–426.

Grant, K.M., Rohling, E.J., Bar-Matthews, M., Ayalon, A., Medina-Elizalde, M., Bronk Ramsey, C., Satow, C., Roberts, A.P., 2012. Rapid coupling between ice volume and polar temperature over the past 150 kyr. Nature 491, 744–747.

Grant, K.M., Rohling, E.J., Bronk Ramsey, C., Cheng, H., Edwards, R.L., Florindo, F., Heslop, D., Marra, F., Roberts, A.P., Tamisiea, M.E., Williams, F., 2014. Sea-level variability over five glacial cycles. Nat. Commun. 5, 5076. http://dx.doi.org/10.1038/ncomms6076.

Grelaud, M., Marino, G., Ziveri, P., Rohling, E.J., 2012. Abrupt shoaling of the nutricline in response to massive freshwater flooding at the onset of the last interglacial sapropel event. Paleoceanography 27, PA3208. http://dx.doi.org/10.1029/ 2012PA002288.

Grimm, R., Maier-Reimer, E., Mikolajewicz, U., Schmiedl, G., Muller-Navarra, K., Adloff, F., Grant, K.M., Ziegler, M., Lourens, L.J., Emeis, K.C., 2015. Late glacial initiation of Holocene eastern Mediterranean sapropel formation. Nat. Commun. (submitted for publication).

Gupta, A.K., Anderson, D.M., Overpeck, J.T., 2003. Abrupt changes in the Asian southwest monsoon during the Holocene and their links to the North Atlantic Ocean. Nature 421, 354–357.

Gupta, A.K., Das, M., Anderson, D.M., 2005. Solar influence on the Indian summer monsoon during the Holocene. Geophys. Res. Lett. 32, L17703. http://dx.doi.org/10.1029/2005GL022685.

Hamad, N., Millot, C., Taupier-Letage, I., 2005. A new hypothesis about the surface circulation in the eastern basin of the Mediterranean Sea. Prog. Oceanogr. 66, 287–298.

Hassan, F.A., 1998. Holocene climatic change and riverine dynamics in the Nile Valley. In: di Lernia, S., Manzi, G. (Eds.), Before Food Production in North Africa, Union Internationale de Sciences Préhistoriques et protohistoriques, XIII world congress, Forli, 1996. A.B.A. C.O Edizioni, Rome, pp. 43–51.

Hassan, F.A. (Ed.), 2002. Droughts, Food, and Culture: Ecological Change and Food Security in Africa's Later Prehistory. Kluwer Academic/ Plenum Publishers, New York.

Hayes, A., Rohling, E.J., De Rijk, S., Zachariasse, W.J., 1999. Mediterranean planktonic foraminiferal faunas during the last glacial cycle. Mar. Geol. 153, 239–252.

Heburn, G.W., La Violette, P.E., 1990. Variations in the structure of the anticyclonic gyres found in the Alboran Sea. J. Geophys. Res. 92, 2901–2906.

Hecht, A., Gertman, I., 2001. Physical features of the eastern Mediterranean resulting from the integration of POEM data with Russian Mediterranean cruises. Deep-Sea Res. I 48, 1847–1876.

Hemleben, C., Spindler, M., Anderson, O.R., 1989. Modern Planktonic Foraminifera. Springer, New York (363 pp.).

Hemleben, Ch., Hoernle, K., Jørgensen, B.B., Roether, W., 2003. Ostatlantik-Mittelmeer-Schwarzes Meer, Cruise 51, 12 September-28 December 2001. Meteor Ber. 03-1 (213 pp.).

Hennekam, R., Jilbert, T., Schnetger, B., de Lange, G.J., 2014. Solar forcing of Nile discharge and sapropel S1 formation in the early to middle Holocene eastern Mediterranean. Paleoceanography 29. http://dx.doi.org/10.1002/2013PA002553.

Herbaut, C., Codron, F., Crépon, M., 1998. Separation of a coastal current at a strait level: case of the Sicily Strait. J. Phys. Oceanogr. 28, 1346–1362.

Herold, M., Lohmann, G., 2009. Eemian tropical and subtropical African moisture transport — an isotope modelling study. Clim. Dyn. 33, 1075–1088.

Higgins, M.B., Robinson, R.S., Carter, S.J., Pearson, A., 2010. Evidence from chlorin nitrogen isotopes for alternating nutrient regimes in the eastern Mediterranean Sea. Earth Planet. Sci. Lett. 290, 102–107.

Higgs, N.C., Thomson, J., Wilson, T.R.S., Croudace, I.W., 1994. Modification and complete removal of eastern Mediterranean sapropels by postdepositional oxidation. Geology 22, 423–426.

Hilgen, F.J., 1991a. Astronomical calibration of Gauss to Matuyama sapropels in the Mediterranean and implication for the geomagnetic Polarity Time Scale. Earth Planet. Sci. Lett. 104, 226–244.

Hilgen, F.J., 1991b. Extension of the astronomically calibrated(polarity) timescale to the Miocene/ Pliocene boundary. Earth Planet. Sci. Lett. 107, 349–368.

Hilgen, F.J., Lourens, L.J., Berger, A., Loutre, M.F., 1993. Evaluation of the astronomically calibrated time scale for the late Pliocene and earliest Pleistocene. Paleoceanography 8, 549–656.

Hilgen, F.J., Krijgsman, W., Langereis, C.G., Lourens, L.J., Santarelli, A., Zachariasse, W.J., 1995. Extending the astronomical (polarity) time scale into the Miocene. Earth Planet. Sci. Lett. 136, 495–510.

Hilgen, F.J., Abdul Aziz, H., Krijgsman, W., Raffi, I., Turco, E., 2003. Integrated stratigraphy and astronomical tuning of the Serravallian and lower Tortonian at Monte dei Corvi (Middle-Upper Miocene, northern Italy). Palaeogeogr. Palaeoclimatol. Palaeoecol. 199, 229–264.

Hoelzmann, P., Kruse, H.J., Rottinger, F., 2000. Precipitation estimates for the eastern Saharan palaeomonsoon based on a water balance model of the West Nubian Palaeolake Basin. Glob. Planet. Chang. 26, 105–120.

Hood, R.R., Michaels, A.F., Capone, D.G., 2000. Answers sought to the enigma of marine nitrogen fixation. Eos 81, 133.

Hoogakker, B.A.A., Klinkhammer, G.P., Elderfield, H., Rohling, E.J., Hayward, C., 2009. Mg/Ca paleothermometry in high salinity environments. Earth Planet. Sci. Lett. 284, 583–589.

Hurst, H.E., 1944. A Short Account of the Nile Basin. Physical Department, Ministry of Public Works, Egypt, Paper 45 (77 pp.).

Irizarry-Ortiz, M.M., Wang, G., Eltahir, E.A.B., 2003. Role of the biosphere in the mid-Holocene climate of West Africa. J. Geophys. Res. 108. http://dx.doi.org/10.1029/2001JD000989.

Ivanova, E., 1999. Late Quaternary monsoon history and paleoproductivity of the western Arabian Sea. (Ph.D. thesis), Free Univ. Amsterdam, Amsterdam (172 pp.).

Jacobson, D.M., Anderson, D.M., 1986. Thecate hetrotrophic dinoflagellates: feeding behaviour and mechanisms. J. Phycol. 22, 249–258.

Jenkins, J.A., Williams, D.F., 1984. Nile water as a cause of eastern Mediterranean sapropel formation: evidence for and against. Mar. Micropaleontol. 9, 521–534.

Jilbert, T., Reichart, G.-J., Mason, P., De Lange, G.J., 2010. Short-time-scale variability in ventilation and export productivity during the formation of Mediterranean sapropel S1. Paleoceanography 25, PA4232. http://dx.doi.org/10.1029/2010PA001955.

Jorissen, F.J., 1999. Benthic foraminiferal successions across Late Quaternary Mediterraenan sapropels. Mar. Geol. 153, 91–101.

Jorissen, F.J., Asioli, A., Borsetti, A.M., Capotondi, De Visser, J.P., Hilgen, F.J., Rohling, E.J., Van der Borg, K., Vergnaud-Grazzini, C., Zachariasse, W.J., 1993. Late Quaternary central Mediterranean biochronology. Mar. Micropaleontol. 21, 169–189.

Josey, S., 2003. Changes in the heat and freshwater forcing of the Eastern Mediterranean and their influence on deep water formation. J. Geophys. Res. 108, 3237. http://dx.doi.org/10.1029/2003JC001778.

Josey, S.A., Somot, S., Tsimplis, M., 2011. Impacts of atmospheric modes of variability on Mediterranean Sea surface heat exchange. J. Geophys. Res. 116, C02032. http://dx.doi.org/10.1029/2010JC006685.

Kallel, N., Paterne, M., Duplessy, J.C., Vergnaud-Grazzini, C., Pujol, C., Labeyrie, L., Arnold, M., Fontugne, M., Pierre, C., 1997a. Enhanced rainfall in the Mediterranean region during the last sapropel event. Oceanol. Acta 20, 697–712.

Kallel, N., Paterne, M., Labeyrie, L., Duplessy, J.C., Arnold, M., 1997b. Temperature and salinity records of the Tyrrhenian Sea during the last 18,000 years. Palaeogeogr. Palaeoclimatol. Palaeoecol. 135, 97–108.

Kallel, N., Duplessy, J.-C., Labeyrie, L., Fontugne, M., Paterne, M., Montacer, M., 2000. Mediterranean pluvial periods and sapropel formation over the last 200 000 years. Palaeogeogr. Palaeoclimatol. Palaeoecol. 157, 45–58.

Kemp, A.E.S., Pearce, R.B., Koizumi, I., Pike, J., Rance, S.J., 1999. The role of mat-forming diatoms in the formation of Mediterranean sapropels. Nature 398, 57–61.

Kemp, A.E.S., Pike, J., Pearce, R.B., Lange, C.B., 2000. The "Fall dump" — a new perspective on the role of a "shade flora" in the annual cycle of diatom production and export flux. Deep-Sea Res. II 47, 2129–2154.

Kidd, R.B., Cita, M.B., Ryan, W.B.F., 1978. Stratigraphy of eastern Mediterranean sapropel sequences recovered during Leg 42A and their paleoenvironmental significance. Initial Rep. Deep Sea Drill. Proj. 42A, 421–443.

Kinder, T.H., Parrilla, G., 1987. Yes, some of the Mediterranean outflow does come from great depth. J. Geophys. Res. 92, 2901–2906.

Klein, B., Roether, W., Manca, B.B., Bregant, D., Beitzel, V., Kovacevic, V., Luchetta, A., 1999. The large deep water transient in the eastern Mediterranean. Deep-Sea Res. 46, 371–414.

Klein, B., Roether, W., Civitarese, G., Gačić, M., Manca, B.B., Ribera d'Alcala, M., 2000. Is the Adriatic returning to dominate production of Eastern Mediterranean Deep Water? Geophys. Res. Lett. 27, 3377–3380.

Kolodny, Y., Stein, M., Machlus, M., 2005. Sea-rain-lake relation in the Last Glacial East Mediterranean revealed by $\delta^{18}O$–$\delta^{13}C$ in Lake Lisan aragonites. Geochim. Cosmochim. Acta 69, 4045–4060.

Koopmans, M.P., Köster, J., Van Kaam-Peters, H.M.E., Kenig, F., Schouten, S., Hartgers, W.A., De Leeuw, J.W., Sinninghe Damsté, J.S., 1996. Diagenetic and catagenetic products of isorenieratene: Molecular indicators for photic zone anoxia. Geochim. Cosmochim. Acta 60, 4467–4496.

Kotthoff, U., Muller, U.C., Pross, J., Schmiedl, G., Lawson, I.T., Schulz, H., 2008. Lateglacial and Holocene vegetation dynamics in the Aegean region: an integrated view based on pollen data from marine and terrestrial archives. The Holocene 18, 1019–1032.

Krahmann, G., Schott, F., 1998. Long-term increase in Mediterranean salinities and temperatures: mixed anthropogenic and climatic sources. Geophys. Res. Lett. 25, 4209–4212.

Krijgsman, W., 2002. The Mediterranean: Mare Nostrum of Earth sciences. Earth Planet. Sci. Lett. 205, 1–12.

Krijgsman, W., Hilgen, F.J., Langereis, C.G., Santarelli, A., Zachariasse, W.J., 1995. Late Miocene magnetostratigraphy, biostratigraphy and cyclostratigraphy in the Mediterranean. Earth Planet. Sci. Lett. 136, 475–494.

Krijgsman, W., Hilgen, F.J., Raffi, I., Sierro, F.J., Wilson, D.S., 1999. Chronology, causes, and progression of the Messinian salinity crisis. Nature 400, 652–655.

Krijgsman, W., Fortuin, A.R., Hilgen, F.J., Sierro, F.J., 2001. Astrochronology for the Messinian Sorbas basin (SE Spain) and orbital (precessional) forcing for evaporite cyclicity. Sediment. Geol. 140, 43–60.

Krishnamurthy, R.V., Meyers, P.A., Lovan, N.A., 2000. Isotopic evidence of sea-surface freshening, enhanced productivity, and improved organic matter preservation during sapropel deposition in the Tyrrhenian Sea. Geology 28, 263–266.

Krom, M.D., Cliff, R.A., Eijsink, L.M., Herut, B., Chester, R., 1999. The characterisation of Saharan dust and Nile particulate matter in surface sediments from the Levantine basin using Sr isotopes. Mar. Geol. 155, 319–330.

Kuhnt, T., Schmiedl, G., Ehrmann, W., Hamann, Y., Hemleben, Ch., 2007. Deep-sea ecosystem variability of the Aegean Sea during the past 22 kyr as revealed by benthic foraminifera. Mar. Micropaleontol. 64, 141–162.

Kullenberg, B., 1952. On the salinity of the water contained in marine sediments. Medd. Oceanogr. Inst. Göteb. 21, 1–38.

Kutzbach, J.E., 1985. Modeling of paleoclimates. In: Manabe, S. (Ed.), Issues in atmospheric and oceanic modeling, A; climate dynamics. Advances in Geophysics 28, pp. 161–196.

Kutzbach, J.E., Guetter, P.J., 1986. The influence of changing orbital parameters and surface boundary conditions on climate simulations for the past 18,000 years. J. Atmos. Sci. 43, 1726–1759.

Kutzbach, J., Bonan, G., Foley, J., Harrison, S.P., 1996. Vegetation and soil feedbacks on the response of the African monsoon to orbital forcing in the early to middle Holocene. Nature 384, 623–626.

Kutzbach, J.E., Chen, G., Cheng, H., Edwards, R.L., Liu, Z., 2014. Potential role of winter rainfall in explaining increased moisture in the Mediterranean and Middle East during periods of maximum orbitally-forced insolation seasonality. Clim. Dyn. 42, 1079–1095.

La Violette, P.E., 1986. Short term measurements of surface currents associated with the Alboran Sea during ?Donde Va? J. Phys. Oceanogr. 16, 262–279.

Lane-Serff, G.F., Rohling, E.J., Bryden, H.L., Charnock, H., 1997. Post-glacial connection of the Black Sea to the Mediterranean and its relation to the timing of sapropel formation. Paleoceanography 12, 169–174.

Larrasoaña, J.C., Roberts, A.P., Rohling, E.J., Winklhofer, M., Wehausen, R., 2003. Three million years of monsoon variability over the northern Sahara. Clim. Dyn. 21, 689–698.

Larrasoaña, J.C., Roberts, A.P., Hayes, A., Wehausen, R., Rohling, E.J., 2006. Detecting missing beats in the Mediterranean climate rhythm from magnetic identification of oxidized sapropels in Ocean Drilling Program Leg 160 marine sediments. Phys. Earth Planet. Inter. 156, 283–293.

Larrasoaña, J.C., Roberts, A.P., Rohling, E.J., 2013. Dynamics of green Sahara periods and their role in hominin evolution. PLoS ONE 8, e76514. http://dx.doi.org/10.1371/journal.pone.0076514.

Lascaratos, A., 1989. Hydrology of the Aegean Sea. Rep. Meteorol. Oceanogr. 40, 313–431.

Lascaratos, A., 1993. Estimation of deep and intermediate water mass formation rates in the Mediterranean Sea. Deep-Sea Res. II 40, 1327–1332.

Lascaratos, A., Roether, W., Nittis, K., Klein, B., 1999. Recent changes in the Eastern Mediterranean Deep Waters: a review. Prog. Oceanogr. 44, 5–36.

Leaman, K.D., Schott, F.A., 1991. Hydrographic structure of the convection regime in the Gulf of Lions: Winter 1987. J. Phys. Oceanogr. 21, 575–598.

Lisiecki, L.E., Raymo, M.E., 2005. A Plio-Pleistocene stack of 57 globally distributed benthic δ^{18}O records. Paleoceanography 20, PA1003. http://dx.doi.org/10.1029/2004PA001071.

Locarnini, R.A., Mishonov, A.V., Antonov, J.I., Boyer, T.P., Garcia, H.E., 2010. World Ocean Atlas 2009, Volume 1: Temperature. In: Levitus, S. (Ed.), NOAA Atlas NESDIS 68. U.S. Government Printing Office, Washington, D.C. (184 pp.).

Lolis, C.J., Bartzokas, A., Katsoulis, B.D., 2002. Spatial and temporal 850 hPa air temperature and sea-surface temperature covariances in the Mediterranean region and their connection to atmospheric circulation. Int. J. Climatol. 22, 663–676.

Lourens, L.J., 2004. Revised tuning of Ocean Drilling Program Site 964 and KC01B (Mediterranean) and implications for the delta O-18, tephra, calcareous nan- nofossil, and geomagnetic reversal chronologies of the past 1.1 Myr. Paleoceanography 19, PA3010. http://dx.doi.org/10.1029/2003PA000997.

Lourens, L.J., Reichart, G.J., 1997. Low latitude forcing of glacial cycles. In: Reichart, G.J. (Ed.), Late Quaternary Variability of the Arabian Sea Monsoon and Oxygen Minimum Zone. Geologica Ultraiectina 154, pp. 153–170.

Lourens, L.J., Antonarakou, A., Hilgen, F.J., Van Hoof, A.A.M., Vergnaud-Grazzini, C., Zachariasse, W.J., 1996. Evaluation of the Plio-Pleistocene astronomical time-scale. Paleoceanography 11, 391–413.

Lourens, L.J., Wehausen, R., Brumsack, H.J., 2001. Geological constraints on tidal dissipation and dynamical ellipticity of the earth over the past three million years. Nature 409, 1029–1033.

Maheras, P., Xoplaki, E., Davies, T., Martin-Vide, J., Bariendos, M., Alcoforado, M.J., 1999. Warm and cold monthly anomalies across the Mediterranean basin and their relationship with circulation; 1860–1990. Int. J. Climatol. 19, 1697–1715.

Major, C.O., Goldstein, S.L., Ryan, W.B.F., Lericolais, G., Piotrowski, A.M., Hajdas, I., 2006. The co-evolution of Black Sea level and composition through the last deglaciation and its paleoclimatic significance. Quat. Sci. Rev. 25, 2031–2047.

Malanotte-Rizzoli, P., Bergamasco, A., 1991. The wind and thermally driven circulation of the eastern Mediterranean Sea. Part II: the baroclinic case. Dyn. Atmos. Oceans 15, 355–419.

Malanotte-Rizzoli, P., Hecht, A., 1988. Large-scale properties of the eastern Mediterranean: a review. Oceanol. Acta 11, 323–335.

Malanotte-Rizzoli, P., Manca, B.B., d'Alcala, M.R., Teocharis, A., Bergemasco, A., Bregant, D., Budillon, G., Civitarese, G., Georgopoulos, D., Michelato, A., Sansone, E., Scarazzato, P., Souvermezoglou, E., 1997. A synthesis of the Ionian Sea hydrography, circulation and water mass pathways during POEM-Phase I. Prog. Oceanogr. 39, 153–204.

Malanotte-Rizzoli, P., Manca, B.B., Ribera d'Alcalà, M., Theocharis, A., Brenner, S., Budillon, G., Ozsoy, E., 1999. The eastern Mediterranean in the 80s and in the 90s: the big transition in the intermediate and deep circulations. Dyn. Atmos. Oceans 29, 365–395.

Maldonado, A., Stanley, D.J., 1976. The Nile cone: submarine fan development by cyclic sedimentation. Mar. Geol. 20, 27–40.

Manca, B.B., Ibello, V., Pacciaroni, M., Scarazzato, P., Giorgetti, A., 2006. Ventilation of deep waters in the Adriatic and Ionian seas following changes in thermohaline circulation of the eastern Mediterranean. Clim. Res. 31, 239–256.

Mandel, R.D., Simmons, A.H., 2001. Prehistoric occupation of Late Quaternary landscapes near Kharga Oasis, Western Desert of Egypt. Geoarchaeology 16, 95–117.

Mangini, A., Schlosser, P., 1986. The formation of eastern Mediterranean sapropels. Mar. Geol. 72, 115–124.

Marino, G., 2008. Palaeoceanography of the interglacial eastern Mediterranean Sea. LPP Contrib. 24 145 pp.

Marino, G., Rohling, E.J., Rijpstra, W.I., Sangiorgi, F., Schouten, S., Sinninghe Damsté, J.S., 2007. Aegean Sea as driver for hydrological and ecological changes in the eastern Mediterranean. Geology 35, 675–678.

Marino, G., Rohling, E.J., Sangiorgi, F., Hayes, A., Casford, J.S.L., Lotter, A.F., Kucera, M., Brinkhuis, H., 2009. Early and middle Holocene in the Aegean Sea: interplay between high and low latitude climate variability. Quat. Sci. Rev. 28, 3246–3262.

Mariolopoulos, E.G., 1961. An outline of the climate of Greece. Publ. Meteorol. Inst. Univ. Athens 6 (51 pp.).

Marshall, J., Schott, F., 1999. Open ocean deep convection: observations, models and theory. Rev. Geophys. 37, 1–64.

Martinez-Ruiz, F., Paytan, A., Kastner, M., Gonzalez-Donoso, J.M., Linares, D., Bernasconi, S.M., Jimenez- Espejo, F.J., 2003. A comparative study of the geochemical and mineralogical characteristics of the S1 sapropel in the western and eastern Mediterranean. Palaeogeogr. Palaeoclimatol. Palaeoecol. 190, 23–37.

Martrat, B., Grimalt, J.O., Lopez-Martinez, C., Cacho, I., Sierro, F.J., Flores, J.A., Zahn, R., Canals, M., Curtis, J.H., Hodell, D.A., 2004. Abrupt temperature changes in the western Mediterranean over the past 250,000 years. Science 306, 1762–1765.

Marullo, S., Santoleri, R., Malanotte-Rizzoli, P., Bergamasco, A., 1999. The sea surface temperature field in the eastern Mediterranean from AVHRR data. Part I: Seasonal variability. J. Mar. Syst. 20, 63–81.

Matthews, A., Ayalon, A., Bar-Matthews, M., 2000. D/H ratios of fluid inclusions of Soreq Cave (Israel) speleothems as a guide to the Eastern Mediterranean Meteoric Line relationships in the last 120 ky. Chem. Geol. 166, 183–191.

Mayewski, P.A., Rohling, E.J., Stager, J.C., Karlén, W., Maasch, K., Meeker, L.D., Meyerson, E., Gasse, F., Van Kreveld, S., Holmgren, K., Lee-Thorp, J., Rosqvist, G., Rack, F., Staubwasser, M., Schneider, R.R., Steig, E., 2004. Holocene climate variability. Quat. Res. 62, 243–255.

McCoy, F.W., 1974. Late Quaternary sedimentation in the eastern Mediterranean Sea. Unpubl. Ph.D. Thesis, Harvard Univ., MA, 132 pp.

McGarry, S., Bar-Matthews, M., Matthews, A., Vaks, A., Schilman, B., Ayalon, A., 2004. Constraints on hydrological and paleotemperature variations in the Eastern Mediterranean region in the last 140 ka given by the δD values of speleothem fluid inclusions. Quat. Sci. Rev. 23, 919–934.

McGill, D.A., 1961. A preliminary study of the oxygen and phosphate distribution in the Mediterranean Sea. Deep-Sea Res. 8, 259–269.

McKenzie, J.A., 1993. Pluvial conditions in the eastern Sahara following the penultimate deglaciation: implications for changes in atmospheric circulation patterns with global warming. Palaeogeogr. Palaeoclimatol. Palaeoecol. 103, 95–105.

MEDAR Group, 2002. Medatlas 2002: Mediterranean and Black Sea Database of Temperature, Salinity and Biochemical Parameters—Climatological Atlas. IFREMER, Brest, France.

MEDATLAS, 1997. Mediterranean Hydrographic Atlas (Mast Supporting Initiative; MAS2-CT93-0074): CD-ROM.

MEDOC group, 1970. Observation of formation of deep water in the Mediterranean Sea. Nature 277, 1037–1040.

Menzel, D., Hopmans, E.C., van Bergen, P.F., de leeuw, J.W., Sinninghe Damsté, J.S., 2002. Development of photic zone euxinia in the eastern Mediterranean Basin during deposition of Pliocene sapropels. Mar. Geol. 189, 215–226.

Mercone, D., Thomson, J., Croudace, I.W., Siani, G., Paterne, M., Troelstra, S., 2000. Duration of S1, the most recent sapropel in the eastern Mediterranean Sea, as indicated by accelerator mass spectrometry radiocarbon and geochemical evidence. Paleoceanography 15, 336–347.

Mercone, D., Thomson, J., Abu-Zied, R.H., Croudace, I.W., Rohling, E.J., 2001. High-resolution geochemical and micropalaeontological profiling of the most recent eastern Mediterranean sapropel. Mar. Geol. 177, 25–44.

MerMex Group, 2011. Marine ecosystems' responses to climatic and anthropogenic forcings in the Mediterranean. Prog. Oceanogr. 91, 97–166.

Meyers, P.A., 2006. Paleoceanographic and paleoclimatic similarities between Mediterranean sapropels and Cretaceous black shales. Palaeogeogr. Palaeoclimatol. Palaeoecol. 235, 305–320.

Meyers, P.A., Doose, H., 1999. Sources, preservation, and thermal maturity of organic matter in Pliocene–Pleistocene organic-carbon-rich sediments of the western Mediterranean Sea. In: Zahn, R., Comas, M.C., Klaus, A. (Eds.), Proceedings of the Ocean Drilling Program. Scientific Results 161. Ocean Drilling Program, College Station, TX, pp. 383–390.

Mikolajewicz, U., 2011. Modelling Mediterranean ocean climate of the Last Glacial Maximum. Clim. Past 7, 161–180.

Miller, A.R., 1963. Physical Oceanography of the Mediterranean Sea: a discourse. Rapp. Comm. Int. Mer Médit. 17, 857–871.

Miller, A.R., 1972. Speculations concerning bottom circulation in the Mediterranean Sea. In: Stanley, D.J. (Ed.), The Mediterranean Sea. Dowden, Hutchinson and Ross, Stroudsburg, Pa., pp. 37–42.

Miller, A.R., 1974. Deep convection in the Aegean Sea. Coll. Int. CNRS 215, 155–163.

Miller, A.R., Tchernia, P., Charnock, H., McGill, D.A., 1970. In: Maxwell, A.E., et al. (Eds.), Mediterranean Sea Atlas of Temperature, Salinity, Oxygen: Profiles and Data From Cruises of R.V. Atlantis and R.V. Chain, With Distribution of Nutrient Chemical Properties. Alpine, Braintree, Mass. (190 pp.).

Millot, C., 1999. Circulation in the western Mediterranean Sea. J. Mar. Syst. 20, 423–442.

Millot, C., 2007. Interannual salinification of the Mediterranean inflow. Geophys. Res. Lett. 34, L21609. http://dx.doi.org/10.1029/2007GL031179.

Millot, C., 2009. Another description of the Mediterranean outflow. Prog. Oceanogr. 82, 101–124.

Millot, C., 2014. Heterogeneities of in- and out-flows in the Mediterranean Sea. Prog. Oceanogr. 120, 254–278.

Millot, C., Taupier-Letage, I., 2005. Circulation in the Mediterranean Sea. The Handbook of Environmental Chemistry. vol. 5: Water Pollution, Part K. Springer-Verlag, Berlin-Heidelberg, pp. 29–66 http://dx.doi.org/10.1007/b107143.

Millot, C., Candela, J., Fuda, J.L., Tber, Y., 2006. Large warming and salinification of the Mediterranean outflow due to changes in its composition. Deep-Sea Res. I 53, 655–666.

Milner, A.M., Collier, R.E.L., Roucoux, K.H., Müller, U.C., Pross, J., Kalaitzidis, S., Christanis, K., Tzedakis, P.C., 2012. Enhanced seasonality of precipitation in the Mediterranean during the early part of the Last Interglacial. Geology 40, 919–922.

Möbius, J., Lahajnar, N., Emeis, K.-C., 2010. Diagenetic control of nitrogen isotope ratios in Holocene sapropels and recent sediments from the Eastern Mediterranean Sea. Biogeosciences 7, 3901–3914.

Moller, T., Schultz, H., Hamann, Y., Dellwig, O., Kucera, M., 2012. Sedimentology and geochemistry of an exceptionally preserved last interglacial sapropel S5 in the Levantine Basin (Mediterranean Sea). Mar. Geol. 291–294, 34–48.

Mommersteeg, H.J.P.M., Loutre, M.F., Young, R., Wijmstra, T.A., Hooghiemstra, H., 1995. Orbital forced frequencies in the 975,000 year pollen record from Tenaghi Philippon (Greece). Clim. Dyn. 11, 4–24.

Moodley, L., Middelburg, J.J., Herman, P.M.J., Soetaert, K., de Lange, G.J., 2005. Oxygenation and organic-matter preservation in marine sediments: direct experimental evidence from ancient organic carbon-rich deposits. Geology 33, 889–892.

Morigi, C., 2009. Benthic environmental changes in the Eastern Mediterranean Sea during sapropel S5 deposition. Palaeogeogr. Palaeoclimatol. Palaeoecol. 273, 258–271.

Moses, T., Kiladis, G.N., Diaz, H.F., Barry, R.G., 1987. Characteristics and frequency of reversals in mean sea level pressure in the North Atlantic sector and their relationship to long-term temperature trends. J. Climatol. 7, 13–30.

Murat, A., 1991. Enregistrement sédimentaire des paléoenvironnements Quaternaires en Méditerranée Orientale. (Thèse de doctorat), Université de Perpignan (280 pp.).

Murat, A., 1999. Pliocene–Pleistocene occurrence of sapropels in the western Mediterranean Sea and their relation to eastern Mediterranean sapropels. In: Zahn, R., Comas, M.C., Klaus, A. (Eds.), Proceedings of the Ocean Drilling Program. Scientific Results 161. Ocean Drilling Program, College Station, TX, pp. 519–527.

Murat, A., Got, H., 1987. Middle and late Quaternary depositional sequences and cycles in the eastern Mediterranean. Sedimentology 34, 885–899.

Murat, A., Got, H., 2000. Organic carbon variations of the eastern Mediterranean Holocene sapropel: a key for understanding formation processes. Palaeogeogr. Palaeoclimatol. Palaeoecol. 158, 241–257.

Myers, P.G., 2002. Flux-forced simulations of the paleocirculation of the Mediterranean. Paleoceanography 17. http://dx.doi.org/10.1029/2000PA000613.

Myers, P.G., Rohling, E.J., 2000. Modelling a 200 year interruption of the Holocene sapropel S1. Quat. Res. 53, 98–104.

Myers, P.G., Haines, K., Rohling, E.J., 1998. Modelling the paleo-circulation of the Mediterranean: The last glacial maximum and the Holocene with emphasis on the formation of sapropel S1. Paleoceanography 13, 586–606.

Myers, P.G., Wielki, C., Goldstein, S.B., Rohling, E.J., 2003. Hydraulic calculations of postglacial connections between the Mediterranean and the Black Sea. Mar. Geol. 201, 253–267.

Naruse, T., Kitagawa, H., Matsubara, H., 1997. Lake level changes and development of alluvial fans in lake Tuz and the Konya basin during the last 24,000 years on the Anatolian Plateau, Turkey. Jpn. Rev. 8, 173–192.

Naval Oceanography Command, 1987. U.S. Navy climatic study of the Mediterranean Sea. Naval Oceanography Command Detachment, Asheville, North Carolina (342 pp.).

Ní Fhlaithearta, S., Reichart, G.J., Jorissen, F.J., Fontanier, C., Rohling, E.J., Thomson, J., De Lange, G.J., 2010. Reconstructing the sea floor environment during sapropel formation using trace metals and sediment composition. Paleoceanography 25, PA4225. http://dx.doi.org/10.1029/2009PA001869.

Nijenhuis, I.A., De Lange, G.J., 2000. Geochemical constraints on Pliocene sapropel formation in the eastern Mediterranean. Mar. Geol. 163, 41–63.

Nijenhuis, I.A., Schenau, S.J., Van der Weijden, C.H., Hilgen, F.J., Lourens, L.J., Zachariasse, W.J., 1996. On the origin of upper Miocene sapropelites: a case study from the Faneromeni section, Crete (Greece). Paleoceanography 11, 633–645.

Nijenhuis, I.A., Brumsack, H.-J., De Lange, G.J., 1998. The trace element budget of the eastern Mediterranean during Pliocene sapropel formation. In: Robertson, A.H.F., Emeis, K.-C., Richter, C., Camerlenghi, A. (Eds.), Proceedings of the Ocean Drilling Program. Scientific Results 160. Ocean Drilling Program, College Station, TX, pp. 199–206.

Nijenhuis, I.A., Bosch, H.-J., Sinninghe Damsté, J.S., Brumsack, H.-J., De Lange, G.J., 1999. Organic matter and trace element rich sapropels and black shales: a geochemical comparison. Earth Planet. Sci. Lett. 169, 277–290.

Nof, D., 1979. On man-induced variations in the circulation of the Mediterranean Sea. Tellus 31, 558–564.

Nolet, G.J., Corliss, B.H., 1990. Benthic foraminiferal evidence for reduced deep-water circulation during sapropel formation in the eastern Mediterranean. Mar. Geol. 94, 109–130.

Olausson, E., 1961. Studies of deep-sea cores. Reports of the Swedish Deep Sea Expedition 1947–1948 8, pp. 353–391.

Olausson, E., 1991. A post-Cromerian rise in sea level. In: Weller, G., Wilson, C.L., Severin, B.A.B. (Eds.), International Conference on the Role of Polar Regions in Global Change: Proceedings of a Conference Held Jun 11–15, 1990 at the University of Alaska Fairbanks vol. II. Geophysical Inst. Univ. of Alaska Fairbanks, pp. 496–498.

O'Neill-Baringer, M., Price, J.F., 1999. A review of the physical oceanography of the Mediterranean outflow. Mar. Geol. 155, 63–82.

Osborne, A.H., Vance, D., Rohling, E.J., Barton, N., Rogerson, M., Fello, N., 2008. A humid corridor across the Sahara for the migration "Out of Africa" of early modern humans 120,000 years ago. Proc. Natl. Acad. Sci. U. S. A. 105, 16444–16447.

Osborne, A., Marino, G., Vance, D., Rohling, E.J., 2010. Eastern Mediterranean surface water Nd during Eemian sapropel S5: monitoring northerly (mid latitude) versus southerly (sub tropical) freshwater contributions. Quat. Sci. Rev. 29, 2473–2483.

Overmann, J., Cypionka, H., Pfennig, N., 1992. An extremely low-light-adapted phototrophic sulphur bacterium from the Black Sea. Limnol. Oceanogr. 37, 150–155.

Ozsoy, E., 1981. On the atmospheric factors affecting the Levantine Sea. European Centre for Medium Range Weather Forecasts Technical Report 25 (29 pp.).

Pachur, H.J., 2001. Holozäne Klimawechsel in den nördlichen Subtropen. Nova Acta Leopoldina NF88 331pp. 109–131.

Pachur, H.J., Braun, G., 1980. The paleoclimate of the central Sahara, Libya and the Libyan Desert. Palaeoecol. Afr. 12, 351–363.

Paillou, P., Schuster, M., Tooth, S., Farr, T., Rosenqvist, A., Lopez, S., Malezieux, J.M., 2009. Mapping of a major paleodrainage system in eastern Libya using orbital imaging radar: the Kufrah River. Earth Planet. Sci. Lett. 277, 327–333.

Paillou, P., Tooth, S., Lopez, S., 2012. The Kufrah paleodrainage system in Libya: a past connection to the Mediterranean Sea? Compt. Rendus Geosci. 344, 406–414.

Painter, S.C., Tsimplis, M.N., 2003. Temperature and salinity trends in the upper waters of the Mediterranean Sea as determined from the MEDATLAS dataset. Cont. Shelf Res. 23, 1507–1522.

Parrilla, G., Kinder, T.H., Preller, R.H., 1986. Deep and intermediate Mediterranean water in the western Alboran Sea. Deep-Sea Res. 33, 55–88.

Passier, H.F., Middelburg, J.J., Van Os, B.J.H., De Lange, G.J., 1996. Diagenetic pyritisation under eastern Mediterranean sapropels caused by downward sulphide diffusion. Geochim. Cosmochim. Acta 60, 751–763.

Passier, H.F., Middelburg, J.J., De Lange, G.J., Böttcher, M.E., 1999a. Modes of sapropel formation in the eastern Mediterranean: some constraints based on pyrite properties. Mar. Geol. 153, 199–220.

Passier, H.F., Bosch, H.-J., Nijenhuis, I.A., Lourens, L.J., Bottcher, M.E., Leenders, A., Sinninghe Damsté, J.S., De Lange, G.J., De Leeuw, J.W., 1999b. Sulphidic Mediterranean surface waters during Pliocene sapropel formation. Nature 397, 146–149.

Pearce, R.B., Kemp, A.E.S., Koizumi, I., Pike, J., Cramp, A.J., Rowland, S.J., 1998. A lamina-scale SEM-based study of a late Quaternary diatom-ooze sapropel from the Mediterranean Ridge. ODP Site 971. Proc. Ocean Drill. Program Sci. Results 160, 349–363.

Peeters, F., 2000. The distribution and stable isotope composition of living planktic foraminifera in relation to seasonal changes in the Arabian Sea. (Ph.D. thesis), Free Univ. Amsterdam, Amsterdam (184 pp.).

Perissoratis, C., Piper, D.J.W., 1992. Age, regional variation and shallowest occurence of S_1 sapropel in the northern Aegean Sea. Geomarine Lett. 12, 49–53.

Perkins, H., Pistek, P., 1990. Circulation in the Algerian Basin during June 1986. J. Geophys. Res. 95, 1577–1585.

Petit-Maire, N., Guo, Z., 1997. In-phase Holocene climate variations in the present-day desert areas of China and Northern Africa. In: Meco, J., Petit-Maire, N. (Eds.), Climates of the Past. Proceedings of the UNESCO-IUGS, June 2–7, 1995, CLIP meeting. Universidad de Las Palmas, Gran Canaria, Spain, pp. 137–140.

Peyron, O., Guiot, J., Cheddadi, R., Tarasov, P.E., Reille, M., de Beaulieu, J.L., Bottema, S., Andrieu, V., 1998. Climatic reconstruction in Europe for 18,000 yr BP from pollen data. Quat. Res. 49, 183–196.

Peyron, O., Goring, S., Dormoy, I., Kotthoff, U., Pross, J., de Beaulieu, J.-L., Drescher-Schneider, R., Vannière, B., Magny, M., 2011. Holocene seasonality changes in the central Mediterranean region reconstructed from the pollen sequences of Lake Accesa (Italy) and Tenaghi Philippon (Greece). The Holocene 21, 131–146.

Piccini, L., Zanchetta, G., Drysdale, R.N., Hellstrom, J., Isola, I., Fallick, A.E., Leone, G., Doveri, M., Mussi, M., Mantelli, F., Molli, G., Lotti, L., Roncioni, A., Regattieri, E., Meccheri, M., Vaselli, L., 2008. The environmental features of the Monte Corchia cave system (Apuan Alps, central Italy) and their effects on speleothem growth. Int. J. Speleol. 37, 153–172.

Pinardi, N., Masetti, E., 2000. Variability of the large scale general circulation of the Mediterranean Sea from observations and modelling: a review. Palaeogeogr. Palaeoclimatol. Palaeoecol. 158, 153–173.

Pinardi, N., Zavatarelli, M., Adani, M., Coppini, G., Fratianni, C., Oddo, P., Simoncelli, S., Tonani, M., Lyubartsev, V., Dobricic, S., Bonaduce, A., 2015. Mediterranean Sea large-scale low-frequency ocean variability and water mass formation rates from 1987 to 2007: a retrospective analysis. Prog. Oceanogr. http://dx.doi.org/10.1016/j.pocean.2013.11.003 (in press).

Pistek, P., De Strobel, F., Montanari, C., 1985. Deep Sea circulation in the Alboran Sea. J. Geophys. Res. 90, 4969–4976.

POEM group, 1992. General circulation of the eastern Mediterranean Sea. Earth Sci. Rev. 32, 285–308.

Pollak, M.I., 1951. The sources of deep water of the eastern Mediterranean Sea. Deep-Sea Res. 10, 128–152.

Poulos, S.E., Drakopoulos, P.G., Collins, M.B., 1997. Seasonal variability in sea surface oceanographic conditions in the Aegean Sea (eastern Mediterranean): an overview. J. Mar. Syst. 13, 225–244.

Price, J.F., O'Neill-Baringer, M., Lueck, R.G., Johnson, G.C., Ambar, I., Parilla, G., Cantos, A., Kenelly, M.A., Sanford, T.B., 1993. Mediterranean outflow mixing and dynamics. Science 259, 1277–1282.

Pross, J., Kotthoff, U., Müller, U.C., Peyron, O., Dormoy, I., Schmiedl, G., Kalaitzidis, S., Smith, A.M., 2009. Massive perturbation in terrestrial ecosystems of the Eastern Mediterranean region associated with the 8.2 kyr BP climatic event. Geology 37, 887–890.

Raicich, F., Pinardi, N., Navarra, A., 2003. Teleconnections between Indian monsoon and Sahel rainfall and the Mediterranean. Int. J. Climatol. 23, 173–186.

Reichart, G.J., Brinkhuis, H., 2003. Cysts of Protoperidinium as indicators of paleoproductivity: the northern Arabian Sea as a natural laboratory. Mar. Micropaleontol. 49, 303–315.

Reid, J.L., 1979. On the contribution of the Mediterranean Sea outflow to the Norwegian-Greenland Sea. Deep-Sea Res. 26A, 1199–1223.

Reiss, Z., Halicz, E., Luz, B., 1999. Late-Holocene foraminifera from the SE Levantine Basin. Israel J. Earth Sci. 48, 1–27.

Repeta, D.J., Simpson, D.J., Jørgensen, B.B., Jannasch, H.W., 1989. Evidence for anoxygenic photosynthesis from the distribution of bacteriochlorophylls in the Black Sea. Nature 342, 69–72.

Revel, M., Ducassou, E., Grousset, F.E., Bernasconi, S.M., Migeon, S., Revillon, S., Mascle, J., Murat, A., Zaragosi, S., Bosch, D., 2010. 100,000 years of African monsoon variability recorded in sediments of the Nile margin. Quat. Sci. Rev. 29, 1342–1362.

Ribera d'Alcalà, M., Civitarese, G., Conversano, F., Lavezza, R., 2003. Nutrient ratios and fluxes hint at overlooked processes in the Mediterranean Sea. J. Geophys. Res. 108, 8106. http://dx.doi.org/10.1029/2002JC001650.

Richez, C., Gascard, J.C., 1986. Mediterranean water flows when approaching the Strait of Gibraltar. Deep-Sea Res. 33, 135–137.

Ritchie, J.C., Eyles, C.H., Haynes, C.V., 1985. Sediment and pollen evidence for an early to mid-Holocene humid period in the eastern Sahara. Nature 314, 352–355.

Roberts, N., Reed, J.M., Leng, M.J., Kuzucuo lu, C., Fontugne, M., Bertaux, J., Woldring, H., Bottema, S., Black, S., Hunt, E., Karabıyıko lu, M., 2001. The tempo of Holocene climatic change in the eastern Mediterranean region: new high-resolution crater-lake sediment data from central Turkey. The Holocene 11, 721–736.

Roberts, N., Brayshaw, D., Kuzucuoglu, C., Perez, R., Sadori, L., 2011. The mid-Holocene climatic transition in the Mediterranean: causes and consequences. The Holocene 21, 3–13.

Robinson, A.R., Golnaraghi, M., 1994. The physical and dynamical oceanography of the Mediterranean Sea. In: Malanotte-Rizzoli, P., Robinson, A.R. (Eds.), Ocean Processes in Climate Dynamics: Global and Mediterranean Examples. Kluwer Academic Publishers, Netherlands, pp. 255–306.

Rodrigues, D., Abell, P.I., Kröpelin, S., 2000. Seasonality in the early Holocene climate of northwest Sudan: interpretation of *Etheria elliptica* shell isotopic data. Glob. Planet. Chang. 26, 181–187.

Rodwell, M.J., Hoskins, B.J., 1996. Monsoons and the dynamics of deserts. Q. J. R. Meteorol. Soc. 122, 1385–1404.

Roether, W., Schlitzer, R., 1991. Eastern Mediterranean deep water renewal on the basis of chlorofluoromethane and tritium data. Dyn. Atmos. Oceans 15, 333–354.

Roether, W., Well, R., 2001. Oxygen consumption in the Eastern Mediterranean. Deep-Sea Res. I 48, 1535–1551.

Roether, W., Schlosser, P., Kuntz, R., Weiss, W., 1983. Transient tracer studies of the thermohaline circulation of the Mediterranean. Manuscripts for Mediterranean circulation. NATO Workshop (44 pp.).

Roether, W., Manca, B.B., Klien, B., Bregant, D., Georgopoulos, D., Beitzel, V., Kovacevic, V., Luchetta, A., 1996. Recent changes in Eastern Mediterranean deep waters. Science 271, 333–335.

Roether, W., Klein, B., Manca, B.B., Theocharis, A., Kioroglou, S., 2007. Transient Eastern Mediterranean deep waters in response to the massive dense-water output of the Aegean Sea in the 1990s. Prog. Oceanogr. 74, 540–571.

Rogerson, M., Cacho, I., Jimenez-Espejo, F., Reguera, M.I., Sierro, F.J., Martinez-Ruiz, F., Frigola, J., Canals, M., 2008. A dynamic explanation for the origin of the western Mediterranean organic rich layers. Geochem. Geophys. Geosyst. 9, Q07U01. http://dx.doi.org/10.1029/2007GC001936.

Rogerson, M., Rohling, E.J., Bigg, G.R., Ramirez, J., 2012a. Palaeoceanography of the Atlantic-Mediterranean Exchange: overview and first quantitative assessment of climatic forcing. Rev. Geophys. 50, RG2003. http://dx.doi.org/10.1029/2011RG000376.

Rogerson, M., Bigg, G.R., Rohling, E.J., Ramirez, J., 2012b. Vertical density gradient in the eastern north Atlantic during the last 30,000 years. Clim. Dyn. 39, 589–598.

Rohling, E.J., 1991a. A simple two-layered model for shoaling of the eastern Mediterranean pycnocline due to glacio-eustatic sea-level lowering. Paleoceanography 6, 537–541.

Rohling, E.J., 1991b. Shoaling of the eastern Mediterranean pycnocline due to reduction of excess evaporation: implications for sapropel formation. Paleoceanography 6, 747–753.

Rohling, E.J., 1994. Review and new aspects concerning the formation of Mediterranean sapropels. Mar. Geol. 122, 1–28.

Rohling, E.J., 1999. Environmental controls on Mediterraneansalinity and δ^{18}O. Paleoceanography 14, 706–715.

Rohling, E.J., 2007. Progress in palaeosalinity: overview and presentation of a new approach. Paleoceanography 22, PA3215. http://dx.doi.org/10.1029/2007PA001437.

Rohling, E.J., 2013. Quantitative assessment of glacial fluctuations in the level of Lake Lisan, Dead Sea rift. Quat. Sci. Rev. 70, 63–72.

Rohling, E.J., Bryden, H.L., 1992. Man-induced salinity and temperature increases in Western Mediterranean deep water. J. Geophys. Res. 97, 11191–11198.

Rohling, E.J., Bryden, H.L., 1994. Estimating past changes in the eastern Mediterranean freshwater budget, using reconstructions of sea level and hydrography. Proc. K. Ned. Akad. Wet. Ser. B 97, 201–217.

Rohling, E.J., De Rijk, S., 1999a. The Holocene Climate Optimum and Last Glacial Maximum in the Mediterranean: the marine oxygen isotope record. Mar. Geol. 153, 57–75.

Rohling, E.J., De Rijk, S., 1999b. Erratum to "The Holocene Climate Optimum and Last Glacial Maximum in the Mediterranean: the marine oxygen isotope record.". Mar. Geol. 161, 385–387.

Rohling, E.J., Gieskes, W.W.C., 1989. Late Quaternary changes in Mediterranean Intermediate Water density and formation rate. Paleoceanography 4, 531–545.

Rohling, E.J., Hilgen, F.J., 1991. The eastern Mediterranean climate at times of sapropel formation: a review. Geol. Mijnb. 70, 253–264.

Rohling, E.J., Pälike, H., 2005. Centennial-scale climate cooling with a sudden cold event around 8,200 years ago. Nature 434, 975–979.

Rohling, E.J., Thunell, R.C., 1999. Five decades of Mediterranean paleoclimate and sapropel studies. Mar. Geol. 153, 7–10.

Rohling, E.J., Jorissen, F.J., Vergnaud-Grazzini, C., Zachariasse, W.J., 1993a. Northern Levantine and Adriatic Quaternary planktic foraminifera; reconstruction of paleoenvironmental gradients. Mar. Micropaleontol. 21, 191–218.

Rohling, E.J., De Stigter, H.C., Vergnaud-Grazzini, C., Zaalberg, R., 1993b. Temporary repopulation by low-oxygen tolerant benthic foraminifera within an upper Pliocene sapropel; evidence for the role of oxygen depletion in the formation of sapropels. Mar. Micropaleontol. 22, 207–219.

Rohling, E.J., Den Dulk, M., Pujol, C., Vergnaud-Grazzini, C., 1995. Abrupt hydrographic change in the Alboran Sea (western Mediterranean) around 8000 yrs BP. Deep-Sea Res. 42, 1609–1619.

Rohling, E.J., Jorissen, F.J., De Stigter, H.C., 1997. 200 Year interruption of Holocene sapropel formation in the Adriatic Sea. J. Micropalaeontol. 16, 97–108.

Rohling, E.J., Hayes, A., Kroon, D., De Rijk, S., Zachariasse, W.J., 1998. Abrupt cold spells in the NW Mediterranean. Paleoceanography 13, 316–322.

Rohling, E.J., Mayewski, P.A., Hayes, A., Abu-Zied, R.H., Casford, J.S.L., 2002a. Holocene atmosphere-ocean interactions: records from Greenland and the Aegean Sea. Clim. Dyn. 18, 587–593.

Rohling, E.J., Cane, T.R., Cooke, S., Sprovieri, M., Bouloubassi, I., Emeis, K.C., Schiebel, R., Kroon, D., Jorissen, F.J., Lorre, A., Kemp, A.E.S., 2002b. African monsoon variability during the previous interglacial maximum. Earth Planet. Sci. Lett. 202, 61–75.

Rohling, E.J., Sprovieri, M., Cane, T.R., Casford, J.S.L., Cooke, S., Bouloubassi, I., Emeis, K.C., Schiebel, R., Hayes, A., Jorissen, F.J., Kroon, D., 2004. Reconstructing past planktic foraminiferal habitats using stable isotope data: a case history for Mediterranean sapropel S5. Mar. Micropaleontol. 50, 89–123.

Rohling, E.J., Hopmans, E.C., Sinninghe-Damsté, J.S., 2006. Water column dynamics during the last interglacial anoxic event in the Mediterranean (sapropel S5). Paleoceanography 21, PA2018. http://dx.doi.org/10.1029/2005PA001237.

Rohling, E.J., Abu-Zied, R., Casford, J.S.L., Hayes, A., Hoogakker, B.A.A., 2009. The marine environment: present and past. In: Woodward, J.C. (Ed.), The Physical Geography of the Mediterranean. Oxford University Press. ISBN: 978-0-19-926803-0, pp. 33–67.

Rohling, E.J., Foster, G.L., Grant, K.M., Marino, G., Roberts, A.P., Tamisiea, M.E., Williams, F., 2014. Sea-level and deep-sea-temperature variability over the past 5.3 million years. Nature 508, 477–482.

Rossignol-Strick, M., 1983. African monsoons, an immediate climate response to orbital insolation. Nature 30, 446–449.

Rossignol-Strick, M., 1985. Mediterranean Quaternary sapropels, an immediate response of the African monsoon to variations of insolation. Palaeogeogr. Palaeoclimatol. Palaeoecol. 49, 237–263.

Rossignol-Strick, M., 1987. Rainy periods and bottom water stagnation initiating brine accumulation and metal concentrations: 1. the Late Quaternary. Paleoceanography 2, 333–360.

Rossignol-Strick, M., 1995. Sea-land correlation of pollen records in the eastern Mediterranean for the glacial-interglacial transition: biostratigraphy versus radiometric timescale. Quat. Sci. Rev. 14, 893–915.

Rossignol-Strick, M., 1999. The Holocene climatic optimum and pollen records of sapropel 1 in the eastern Mediterranean, 9000–6000BP. Quat. Sci. Rev. 18, 515–530.

Rossignol-Strick, M., Paterne, M., 1999. A synthetic pollen record of the eastern Mediterranean sapropels of the last 1 Ma: implications for the time-scale and formation of sapropels. Mar. Geol. 153, 221–237.

Rossignol-Strick, M., Nesteroff, V., Olive, P., Vergnaud-Grazzini, C., 1982. After the deluge; Mediterranean stagnation and sapropel formation. Nature 295, 105–110.

Rozanski, K., 1985. Deuterium and oxygen-18 in European groundwaters — links to atmospheric circulation in the past. Chem. Geol. (Isot. Geosci. Sect.) 52, 349–363.

Rumney, G.R., 1968. Climatology and the World's Climates. Macmillan Company, New York (656 pp.).

Ryan, W.B.F., Cita, M.B., 1977. Ignorance concerning episodes of ocean-wide stagnation. Mar. Geol. 23, 193–215.

Saaroni, H., Bitan, A., Alpert, P., Ziv, B., 1996. Continental Polar outbreaks into the Levant and Eastern Mediterranean. Int. J. Climatol. 16, 1175–1191.

Sachs, J., Repeta, D.J., 1999. Oligotrophy and Nitrogen fixation during eastern Mediterranean sapropel events. Science 286, 2485–2488.

Said, R., 1981. The Geological Evolution of the River Nile. Springer-Verlag, New York (151 pp.).

Samuel, S., Haines, K., Josey, S., Myers, P.G., 1999. Response of the Mediterranean Sea thermohaline circulation to observed changes in the winter wind stress field in the period 1980–1993. J. Geophys. Res. 104, 7771–7784.

Sancetta, C., 1994. Mediterranean sapropels: seasonal stratification yields high production and carbon flux. Paleoceanography 9, 195–196.

Sangiorgi, F., Capotondi, L., Combourieu Nebout, N., Vigliotti, L., Brinkhuis, H., Giunta, S., Lotter, A.F., Morigi, C., Negri, A., Reichart, G.J., 2003. Holocene seasonal sea surface temperature variations in the South Adriatic Sea inferred from a multi-proxy approach. J. Quat. Sci. 18, 723–732.

Sangiorgi, F., Dinelli, E., Maffioli, P., Capotondi, L., Giunta, S., Morigi, C., Speranza Principato, M., Negri, A., Emeis, K.-C., Corselli, C., 2006. Geochemical and micropaleontological characterisation of a Mediterranean sapropel S5: a case study from core BAN89GC09 (south of Crete). Palaeogeogr. Palaeoclimatol. Palaeoecol. 235, 192–207.

Santarelli, A., Brinkhuis, H., Hilgen, F.J., Lourens, L.J., Versteegh, G.J.M., Visscher, H., 1998. Orbital signatures in a Late Miocene dinoflagellate record from Crete (Greece). Mar. Micropaleontol. 33, 273–297.

Schenau, S.J., Antonarakou, A., Hilgen, F.J., Lourens, L.J., Nijenhuis, I.A., Van der Weijden, C.H., Zachariasse, W.J., 1999. Organic-rich layers in the Metochia section (Gavdos, Greece): evidence for a single mechanism of sapropel formation during the past 10 My. Mar. Geol. 153, 117–135.

Schlitzer, R., 2014. Ocean Data View. http://odv.awi.de.

Schlitzer, R., Roether, W., Oster, H., Junghans, H.G., Hausmann, M., Johannsen, H., Michelato, A., 1991. Chlorofluoromethane and oxygen in the eastern Mediterranean. Deep-Sea Res. 38, 1531–1551.

Schmiedl, G., Mitschele, A., Beck, S., Emeis, K.C., Hemleben, Ch., Schultz, H., Sperling, M., Weldeab, S., 2003. Benthic foraminiferal record of ecosystem variability in the eastern Mediterranean Sea during times of sapropel S_5 and S_6 deposition. Palaeogeogr. Palaeoclimatol. Palaeoecol. 190, 139–164.

Schmiedl, G., Kuhnt, T., Ehrmann, W., Emeis, K.-C., Hamann, Y., Kotthoff, U., Dulski, P., Pross, J., 2010. Climatic forcing of eastern Mediterranean deep-water formation and benthic ecosystems during the past 22 000 years. Quat. Sci. Rev. 29, 3006–3020.

Schott, F., Leaman, K., 1991. Observations with moored acoustic Doppler current profilers in the convection regime in the Gulf of Lions. J. Phys. Oceanogr. 21, 558–574.

Schrader, H., Matherne, A., 1981. Sapropel formation in the eastern Mediterranean Sea: evidence from preserved opal assemblages. Micropaleontology 27, 191–203.

Schröder, K., Gasparini, G.P., Tangherlini, M., Astralidi, M., 2006. Deep and intermediate water in the western Mediterranean under the influence of the Eastern Mediterranean Transient. Geophys. Res. Lett. 33, L21607. http://dx.doi.org/10.1029/2006GL027121.

Schröder, K., Ribotti, A., Borghini, M., Sorgente, R., Perilli, A., Gasparini, G.P., 2008. An extensive Western Mediterranean Deep Water renewal between 2004 and 2006. Geophys. Res. Lett. 35, L18605. http://dx.doi.org/10.1029/2008GL035146.

Schubert, C.J., Villanueva, J., Calvert, S.E., Cowie, G.L., von Rad, U., Schulz, H., Berner, U., Erlenkeusser, H., 1998. Stable phytoplankton community structure in the Arabian Sea over the past 200,000 years. Nature 394, 563–566.

Scrivner, A., Vance, D., Rohling, E.J., 2004. New neodymium isotope data quantify Nile involvement in Mediterranean anoxic episodes. Geology 32, 565–568.

Seim, H., Gregg, M.C., 1997. The importance of aspiration and channel curvature in producing strong vertical mixing over a sill. J. Geophys. Res. 102, 3451–3472.

Send, U., Font, J., Krahmann, G., Millot, C., Rhein, M., Tintoré, J., 1999. Recent advances in observing the physical oceanography of the western Mediterranean Sea. Prog. Oceanogr. 44, 37–64.

Sharaf El Din, S.H., 1977. Effect of Aswan High Dam on the Nile flood and on the estuarine and coastal circulation pattern along the Mediterranean Egyptian coast. Limnol. Oceanogr. 22, 194–207.

Shaw, H.F., Evans, G., 1984. The nature, distribution and origin of a sapropelic layer in sediments of the Cilicia Basin, northeastern Mediterranean. Mar. Geol. 61, 1–12.

Siddall, M., Rohling, E.J., Almogi-Labin, A., Hemleben, Ch., Meischner, D., Schmeltzer, I., Smeed, D.A., 2003. Sea-level fluctuations during the last glacial cycle. Nature 423, 853–858.

Sierro, F.J., Flores, J.A., Zamarreño, I., Vázquez, A., Utrilla, R., Francés, G., Hilgen, F.J., Krijgsman, W., 1999. Messinian pre-evaporite sapropels and precession-induced oscillations in western Mediterranean climate. Mar. Geol. 153, 137–146.

Skliris, N., Lascaratos, A., 2004. Impacts of the Nile River damming on the thermohaline circulation and water mass characteristics of the Mediterranean Sea. J. Mar. Syst. 52, 121–143.

Skliris, N., Sofianos, S., Lascaratos, A., 2007. Hydrological changes in the Mediterranean Sea in relation to changes in the freshwater budget: a numerical modelling study. J. Mar. Syst. 65, 400–416.

Slomp, C.P., Thomson, J., De Lange, G.J., 2002. Enhanced regeneration of phosphorus during formation of the most recent eastern Mediterranean sapropel (S1). Geochim. Cosmochim. Acta 66, 1171–1184.

Smith, J.R., Giegengack, R., Schwarcz, H.P., McDonald, M.M.A., Kleindienst, M.R., et al., 2004. A reconstruction of Quaternary pluvial environments and human occupations using stratigraphy and geochronology of fossil-spring tufas, Kharga Oasis, Egypt. Geoarchaeology 19, 407–439.

Smith, R.O., Bryden, H.L., Stansfield, K., 2008. Observations of new western Mediterranean deep water formation using Argo floats 2004–2006. Ocean Sci. 4, 133–149.

Sonntag, C., Klitzsch, E., Löhnert, E.P., El Shazly, E.M., Münnich, K.O., Junghans, Ch., Thorweihe, U., Weistroffer, K., Swailem, F.M., 1979. Paleoclimatic information from deuterium and oxygen-18 in carbon-14-dated north Saharan groundwaters. Isotope Hydrology 1978, II. International Atomic Energy Agency, Vienna, pp. 569–580.

Sperling, M., Schmiedl, G., Hemleben, Ch., Emeis, K.C., Erlenkeuser, H., Grootes, P.M., 2003. Black Sea impact on the formation of eastern Mediterranean sapropel S1? Evidence from the Marmara Sea. Palaeogeogr. Palaeoclimatol. Palaeoecol. 190, 9–21.

Spötl, C., Nicolussi, K., Patzelt, G., Boch, R., Daphne Team, 2010. Humid climate during deposition of sapropel 1 in the Mediterranean Sea: assessing the influence on the Alps. Glob. Planet. Chang. 71, 242–248.

Sprovieri, R., Di Stefano, E., Incarbona, A., Oppo, D.W., 2006. Suborbital climate variability during Marine Isotopic Stage 5 in the central Mediterranean basin: evidence from calcareous plankton record. Quat. Sci. Rev. 25, 2332–2342.

Stanford, J.D., Hemingway, R., Rohling, E.J., Challenor, P.G., Medina-Elizalde, M., Lester, A.J., 2011. Sea-level probability for the last deglaciation: a statistical analysis of far-field records. Glob. Planet. Chang. 79, 193–203.

Stanley, D.J., 1996. Nile Delta: extreme case of sediment entrapment on a delta plain and consequent coastal land loss. Mar. Geol. 129, 189–195.

Stanley, D.J., Maldonado, A., 1977. Nile Cone: Late Quaternary stratigraphy and sediment dispersal. Nature 266, 129–135.

Stanley, D.J., Maldonado, A., 1979. Levantine Sea–Nile Cone lithostratigraphic evolution: quantitative analysis and correlation with paleoclimatic and eustatic oscillations in the Late Quaternary. Sediment. Geol. 23, 37–65.

Stanley, D.J., Maldonado, A., Stuckenrath, R., 1975. Strait of Sicily depositional rates and patterns, and possible reversal of currents in the late Quaternary. Palaeogeogr. Palaeoclimatol. Palaeoecol. 18, 279–291.

Stanley, D.J., Nir, Y., Galili, E., 1998. Clay mineral distributions to interpret Nile cell provenance and dispersal: II. Offshore margin between Nile to delta and northern Israel. J. Coast. Res. 14, 196–217.

Stansfield, K., Gasparini, G.P., Smeed, D.A., 2003. High-resolution observations of the path of the overflow from the Sicily Strait. Deep-Sea Res. I 50, 1129–1149.

Stommel, H., Bryden, H., Mangelsdorf, P., 1973. Does some of the Mediterranean outflow come from great depth? Pure Appl. Geophys. 105, 879–889.

Stratford, K., Williams, R.G., Myers, P.G., 2000. Impact of the circulation on sapropel formation in the eastern Mediterranean. Glob. Biogeochem. Cycles 14, 683–695.

Strohle, K., Krom, M.D., 1997. Evidence for the evolution of an oxygen minimum layer at the beginning of S-1 sapropel deposition in the eastern Mediterranean. Mar. Geol. 140, 231–236.

Struck, U., Emeis, K.C., Voss, M., Krom, M.D., Rau, G.H., 2001. Biological productivity during sapropel S5 formation in the Eastern Mediterranean Sea: evidence from stable isotopes of nitrogen and carbon. Geochim. Cosmochim. Acta 65, 3249–3266.

Szabo, B.J., Haynes Jr., C.V., Maxwell, T.A., 1995. Ages of Quaternary pluvial episodes determined by uranium-series and radiocarbon dating of lacustrine deposits of Eastern Sahara. Palaeogeogr. Palaeoclimatol. Palaeoecol. 113, 227–242.

Tang, C.M., Stott, L.D., 1993. Seasonal salinity changes during Mediterranean sapropel deposition 9000 years B.P.: evidence from isotopic analyses of individual planktonic foraminifera. Paleoceanography 8, 473–493.

Targarona, J., Alonso, B., Brinkhuis, H., Canals, M., Rohling, E.J., Versteegh, G.J.M., 1997. Productivity variations in the Alboran Sea over the last 20,000 years from Protoperidinium dinoflagellate cyst records. LPP Contrib. 7, 43–66.

Theocharis, A., 1989. Deep water formation and circulation in the Aegean Sea. Rep. Meteorol. Oceanogr. 40 (I), 335–359.

Theocharis, A., 2009. Variability of the thermohaline properties in the Eastern Mediterranean during the post-EMT period (1995–2008) and SST changes in the Aegean (1985–2008). In: Briand, F. (Ed.), CIESM, 2009, Dynamics of Mediterranean deep waters. CIESM Workshop Monographs 38, pp. 35–40 (Monaco).

Theocharis, A., Georgopoulos, D., 1993. Dense water formation over the Samothraki and Limnos Plateaux in the north Aegean Sea (eastern Mediterranean Sea). Cont. Shelf Res. 13, 919–939.

Theocharis, A., Klein, B., Nittis, K., Roether, W., 2002. Evolution and Status of the Eastern Mediterranean Transient (1997–1999). J. Mar. Syst. 33–34, 91–116.

Thomson, J., Higgs, N.C., Wilson, T.R.S., Croudace, I.W., De Lange, G.J., Van Santvoort, P.J.M., 1995. Redistribution and geochemical behaviour of redox-sensitive elements around S1, the most recent eastern Mediterranean sapropel. Geochim. Cosmochim. Acta 59, 3487–3501.

Thomson, J., Mercone, D., de Lange, G.J., van Santvoort, P.J.M., 1999. Review of recent advances in the interpretation of eastern Mediterranean sapropel S1 from geochemical evidence. Mar. Geol. 153, 77–89.

Thomson, J., Crudeli, D., De Lange, G.J., Slomp, C.P., Erba, E., Corselli, C., Calvert, S.E., 2004. Florisphaera profunda and the origin and diagenesis of carbonate phases in eastern Mediterranean sapropel units. Paleoceanography 19, PA3003. http://dx.doi.org/10.1029/2003PA000976.

Thunell, R.C., Williams, D.F., 1983. Paleotemperature and paleosalinity history of the eastern Mediterranean during the late Quaternary. Palaeogeogr. Palaeoclimatol. Palaeoecol. 44, 23–39.

Thunell, R.C., Williams, D.F., 1989. Glacial-Holocene salinity changes in the Mediterranean Sea: hydrographic and depositional effects. Nature 338, 493–496.

Tierney, J.E., deMenocal, P.B., 2013. Abrupt shifts in Horn of Africa hydroclimate since the Last Glacial Maximum. Science 342, 843–846.

Tintoré, J.D., La Violette, P.E., Blade, I., Cruzado, A., 1988. A study of an intense density front in the eastern Alboran Sea: The Almeria-Oran Front. J. Phys. Oceanogr. 18, 1384–1397.

Trewartha, G.T., 1966. The earth's problem climates. Methuen & Co., London (334 pp.).

Triantaphyllou, M.V., Ziveri, P., Gogou, A., Marino, G., Lykousis, V., Bouloubassi, I., Emeis, K.-C., Kouli, K., Dimizia, M., Rosell-Melé, A., Papanikolaou, M., Katsouras, G., Nunez, N., 2009. Late Glacial–Holocene climate variability at the south-eastern margin of the Aegean Sea. Mar. Geol. 266, 182–197.

Trigo, I.F., Davies, T.D., Bigg, G.R., 1999. Objective climatology in the Mediterranean region. J. Clim. 12, 1685–1696.

Tsimplis, M.N., Bryden, H.L., 2000. Estimation of the transports through the Strait of Gibraltar. Deep-Sea Res. I 47, 2219–2242.

Tzedakis, P.C., 1993. Long-term tree populations in northwest Greece through multiple climatic cycles. Nature 364, 437–440.

Tzedakis, P.C., 2007. Seven ambiguities in the Mediterranean palaeoenvironmental narrative. Quat. Sci. Rev. 26, 2042–2066.

Tzedakis, P.C., 2009. Cenozoic climate and vegetation change. In: Woodward, J.C. (Ed.), The Physical Geography of the Mediterranean. Oxford University Press, Oxford, pp. 89–137.

UNDP/UNESCO, 1978. Coastal protection studies. Project Findings and Recommendations (Paris: UNDP/EGY/73/063) (483 pp.).

Vaks, A., Bar-Matthews, M., Ayalon, A., Schilman, B., Gilmour, M., Hawkesworth, C.J., Frumkin, A., Kaufman, A., Matthews, A., 2003. Paleoclimate reconstruction based on the timing of speleothem growth and oxygen and carbon isotope composition in a cave located in the rain shadow in Israel. Quat. Res. 59, 182–193.

Vaks, A., Bar-Matthews, M., Ayalon, A., Matthews, A., Frumkin, A., Dayan, U., Halicz, L., Almogi-Labin, A., Schilman, B., 2006. Paleoclimate and location of the border between Mediterranean climate region and the Saharo-Arabian Desert as revealed by speleothems from the northern Negev Desert, Israel. Earth Planet. Sci. Lett. 249, 384–399.

Vaks, A., Bar-Matthews, M., Ayalon, A., Matthews, A., Halicz, L., Frumkin, A., 2007. Desert speleothems reveal climatic window for African exodus of early modern humans. Geology 35, 831–834.

Vaks, A., Bar-Matthews, M., Matthews, A., Ayalon, A., Frumkin, A., 2010. Middle-Late Quaternary paleoclimate of northern margins of the Saharan-Arabian Desert: reconstruction from speleothems of Negev Desert, Israel. Quat. Sci. Rev. 29, 2647–2662.

Van der Meer, M.T.J., Baas, M., Rijpstra, W.I.C., Marino, G., Rohling, E.J., Sinninghe Damsté, J.S., Schouten, S., 2007. Hydrogen isotopic compositions of long-chain alkenones record freshwater flooding of the eastern Mediterranean at the onset of sapropel deposition. Earth Planet. Sci. Lett. 262, 594–600.

Van der Zwaan, G.J., Gudjonsson, L., 1986. Middle Miocene–Pliocene stable isotope stratigraphy and paleoceanography of the Mediterranean. Mar. Micropaleontol. 10, 71–90.

Van Santvoort, P.J.M., De Lange, G.J., Thomson, J., Cussen, H., Wilson, T.R.S., Krom, M.D., Strohle, K., 1996. Active post-depositional oxidation of the most recent sapropel (S1) in sediments of the eastern Mediterranean Sea. Geochim. Cosmochim. Acta 60, 4007–4024.

Van Santvoort, P.J.M., de Lange, G.J., Langereis, C.G., Dekkers, M.J., Paterne, M., 1997. Geochemical and paleomagnetic evidence for the occurrence of "missing" sapropels in eastern Mediterranean sediments. Paleoceanography 12, 773–786.

Van Straaten, L.M.J.U., 1966. Micro-malacological investigation of cores from the southeastern Adriatic Sea. Proc. K. Ned. Akad. Wet. Ser. B 69, 429–445.

Van Straaten, L.M.J.U., 1972. Holocene stages of oxygen depletion in deep waters of the Adriatic Sea. In: Stanley, D.J. (Ed.), The Mediterranean Sea. Dowden, Hutchingson & Ross Inc., Stroudsburg, Pa., pp. 631–643.

Vergnaud-Grazzini, C., 1985. Mediterranean late Cenozoic stable isotope record: stratigraphic and paleoclimatic implications. In: Stanley, D.J., Wezel, F.C. (Eds.), Geological Evolution of the Mediterranean Basin. Springer-Verlag, New York, pp. 413–451.

Vergnaud-Grazzini, C., Ryan, W.B.F., Cita, M.B., 1977. Stable isotope fractionation, climatic change and episodic stagnation in the eastern Mediterranean during the late Quaternary. Mar. Micropaleontol. 2, 353–370.

Verhallen, P.J.J.M., 1991. Late Pliocene to Early Pleistocene Mediterranean mud-dwelling foraminifera; influence of a changing environment on community structure and evolution. Utrecht Micropaleontol. Bull. 40 (219 pp.).

Versteegh, G.J.M., Zonneveld, K.A.F., 2002. Use of selective degradation to separate preservation from productivity. Geology 30, 615–618.

Wahby, S.D., Bishara, N.F., 1981. The effect of the river Nile on Mediterranean water, before and after the construction of the High Dam at Aswan. In: Martin, J.M., Burton, J.D., Eisma, D. (Eds.), River Inputs to Ocean Systems. UNEP-UNESCO, Switzerland, pp. 311–318.

Wang, Y., Cheng, H., Edwards, R.L., Kong, X., Xiaohua, S., Chen, S., Wu, J., Jiang, X., Wang, X., Zhisheng, A., 2008. Millennial- and orbital-scale changes in the East Asian monsoon over the past 224,000 years. Nature 28, 1090–1093.

Warning, B., Brumsack, H.J., 2000. Trace metal signatures of eastern Mediterranean sapropels. Palaeogeogr. Palaeoclimatol. Palaeoecol. 158, 293–309.

Wegwerth, A., Dellwig, O., Kaiser, J., Menot, G., Bard, E., Shumilovskikh, L., Schnetger, B., Kleinhanns, I.C., Wille, M., Arz, H.W., 2014. Meltwater events and the Mediterranean reconnection at the Saalian-Eemian transition in the Black Sea. Earth Planet. Sci. Lett. 404, 124–135.

Wehausen, R., Brumsack, H.J., 1999. Cyclic variations in the chemical composition of eastern Mediterranean Pliocene sediments: a key for understanding sapropel formation. Mar. Geol. 153, 161–176.

Wehausen, R., Brumsack, H.J., 2000. Chemical cycles in Pliocene sapropel-bearing and sapropel-barren eastern Mediterranean sediments. Palaeogeogr. Palaeoclimatol. Palaeoecol. 158, 325–352.

Weldeab, S., Siebela, W., Wehausen, R., Emeis, K.-C., Schmiedl, G., Hemleben, Ch., 2003. Late Pleistocene sedimentation in the Western Mediterranean Sea: implications for productivity changes and climatic conditions in the catchment areas. Palaeogeogr. Palaeoclimatol. Palaeoecol. 190, 121–137.

Weldeab, S., Menke, V., Schmiedl, G., 2014. The pace of East African monsoon evolution during the Holocene. Geophys. Res. Lett. 41. http://dx.doi.org/10.1002/2014GL059361.

Weninger, B., Clare, L., Rohling, E.J., Bar-Yosef, O., Boehner, U., Budja, M., Bundschuh, M., Feurdean, A., Gebel, H.G., Joeris, O., Lindstaedter, J., Mayewski, P., Muehlenbruch, T., Reingruber, A., Rollefson, G., Schyle, D., Thissen, L., Todorova, H., Zielhofer, C., 2009. The impact of rapid climate change on prehistoric societies during the Holocene in the Eastern Mediterranean. Doc. Praehist. 36 (Neolithic Studies 16), 7–59.

Whiting-Blome, M., Cohen, A.S., Tyron, C.A., Brooks, A., Russell, J., 2012. The environmental context for the origins of modern human diversity: a synthesis of regional variability in African climate 150,000–30,000 years ago. J. Hum. Evol. 62, 563–592.

Wijmstra, T.A., Young, R., Witte, H.J.L., 1990. An evaluation of the climatic conditions during the Late Quaternary in northern Greece by means of multivariate analysis of palynological data and comparison with recent phytosociological and climatic data. Geol. Mijnb. 69, 243–251.

Williams, M.A.J., Adamson, D.A., Cock, B., McEvedy, R., 2000. Late Quaternary environments in the White Nile region, Sudan. Glob. Planet. Chang. 26, 305–316.

Wilson, C., 2003. Late summer chlorophyll blooms in the oligotrophic North pacific subtropical gyre. Geophys. Res. Lett. 30, 1942. http://dx.doi.org/10.1029/2003 GL017770.

Wu, P., Haines, K., 1996. Modeling the dispersal of Levantine Intermediate Water and its role in Mediterranean deep water formation. J. Geophys. Res. 101, 6591–6607.

Wüst, G., 1960. Die tiefenzirkulation des Mittelländischen Meeres in den Kernschichten des Zwischen- und des Tiefenwassers. Dtsch. Hydrographische Z. 13, 105–131.

Wüst, G., 1961. On the vertical circulation of the Mediterranean Sea. J. Geophys. Res. 66, 3261–3271.

Yavuz, V., Akcar, N., Schluchter, C., 2007. The frozen Bosphorus and its paleoclimatic implications based on a summary of historical data. In: Yanko-Hombach, V., Gilbert, A.S., Panin, N., Dolukhanov, P.M. (Eds.), The Black Sea Flood Question: Changes in Coastline, Climate and Human Settlement. Springer Verlag New York Inc.

Yüce, H., 1995. Northern Aegean water masses. Estuar. Coast. Shelf Sci. 41, 325–343.

Zanchetta, G., Drysdale, R.N., Hellstrom, J.C., Fallick, A.E., Isola, I., Gagan, M.K., Pareschi, M.T., 2007. Enhanced rainfall in the Western Mediterranean during deposition of sapropel S1: stalagmite evidence from Corchia cave (Central Italy). Quat. Sci. Rev. 26, 279–286.

Zavatarelli, M., Mellor, G.L., 1995. A numerical study of the Mediterranean Sea circulation. J. Phys. Oceanogr. 25, 1384–1414.

Zehr, J.P., Carpenter, E.J., Villareal, T.A., 2000. New perspectives on nitrogen-fixing microorganisms in tropical and subtropical oceans. Trends Microbiol. 68, 68–73.

Zhao, Y., Colin, C., Liu, Z., Paterne, M., Siani, G., Xie, X., 2012. Reconstructing precipitation changes in northeastern Africa during the Quaternary by clay mineralogical and geochemical investigations of Nile deep-sea fan sediments. Quat. Sci. Rev. 57, 58–70.

Ziegler, M., Tuenter, E., Lourens, L.J., 2010. The precession phase of the boreal summer monsoon as viewed from the eastern Mediterranean (ODP Site 968). Quat. Sci. Rev. 29, 1481–1490.

Ziv, B., Saaroni, H., Alpert, P., 2004. The factors governing the summer regime of the eastern Mediterranean. Int. J. Climatol. 24, 1859–1871.

Zonneveld, K.A.F., Versteegh, G.J.M., de Lange, G.J., 2001. Palaeo-productivity and postdepositional aerobic organic matter decay reflected by dinoflagellate cyst assemblages of the Eastern Mediterranean S1 sapropel. Mar. Geol. 172, 181–195.

Zonneveld, K.A.F., Bockelmann, F., Holzwarth, U., 2007. Selective aerobic degradation of organic walled dinoflagellates as tool to quantify past net primary production and bottom water oxygen concentrations. Mar. Geol. 237, 109–126.